Synthesis and Physicochemical Characterisation of Poly (ε-caprolactone) Nanoparticles for Delivery of Propranolol

UNIVERSITY *of the*
WESTERN CAPE

Hanan Belhaja

A thesis submitted in fulfillment of the requirements for the degree for the degree of Magister Pharmaceuticiae in the School of Pharmacy at the University of the Western Cape, Bellville, South Africa.

Supervisor: Dr. Admire Dube

Co-supervisor: Dr. Kenechukwu Obikeze

May 2017

Synthesis and Physicochemical Characterisation of Poly (ε-caprolactone) Nanoparticles for Delivery of Propranolol

Keywords:

Poly(ε-caprolactone) nanoparticles

Surfactant type

Propranolol

Drug release kinetics

UNIVERSITY of the
WESTERN CAPE

http://etd.uwc.ac.za/

ABSTRACT

Purpose: Cardiovascular diseases (CVDs) are a major cause of morbidity and mortality in both developed and developing countries; and account for around 30% of all deaths worldwide. Reports indicate that nanoparticle (NP) based drug systems are likely to meet the urgent demand for breakthrough innovation in CVDs therapy and diagnosis. NPs have the potential to improve pharmacokinetics and efficacy and reduce the toxicity of cardiovascular drugs. Propranolol is a non-selective beta blocker, and has long been used in the treatment of hypertension, angina and other CVDs. Propranolol has a short half-life (between 2-3 h) and exhibits toxicity, including bronchospasm, due to non-selective beta receptor stimulation. The aim of this study was to develop an NP drug delivery system for propranolol; studying the parameters around formulation of the NPs and their performance *in-vitro*.

Methods: The double emulsion solvent evaporation technique was used to synthesise water-in-oil-in-water poly (ε-caprolactone) (PCL) propranolol loaded NPs using various surfactants, i.e. Span 80, polyvinyl alcohol (PVA), and vitamin E- D-α-Tocopherol polyethylene glycol succinate (TPGS). Characterisation of NPs was performed in terms of particle size, polydispersity index (PDI) and zeta potential (ZP). Using dynamic light scattering (DLS); particle shape was analysed using scanning electron microscopy; short term stability of freeze dried NPs was assessed in deionized water over seven days, at 4°C, 20°C and 37°C. Stability of NPs in human serum albumin (HSA) over 24 h, at 37°C, was also assessed. The extent of NP to albumin binding was assessed using fluorescence measurements. Propranolol loading percentage was determined using a UV-vis spectrophotometer and drug release kinetics was determined in phosphate buffered saline (pH 7.4 at 37°C) in test tubes (Magnetic stirrer, multi positions-Multistirrer series apparatus).

UNIVERSITY of the WESTERN CAPE

http://etd.uwc.ac.za/

Results: The z-average size of the Span 80 and PVA formulations was 378 ± 3.90 nm, and TPGS containing NP formulations had a smaller z-average particle size within the range of 247 ± 0.60 and 276.30 ± 5.01 nm. All NP formulations were relatively monodisperse and the PDI ranged from 0.15 ± 0.13 to 0.41 ± 0.05, with negative ZP ≤ -32 mV. Particle shape was near spherical for all formulations. There was no significant increase ($p > 0.05$) in particle size over seven days in aqueous media whereas in HSA over 24 h, particle size of all formulations increased from 300 nm to 800 nm. The percentage protein binding was affected by the incubation temperature. The type of surfactant was found to have a significant effect on the mean percentage of protein binding; whereby Span 80 stabilized NP formulations had a higher % protein binding than TPGS stabilized NPs.

In comparison to the blank NPs, the size of propranolol loaded NPs were not significantly different with ($p < 0.05$) PDI values below 0.47 ± 0.04. ZP values were ≤ 57.43 ± 0.15. The actual drug loading content was found to be in the range of 0.44% to 5.91% w/w. Encapsulation efficiency (EE%) was within the range of 7.56 ± 0.64 and 36.85 ± 1.16%. SP (Span 80, PVA) and TST (TPGS, Span 80, TPGS) NP formulations showed biphasic Fickian diffusion release kinetics, while ST (Span 80, TPGS) and TT (TPGS, TPGS) formulations showed non Fickian release.

UNIVERSITY of the
WESTERN CAPE

Conclusions: The double emulsion solvent evaporation technique enabled preparation of PCL NPs loaded with propranolol. NPs provided sustained drug release. Based upon the drug release profiles and percent protein binding, the TPGS stabilised PCL NPs appear to be the most suitable carrier for propranolol. These NPs can be evaluated for drug delivery in future *in-vitro* and *in-vivo* studies.

http://etd.uwc.ac.za/

DECLARATION

I, Hanan Belhaja, declare that the thesis **"***Synthesis and Physicochemical Characterisation of Poly (ε-caprolactone) Nanoparticles for Delivery of Propranolol***"** is my own work and has not been submitted before for any degree or examination at this university or any other tertiary institute. All sources used have been acknowledged in the references section.

UNIVERSITY of the
WESTERN CAPE

Signature…….

Date…….. 17/05/2017

http://etd.uwc.ac.za/

DEDICATION

For my dearest family...

The Prophet Muhammad (Peace Be upon Him) said, regarding knowledge:

"Acquire knowledge and impart it to the people...One who treads a path in search of knowledge, has his path to Paradise made easy by God" (Sunan Tirmidhi, Hadith 107; Riyadh us-Saleheen, 245).

http://etd.uwc.ac.za/

Acknowledgments

Above all, I would like to acknowledge my Creator for giving me the faith, strength, good health, wisdom and perseverance, without him I would not have completed my Masters!

I would like to express my deepest gratitude to my supervisor Dr Admire Dube for the knowledge gained, encouragement, for his confidence, patience, support and motivation throughout the duration and the completion of this research, and I acknowledge him for proofreading my thesis. THANK YOU! I also thank Dr Kenechukwu Obikeze, my co-supervisor whose contributions were invaluable.

A special thanks to my husband who stood by me through all the rough times and my children whose presence always brings joy to my life.

- I would also like to thank my parents, brothers and sisters for their love, care, prayers, and support during the course of my research work.
- I am thankful to Dr Mustafa Drah from the Biotechnology Department at the University of the Western Cape, for his invaluable advice, and editing assistance.
- I would like to acknowledge Nanomedicine Research Group: Somaya, Ephraim, Myolisi, Zipho, Tendai and Alkassim, for their moral support and constructive criticism.
- I would like also to thank my friends Suad and Reem for the support and invaluable advice.
- I would also like to sincerely acknowledge Mr. Adrian Josephs for his assistance with the SEM analysis. Mr. Sandile Dyantyi for procurement of the essentials of the project and Mr. Yunus Kippie for the analytical expertise he shared.
- To the stuff and colleagues at the School of Pharmacy, University of the Western Cape, South Africa, I say thank you for your kind and cordial working relationship I enjoyed during my studies.
- To Prof Mervin Meyer for the opportunity to use his laboratory.
- Lastly, but by no means the least I would like to thank the Libyan government for assisting me financially.

UNIVERSITY of the WESTERN CAPE

http://etd.uwc.ac.za/

Table of Contents

Title page i

Keywords: ii

Abstract iii

Declaration v

Dedication vi

Acknowledgments vii

Table of Contents viii

List of Figures xiv

List of Tables xviii

List of abbreviations and units xix

Chapter 1 1

Introduction 1

Chapter 2 4

Literature review 4

2.1 The burden of cardiovascular diseases (CVDs) 4

2.1.1 CVDs and nanomedicines for the treatment of CVDs 4

2.2 Nanoscience, nanotechnology and nanomedicine 6

2.3 NP drug delivery systems 8

2.4 Types of NPs 10

2.4.1 Liposomes 10

UNIVERSITY of the
WESTERN CAPE

http://etd.uwc.ac.za/

2.4.2 Solid lipid nanoparticles (SLNs)....10
2.4.3 Dendrimers....11
2.4.4 Polymeric NPs (PNPs)....11
2.5 Polymers used in the formulation of PNPs....13
2.5.1 The synthetic polymer PCL....14
2.6 Nanomedicine and treatment of CVDs....17
2.7 Emulsions....19
2.7.1 Surfactants used in the stabilization of NP drug delivery systems....22
2.8 Emulsion Stability Mechanisms....23
2.8.1 Polyvinyl alcohol (PVA)....24
2.8.2 D-α-tocopheryl polyethylene glycol succinate....25
2.8.3 Span 80....26
2.9 Methods for the formulation of polymeric NPs....27
2.9.1 The emulsion-solvent evaporation method (EEM)....27
2.9.1.1 The mechanism of formation of PNPs by EEM....28
2.9.2 The double emulsion and solvent evaporation method....30
2.9.3 The emulsion solvent diffusion method....32
2.9.4 The solvent displacement / nanoprecipitation method....33
2.9.5 The salting out method....34
2.10 Characterisation of nanoparticles....35
2.10.1 Determination of average particle size....35
2.10.2 Determination of particle shape and surface morphology....36
2.10.2.1 Scanning electron microscopy (SEM)....36
2.10.2.2 Transmission electron microscope (TEM)....37

UNIVERSITY of the WESTERN CAPE
http://etd.uwc.ac.za/

2.10.3 Measurement of particle zeta potential (ZP) 37

2.11 Determination of the kinetics of drug release from NPs 39

2.11.1 Drug release mechanisms 42

2.11.2 Modelling drug release 43

Chapter 3 47

Formulation, development and characterisation of poly (ε-caprolactone) nanoparticles 47

3.1 Introduction 47

3.2 Aims 47

3.3 Hypothesis 47

3.4 Materials 48

3.4.1 Equipment and materials 48

Equipments used 48

Chemicals used 48

3.5 Methods 49

3.5.1 Synthesis of PCL NPs 49

3.5.2 Characterisation of particle size, PDI and ZP of the NPs 51

3.5.3 Determination of influence of surfactant type on the physiochemical characteristics of the NPs 51

3.5.3.1 Calculation of HLB values of surfactant mixtures 52

3.5.4 Determination of surface morphology of NPs 54

3.5.5 Assessment of NP stability 54

3.5.5.1 Evaluation of NP stability in aqueous solution 55

3.5.5.2 Evaluating NP stability in human serum 55

3.5.6 Assessment of the extent of albumin binding to NPs 55

UNIVERSITY of the WESTERN CAPE

http://etd.uwc.ac.za/

3.5.6.1 Quantification of albumin 56

3.5.6.2. Assessment of extent of albumin binding to NPs 56

Statistical analysis 57

3.6 Results and discussion 57

3.6.1 Synthesis and characterization of PCL NPs 57

3.6.2 The effect of different surfactants on the physiochemical characteristics of 33% SOR PCL NPs 60

3.6.3 Characterisation of the physiochemical properties of NPs prepared with PVA, TPGS and Span 80 surfactants 60

3.6.4 Evaluation of surface morphology of the NPs 63

3.6.5 Stability of the NPs in aqueous media 65

3.6.6 Evaluating NP stability in human serum 72

3.6.7 Assessment of the extent of albumin binding to NPs 74

3.6.7.1 Standard curve determination for quantification of HSA in PBS 74

3.6.7.2 Determination of the extent of albumin binding to NPs 76

Chapter 4 80

Preparation and Characterisation of Propranolol-HCL loaded PCL NPs 80

4.1 Introduction 80

4.2 Aims 80

4.3 Hypothesis 80

4.4 Materials 80

4.4.1 Equipment and Materials 80

4.5 Methods 82

UNIVERSITY of the WESTERN CAPE

http://etd.uwc.ac.za/

4.5.1 Preparation of propranolol loaded PCL NPs 82
4.5.2 Characterisation of propranolol loaded NPs 82
4.5.3 Quantitation of propranolol loading in NPs 83
4.5.3.1 Determination of drug loading 83
4.5.3.2 Validation of UV-vis analytical procedure for quantitation of propranolol in NPs 84
4.5.4 Differential Scanning Calorimetry (DSC): Thermo analytical analysis of the NPs 85
4.5.5 Fourier Transform Infrared spectroscopy (FTIR) analysis of NPs 86
4.5.6 Determination of kinetics of propranolol release from NPs 86
4.5.6.1 Validation of UV-vis assay of propranolol-HCL in PBS pH 7.4 87
4.5.6.2 Determination of the kinetics of drug release 87
4.6 Results and discussion 87
4.6.1 Properties of the propranolol loaded PCL NPs 87
4.6.3 Quantitation of propranolol loading in NPs 90
4.6.3.1 Validation of UV-vis analytical procedure for quantitation of propranolol in NPs 90
4.6.3.2 Determination of propranolol loading and encapsulation efficiency in NPs ... 92
4.6.5 Differential Scanning Calorimetry (DSC) 94
4.6.6 Fourier Transform Infrared spectroscopy (FTIR) of NPs (Drug–polymer interactions) 97
4.6.7 Determination of propranolol release from NPs 103
4.6.7.1 Validation of UV-visible assay of propranolol-HCL 103
4.6.7.2 Determination of propranolol release kinetics from NPs 105
4.6.8 Determination of the mechanism of drug release 108
4.6.8.1 Release profiles and kinetics at pH 7.4 for SP formulation 110

UNIVERSITY of the
WESTERN CAPE

http://etd.uwc.ac.za/

4.6.8.2 Release profiles and kinetics at pH 7.4 for ST formulation.....110

4.6.8.3 Release profiles and kinetics at pH 7.4 for TT formulation 112

4.6.8.4 Release profiles and kinetics at pH 7.4 for TST formulation 113

4.6.8.5 Summary of drug release fitting 114

Chapter5.....116

Conclusion and future recommendations.....116

References.....119

UNIVERSITY of the
WESTERN CAPE

http://etd.uwc.ac.za/

List of Figures

Chapter 2

Figure 2.1	Chemical structure of propranolol-HCL……	5
Figure 2.2	Nanoparticle (applied in drug delivery) in relation to other scales…….	7
Figure 2.3	Schematic representation of nanospheres and nanocapsules.	12
Figure 2.4	Chemical structure of Poly (ε-caprolactone) (PCL)……...	15
Figure 2.5	Schematic representations of (a) an oil-in-water emulsion and (b) a water-in-oil emulsion……..	20
Figure 2.6	Schematic representations of a multiple w/o/w emulsion and o/w/o emulsion…….	20
Figure 2.7	Mechanism of stabilization of two emulsion phases by a surfactant……	21
Figure 2.8	Structural formula for PVA…….	24
Figure 2.9	Chemical structure of TPGS……	26
Figure 2.10	Chemical structure of Span 80…….	27
Figure 2.11	Schematic representation of the emulsification-solvent evaporation method……..	28
Figure 2.12	Description of the possible mechanisms of formation of the NPs by emulsion solvent evaporation EEM……	30
Figure 2.13	A typical process of double emulsion formation…….	32

UNIVERSITY of the WESTERN CAPE

http://etd.uwc.ac.za/

Figure 2.14 Schematic representation of the emulsion-solvent diffusion method…….. 33

Figure 2.15 Schematic representation of the solvent displacement technique…… 34

Figure 2.16 Schematic representation of the salting out method…….…… 35

Figure 2.17 Schematic of a Dynamic Light Scattering instrument……. 36

Figure 2.18 Schematic showing the electrical double layer that surrounds a particle in an aqueous medium and the position of the slipping plane…….. 38

Figure 2.19 Schematic of drug release mechanisms from NPs…… 42

Chapter 3

Figure 3.1 Schematic representation of the emulsion-solvent evaporation method for synthesis of PCL NPs……. 50

UNIVERSITY of the
WESTERN CAPE

Figure 3.2 Average (z-average) hydrodynamic particle size of PCL NPs at various SOR%..... 58

Figure 3.3 PDI and ZP of PCL NPs prepared with different SOR% …… 59

Figure 3.4 Z-average particle size and PDI of PCL NPs prepared with PVA, Span 80 and TPGS surfactants……... 61

Figure 3.5 Plot of average particle size distribution of SP, ST, TT and TST NP formulations…….. 61

Figure 3.6 HR-SEM images of PCL NPs…… 64

Figure 3.7 Trends in the z-average particle size of SP, ST, TT, and TST NPs over seven days……... 67

http://etd.uwc.ac.za/

Figure 3.8 Trends in the PDI of SP, ST, TT, and TST NPs over seven days……. 69

Figure 3.9 Trends in the ZP of SP, ST, TT, and TST NPs over seven days 70

Figure 3.10 Trends in z-average particle size of SP, ST, TT, and TST NPs over 24 h at 37°C in HSA solution……. 73

Figure 3.11 Linear relationship between HSA concentration and fluorescence intensity…… 75

Figure 3.12 Fluorescence intensity of serial dilutions from NP stock solution -1 mg/mL in PBS pH 7.4…… 76

Figure 3.13 Percentage of protein binding of SP, ST, TT and TST NPs at three concentration levels (1, 0.25, 0.0625 mg/mL NPs)…… 78

Chapter 4

Figure 4.1 Z-average particle size and PDI of propranolol loaded PCL NPs, SP, ST, TT, and TST……. 88

UNIVERSITY of the
WESTERN CAPE

Figure 4.2 ZP values of propranolol loaded PCL NPs, SP, ST, TT, and TST…….. 90

Figure 4.3 Propranolol-HCL calibration curve in Methanol: Water: Chloroform (7:2:1)…… 91

Figure 4.4 DSC thermo grams of individual compounds; (TPGs, PCL, propranolol, glucose and PVA), and physical mixtures of NP components…… 96

Figure 4.5 DSC thermo grams of propranolol loaded PCL NP formulations (SP, ST, TT and TST)…… 97

http://etd.uwc.ac.za/

Figure 4.6 FTIR spectra of PCL, propranolol-HCl, PVA and SP drug loaded NPs……. 99

Figure 4.7 FTIR spectra of PCL, propranolol-HCl, TPGS and ST drug loaded NPs……. 100

Figure 4.8 FTIR spectra of PCL, propranolol-HCl, TPGS and TT drug loaded NPs……. 101

Figure 4.9 FTIR spectra of PCL, propranolol-HCl, TPGS and TST drug loaded NPs…….. 102

Figure 4.10 Calibration curve of propranolol-HCL in PBS pH 7.4. Absorbance measured at 290 nm…… 105

Figure 4.11 *In-vitro* release of propranolol loaded NPs in PBS pH 7.4 at 37°C over 48 h…… 106

Figure 4.12 The initial (burst) release of propranolol loaded NPs in PBS pH 7.4 at 37°C over the first 3h…… 107

Figure 4.13 Models of fit for *in-vitro* release of propranolol from SP NP formulation at pH 7.4……. 111

Figure 4.14 Models of fit for *in-vitro* release of propranolol from ST NP formulation at pH 7.4……. 112

Figure 4.15 Models of best fit for in-vitro release of propranolol from TT NP formulation at pH 7.4…….. 113

Figure 4.16 Models of best fit for in-vitro release of propranolol from TST NP formulation at pH 7.4……... 115

http://etd.uwc.ac.za/

List of Tables

Chapter 2

Table 2.1	Most widely used polymers for preparing NPs in drug delivery…….	14
Table 2.2	Tabular summary of selected studies employing PCL NPs for drug delivery…….	16
Table 2.3	NP-mediated drug delivery system for hypertension treatment	18
Table 2.4	The major potential and limitations of commonly used methods for drug release assessment……	40

Chapter 3

Table 3.1	Distribution of the surfactants in the double emulsion phases and the calculated HLB values of the surfactant mixture……	53

UNIVERSITY of the WESTERN CAPE

Chapter 4

Table 4.1	Intra-day and inter-day precision of the propranolol assay…..	92
Table 4.2	Accuracy and recovery data for quantification of propranolol	92
Table 4.3	DL *theoretical* %, DL *actual* % and EE% of propranolol in the NP formulations……	93
Table 4.4	Intra-day and inter-day precision of the propranolol assay in PBS …….	105
Table 4.5	Accuracy and recovery data of the propranolol assay in PBS.	105
Table 4.6	Kinetic release rate constants, correlation coefficient and diffusion exponent of various propranolol release models …	110

http://etd.uwc.ac.za/

List of abbreviations and units

Abbreviation	Full name
AFM	Atomic force microscopy
ANOVA	Analysis of variance
AUC	Area under curve
BP	Blood pressure
CVDs	Cardiovascular diseases
°C	Degrees Celsius
cm^{-1}	Reciprocal centimetre
DDS	Drug delivery system
DL	Drug loading
DLS	Dynamic light scattering
DSC	Differential scanning calorimetry
EE%	Encapsulation efficiency
EEM	Emulsion solvent evaporation method
Eq.	Equation
FDA	Food and drug administration
FTIR	Fourier Transform Infrared spectroscopy
g	G-force
H	Hour
HCl	Hydrochloride
HLB	Hydrophilic-Lipophilic balance
HR-SEM	High resolution scanning electron microscopy
HSA	Human serum albumin
IR	Infrared spectra
ICH	International Council on Harmonization
ISO	International Organization for Standardization
J/g	Joule per gram
KV	Kilovolts

UNIVERSITY of the
WESTERN CAPE

http://etd.uwc.ac.za/

MCT	Monocrotaline rat model
Mw	Molecular weight
Mg	Milligrams
mL	Millilitres
mmHg	Millimetres of mercury
mV	Millivolts
µl	Microliters
µg	Micrograms
NDDS	Nanoparticle drug delivery system
NF-kB	Nuclear factor kappa B
Nm	Nanometres
NP	Nanoparticle
NPs	Nanoparticles
O	Oil (organic) phase
O/W	Oil-in-water emulsion
PBS	Phosphate buffered saline
PCL	Poly(ε-caprolactone)
PCS	Photon correlation spectroscopy
PDI	Polydispersity index
PEG	Polyethylene glycol
PIBCA	Poly(isobutyl cyanoacrylate)
PIHCA	Poly (isohexylcyanoacrylate)
PBCA	Poly (n-butyl cyanoacrylate)
PLA	Poly(lactic acid)
PLGA	Poly(lactic-co-glycolic acid)
PNPs	Polymeric nanoparticles
PVA	Polyvinyl alcohol
Rpm	Revolutions per minute
SD	Standard deviation
Sec	Second
SEM	Scanning electron microscopy
SLNs	Solid lipid nanoparticles
SOR(%)	Surfactant-oil ratio

UNIVERSITY of the WESTERN CAPE
http://etd.uwc.ac.za/

TEM	Transmission electron microscopy
TPGS	D-α-tocopheryl polyethylene glycol succinate
$t_{1/2}$	Half-life
UK	United Kingdom
USA	United States of America
v/v	Volume per volume
W/O/W	Water-in-oil-in-water emulsion
w/v	Weight per volume
w/w	Weight per weight
ZP	Zeta potential

UNIVERSITY of the
WESTERN CAPE

http://etd.uwc.ac.za/

CHAPTER 1

Introduction

The challenge of developing suitable drug delivery systems for the targeted treatment of cardiovascular diseases (CVDs) is currently a major focus for pharmaceutical scientists. Recently, particulate carriers have been gaining more attraction due to their potential application in targeted drug delivery [1]. Over the past few decades, there has been extensive interest in developing biodegradable polymeric nanoparticles (PNPs) as effective drug delivery strategies. The controlled release of pharmacologically active agents to the specific site of action at an optimal rate and dose regimen has been a major goal in utilising NPs [2].

NPs are colloidal drug carriers, having a size range between 1-1000 nm and providing improved drug bioavailability. Propranolol hydrochloride (HCl) is a non-selective beta blocker used in the treatment of essential hypertension, myocardial infarction and arrhythmia. Propranolol-HCL undergoes extensive hepatic first pass metabolism. It is about 90% bound to plasma proteins; has a bioavailability of approximately 23% and a biological half-life ($t_{1/2}$) of 2-3 h. Propranolol may benefit from delivery using a targeted and extended release NP formulation [3]. The water-in-oil-in-water (w/o/w) emulsification process is the method of choice for encapsulation inside PNPs of hydrophilic drugs such as propranolol-HCl [4]. The stability of the emulsion's oil and water phases, during the emulsification process, is assured by the addition of surfactants. A wide range of surfactants are available for emulsion stabilisation and include ionic surfactants (cationic, anionic, zwitterionic) and non-ionic surfactants. Non-ionic surfactants are macromolecules formed by copolymers or tripolymers (amphiphilic) which can form stable micelles due to the hydrophobic and hydrophilic interactions with the oil and water phases. The major non-ionic surfactants used in the

UNIVERSITY of the WESTERN CAPE
http://etd.uwc.ac.za/

emulsion-solvent evaporation method (EEM) are poly(vinyl alcohol) (PVA), the poloxamer and poloxamines family, the pluronic family (F68, F127, and others), sodium cholate, and tween 80 [5]. However, the impact of these surfactants on NP properties i.e. particle size, drug loading and drug release kinetics, as well as protein (albumin) binding *in-vitro,* is unknown. The objective of this study was to synthesise NPs from the polymer poly (ε-caprolactone) (PCL) encapsulating propranolol-HCL and determine the impact of various surfactants on NP properties and drug release kinetics. It was hypothesised that:

i. The EEM technique can produce nano-sized PCL (w/o/w) particles and that the formulation variable (i.e. surfactant to polymer ratio), has a noticeable effect on the resultant NP properties.

ii. Surfactant type influences the physicochemical characteristics of PCL NPs and influences albumin adsorption onto the NPs.

UNIVERSITY of the

iii. Surfactant type modulates the encapsulation efficiency and kinetics of release of propranolol from PCL NPs.

The goal of this study was to develop a NP drug delivery system for propranolol; studying parameters around formulation of the NPs and their performance *in-vitro.*

Chapter 2 of this dissertation discusses the relevant literature; including prior art in the development of polymeric NPs drug delivery systems. Chapter 3 describes the experimental methods used in the synthesis of, and characterisation of the PCL NPs. A suitable preparation method was selected and the effect of different surfactants on NP characteristics was determined. The stability of NPs in aqueous media and in human serum albumin and the

http://etd.uwc.ac.za/

assessment of the extent of albumin binding to NPs, were also characterised. The results obtained are presented and discussed. Chapter 4 focuses on the methods of preparation and characterisation of propranolol-HCL loaded PCL NPs, as well as the quantification of propranolol loading of the NPs. The effect of surfactant type on propranolol loading was also investigated. Finally determination of kinetics of propranolol release from the NPs was investigated. Part of the investigation involved understanding the rate and mechanism of propranolol release from PCL NPs. The results obtained are presented and discussed. The conclusion of this study and recommendations for further work are presented in Chapter 5.

http://etd.uwc.ac.za/

CHAPTER 2

Literature review

2.1 The burden of cardiovascular diseases (CVDs)

2.1.1 CVDs and nanomedicines for the treatment of CVDs

CVDs are a major source of morbidity and mortality in both developed and developing countries and account for approximately 30% of all deaths [6][7]. CVDs include ischemic heart diseases, stroke, hypertension, rheumatic heart disease, cardiomyopathies and peripheral artery diseases [8]. There are several factors that cause CVDs such as tobacco use, obesity, alcohol, physical inactivity, hypertension, diabetes, age, psychological factors and genetic factors [9][10].

UNIVERSITY of the
WESTERN CAPE

The World Health Organization (WHO) estimates that about 60% of deaths in the world are caused by non-communicable diseases (i.e. cancer, CVDs and other chronic diseases) [11]. It is further predicted that by 2020 the mortality rate from CVDs is expected to increase by 120% for women and 137% for men [11].

Today, CVDs are the number one cause of death in sub-Saharan Africa in adults over the age of 30 in 2015. Globally, low- and middle-income countries bear 80% of the world's death burden from CVDs. One of the strongest drivers is undiagnosed and untreated hypertension, which affects nearly one in two Africans over the age of 25 — the highest rate of any continent in the world [12].

Hypertension is one of the most common health conditions in primary care and one of the key risk factors, along with hyperlipidaemias, hyperglycaemia, obesity and smoking, which

http://etd.uwc.ac.za/

contribute to other diseases like myocardial infarction, stroke, renal failure and death. As per the WHO report on World Health Statistics 2012, one in every three adults has hypertension [13]. Hypertension is usually defined by the presence of a chronic elevation of systemic arterial pressure above a certain threshold value; an elevation of blood pressure (BP) above approximately115⁄75 mm Hg [14][15][16].

Although drugs are available for the treatment of CVDs, they have several limitations such as non-specific toxicity, the lack of drug affinity to the pathological site, low bioavailability, short half-life and low efficacy at tolerated doses [6]. This has promoted the development of alternative strategies to treat CVDs.

One of the key drugs that are used to treat hypertension is the beta blocker, propranolol (see Figure 2.1).

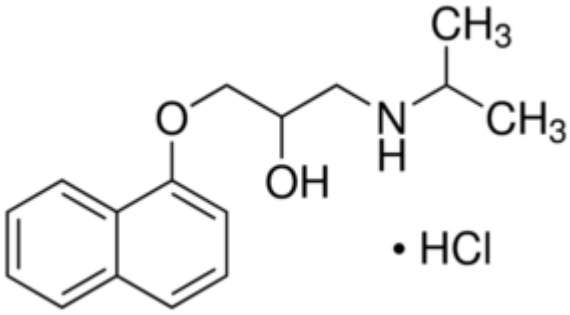

Figure 2.1 *Chemical structure of propranolol-HCL* [17]

Propranolol is a non-selective beta blocker, and has long been used in the treatment of hypertension, and other CVDs [18]. After oral administration, propranolol is subjected to extensive hepatic first pass metabolism and has a systemic bioavailability between 15 and 23% and a short plasma half-life between 1 – 2 h. These properties indicate that propranolol cannot be fully available for the treatment of CVDs [19]. Propranolol functions through non-

http://etd.uwc.ac.za/

specific blocking of the beta 1 and beta 2 receptors. Beta 1 receptors are located in the heart and in the kidneys, whereas beta 2 receptors are mainly located in the lungs, gut liver, uterus, vascular smooth muscle and skeletal muscle. Blocking the activity of beta receptors results in a decreasing heart rate and force of contractions which results in the lowering of high blood pressure [18]. Propranolol is reported to have poor patient compliance and side effects which result from its non-selective blockage of beta adeno-receptors and include tightness in the chest (bronchoconstriction) and bradycardia (slower than normal heart rate). These side effects are due to the blockage of beta 2 receptors, and the beta 1 receptors respectively [20].

2.2 Nanoscience, nanotechnology and nanomedicine

Nanoscience is the study of phenomena and manipulation of materials at atomic, molecular and macromolecular scales, where properties differ significantly from those at a larger scale [21]. Nanotechnology is the application of nanoscience in various fields. Nanotechnology is considered by many as the next revolution [21]. This technological leap in the control, manipulation, study, and design of structures and materials at the nanometre size range (one-billionth of a meter), in the past decade, has driven developments enabling the use of nano-sized objects, i.e., nanoparticles (NPs) in fields ranging from electronics and communications, through to optics, chemistry, energy and biology [22][23].

Nanoscience and nanotechnologies encompass a range of techniques rather than a single discipline, and stretch across the whole spectrum of science, touching medicine, physics, engineering and chemistry. They are widely seen as having huge potential to bring about benefits in areas as diverse as drug development [24].

The International Standards Organization (ISO) defines a NP as a particle that has a size range between 1-100 nanometres (nm) [25]. It is important to understand that this range is not

http://etd.uwc.ac.za/

definitive and that the size of NPs may differ (i.e. some literature reviews utilize a 1-1000 nm as the range) [26][27][28]. Figure 2.2 shows the different types of NPs and their relation to other scales.

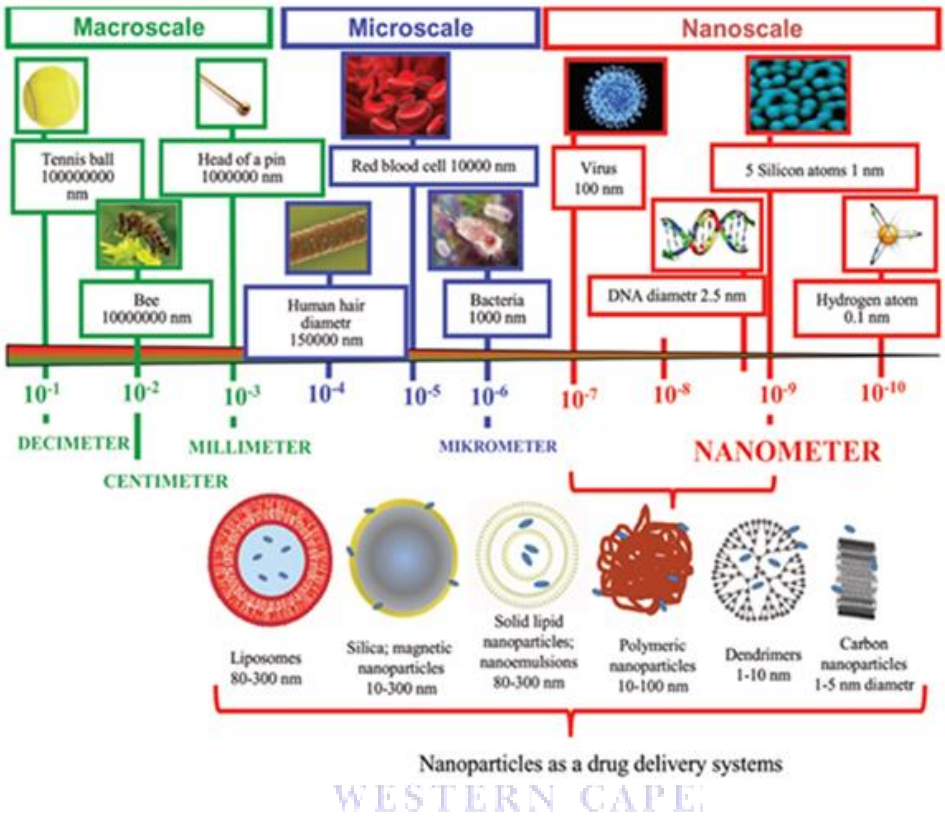

WESTERN CAPE

Figure 2.2 *NPs (applied in drug delivery) in relation to other scales* [29]

NP shapes vary from spherical particles to discoidal, hemispherical, cylindrical and conical [30]. The term NP collectively includes nanospheres and nanocapsules. Nanospheres are matrix-type particles and the active compound for delivery may be adsorbed on the surface, encapsulated or dissolved within the matrix of the NP. Nanocapsules on the other hand, are vesicular systems in which the active compound is confined to a cavity or inner liquid core surrounded by the polymer membrane. In this case the active compounds are usually dissolved in the inner core; however, they may also be adsorbed onto the NP surface [31][32].

http://etd.uwc.ac.za/

The implementation of nanotechnology in the field of medicine has been termed nanomedicine. Nanomedicine brings hope for revolutionising medical treatments and therapies in areas, such as imaging, faster diagnosis, drug delivery and tissue regeneration, as well as the development of new medical products [23][33]. Indeed, materials and devices of nanometric dimensions are already approved for clinical use and numerous products are being evaluated in clinical trials [23][30][34]. Among these products, liposomal drugs and polymer–drug conjugates are two dominant classes, accounting for more than 80% of the total number of nanomedicines e.g. liposomal doxorubicin, albumin-bound paclitaxel and nanocrystalline fenofibrate [35].

One of the major focuses of nanomedicines is in the treatment of CVDs [30]. Varieties of NP-based drug delivery systems have been and are being developed for applications in cancer, CVDs and other conditions. Nanomedicines have advantages over standard low-molecular-weight drugs. They reduce renal excretion and/or hepatic degradation, which lead to prolonged circulation times; they reduce the volume of distribution, leading to less accumulation in healthy non-target tissues (site-avoidance drug delivery) [36][37]. Moreover, they improve the ability of drugs to accumulate at pathological sites (site-specific drug delivery); and improve the therapeutic index of drugs, by increasing their accumulation at the target site and/or reducing their localisation in potentially endangered healthy organs [38]. In addition, nanomedicine formulations assist low-molecular-weight therapeutic agents in overcoming several additional barriers to efficient drug delivery to pathological sites [37].

UNIVERSITY of the
WESTERN CAPE

2.3 Nanoparticle drug delivery systems

Delivering therapeutic compounds to the target site is a major challenge in the treatment of many diseases. The conventional delivery of drugs in dosage forms such as solutions, suspensions or emulsions suffer from certain limitations including limited bioavailability,

http://etd.uwc.ac.za/

first pass effect, lack of selectivity, and fluctuations in plasma drug levels in the absence of sustained therapeutic effect [26]. These limitations and drawbacks can be overcome by sustaining drug delivery. In sustained drug delivery systems, the drug is transported to the site of action, thus, its influence on vital tissues and undesirable side effects can be minimised. In addition, the delivery system protects the drug from rapid degradation or clearance and enhances drug concentration in target tissues; therefore, lower doses of drug are required. [26][29].

NPs, due to their small size, can extravasate through the endothelium in inflammatory sites, epithelium (e.g., intestinal tract and liver), tumours, or penetrate micro-capillaries. In general, the nanometre size of these particles allows for efficient uptake by a variety of cell types and selective drug accumulation at target sites in the body (its site of action). This results in concomitant reduction in the quantity of the drug required and dosage toxicity, enabling the safe delivery of toxic therapeutic drugs and protection of non-target tissues and cells from severe side effects [26][39]. The use of polymeric biodegradable materials for NP preparation allows for sustained drug release within the target site over a period of days or even weeks [26][39]. This results in increasing drug residence time in the body [26][39]. In addition particle size and surface characteristics of NPs can be easily manipulated to achieve both passive and active drug targeting after parenteral administration [40]. Moreover, ligands on the surface of particles can be used to achieve site-specific targeting [40].

http://etd.uwc.ac.za/

2.4 Types of NPs

2.4.1 Liposomes

Liposomes are vesicular structures composed of an aqueous core surrounded by a hydrophobic lipid bilayer, created by the extrusion of phospholipids and steroids (e.g., cholesterol) [41]. The typical size range of a liposome is 80–300 nm [42][29]. The utilisation of liposomal platforms for drug delivery has had a significant impact on pharmacology. There are several examples of successful liposomal drug formulations, such as anticancer drugs, neurotransmitters (serotonin), antibiotics, anti-inflammatories, anti-bacterials, antivirals, and anti-rheumatic drugs [41]. The main disadvantages of using liposomes as drug delivery systems include low encapsulation efficiency, poor stability in biological fluid and during storage, and poor storage stability [43][29].

UNIVERSITY of the
WESTERN CAPE

2.4.2 Solid lipid nanoparticles (SLNs)

SLNs are comprised of a solid lipid matrix, i.e., lipids that are solid at body temperature [44]. They have been exploited for dermal, oral, parenteral, ocular, pulmonary, and rectal drug delivery. SLNs are particles prepared from solid lipids, e.g., highly purified triglycerides, complex glyceride mixtures or waxes stabilised by various surfactants. The main advantages of SLNs include good physical stability, protection of incorporated drug molecules from the environment (water, light), controlled and/or targeted drug release, and good tolerability [44][26][29]. However, some disadvantages have been observed, which include low loading capacity (limited by the solubility of drug in the lipid and the structure and polymorphic state of the lipid matrix) and drug expulsion after crystallisation[43][29].

http://etd.uwc.ac.za/

2.4.3 Dendrimers

Dendrimers are unimolecular, monodisperse, micellar nanostructures, around 20 nm in size, with a well-defined, regularly branched symmetrical structure and a high density of functional end groups at their periphery [26]. The drug may be encapsulated in the internal structure of dendrimers or it can be chemically attached or physically adsorbed on the dendrimer's surface [45]. An example of a drug entrapped within the dendrimetric architecture is cisplatin [46]. Further examples are anticancer drugs, including methotrexate [47] and doxorubicin [48]. The disadvantages of using dendrimers as drug delivery systems are the extra obstacles of multistep syntheses, and the associated higher cost [43].

2.4.4 Polymeric NPs (PNPs)

PNPs are among the simplest form of soft materials for nanomedicine applications due to their facile synthesis and wide applicability to all aspects of the field [41]. Biodegradable PNPs have been used frequently as drug delivery vehicles due to better encapsulation, great bioavailability, controlled release and less toxic properties [49]. Indeed, two of the top 10 best-selling drugs in the United States in 2013 were PNP loaded drugs (Copaxone® and Neulasta®) [41]. PNPs fall into one of two categories: (a) biodegradable polymer architectures for controlled release applications, and (b) polymer-drug conjugates for increased drug half-life and bioavailability [41].

PNPs are obtained from synthetic polymers, such as poly-ε-caprolactone (PCL), polyacrylamide and polyacrylate, or natural polymers, such as albumin, DNA, chitosan, and gelatine [50]. Based on *in-vivo* behaviour, PNPs may be classified as biodegradable, i.e., poly (L-lactide) (PLA), polyglycolide (PGA), and non-biodegradable, e.g., polyurethane. PNPs are usually coated with non-ionic surfactants in order to reduce immunological interactions e.g., opsonisation as well as to reduce intermolecular interactions between the surface chemical

http://etd.uwc.ac.za/

groups of PNPs e.g., van der Waals forces, hydrophobic interaction or hydrogen bonding [51]. Kumari and co-workers in 2010 reported that minimal systemic toxicity associated with the use of poly lactide-co-glycolide (PLGA) for drug delivery or biomaterial applications [52].

A drug is typically dissolved, entrapped, encapsulated or covalently attached to the PNP. Depending upon the method of preparation (methods of PNP preparation are discussed in section 2.9) nanospheres or nanocapsules can be obtained. Nanospheres are matrix systems in which the drug is physically and uniformly dispersed whereas nanocapsules are systems in which the drug is contained within a cavity surrounded by a unique polymer membrane [31][32], as shown in Figure 2.3.

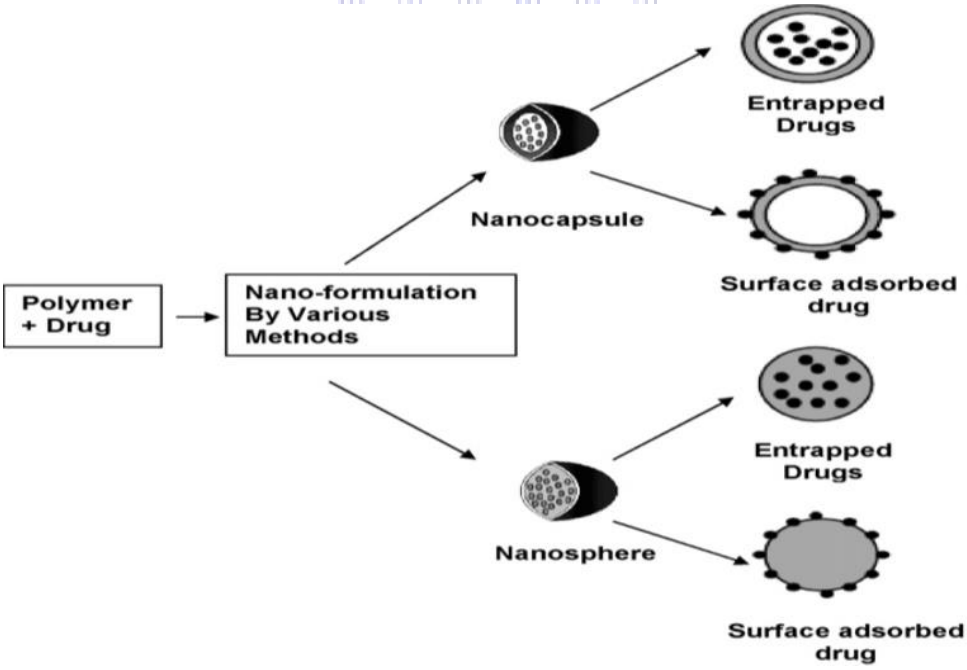

Figure 2.3 *Schematic representation of nanospheres and nanocapsules: Drug molecules are either entrapped inside or adsorbed on the surface, depending on method of preparation* [49].

http://etd.uwc.ac.za/

Polymer drug conjugates have been shown to be stable in blood, non-toxic, and non-thrombogenic [29]. Moreover, polymer drug conjugates have been applied to deliver anticancer drugs such as carboplatin [53], 5-fluorouracil [54] and doxorubicin [55] and anti-infective drugs such as rifampicin [56], lamivudine[57] and clotrimazole [58].

2.5 Polymers used in the formulation of PNPs

The type of polymer used in the preparation of NPs highly affects the properties of NPs. Currently, several types of polymers are available for the preparation of PNPs [31]. Table 2.1 lists some of the common polymers classified as synthetic, natural or co-polymers. The characteristics and performance *in vivo*, of NPs prepared using natural polymers may be less predictable due as these polymers vary widely in chemical composition and hence their physical properties. On the contrary, it is possible to synthesize polymers with specific chemical composition resulting in highly predictable physical properties such as solubility, permeability and rates of biodegradation. As a result synthetic polymers are also easily designed for specific applications such as controlled rates of dissolution, degradation, and erosion, as well as targeting [59]. An appropriate polymer needs to fulfil several requirements in order to be useful in a drug delivery application. Firstly, it needs to be biodegradable and eliminated from the body in a short period of time, allowing repeated administration without any risk of uncontrolled accumulation. Secondly, its degradation products, if any, must be non-toxic and non-immunogenic [60]. PCL is among the most extensively used polymers for NP preparation, attributed to its biodegradability and slow degradation which result in NPs possessing favorable properties for long-term delivery extending over a period of more than one year [61].

UNIVERSITY of the
WESTERN CAPE

http://etd.uwc.ac.za/

Table 2.1 *Most widely used polymers for preparing NPs in drug delivery* [60].

Classification	Material name
Synthetic homopolymers	Poly (lactide) (PLA)
	Poly (lactide-co-glycolide) (PLGA)
	Poly (ε-caprolactone) (PCL)
	Poly (isobutylcyanoacrylate) (PIBCA)
	Poly (isohexylcyanoacrylate) (PIHCA) Poly (n-butylcyanoacrylate) (PBCA)
	Poly (acrylate) and Poly (mathacrylate)(PMA)
Natural polymers	Chitosan
	Alginate
	Gelatine
	Albumin
Copolymers	Poly (lactide)-poly (ethylene glycol) (PLA-PEG)
	Poly (lactide-co-glycolide)- poly (ethylene glycol) (PLGA-PEG)
	Poly (ε-caprolactone)- poly (ethylene glycol) (PCL-PEG)
	Poly(hexadecylcyanoacrylate co-poly (ethylene glycol) cyanoacrylate) Poly (HDCA-PEGCA)

UNIVERSITY of the
WESTERN CAPE

2.5.1 The synthetic polymer PCL

PCL is a semi-crystalline polymer having a glass transition temperature of -60°C and a melting point ranging between 59 and 64°C [62]. PCL is a biodegradable, biocompatible and

http://etd.uwc.ac.za/

water insoluble synthetic polymer. PCL is soluble in chloroform, dichloromethane, carbon tetrachloride, benzene, toluene, cyclohexanone and 2-nitropropane at room temperature. It is suitable for use in controlled drug delivery systems due to a high compatibility with many drugs and at the same time having a relatively low toxicity. It has the ability to form compatible blends with other polymers such as cellulose propionate, cellulose acetate butyrate, PLA and PLGA [61]. PCL is degraded by hydrolysis of its ester linkages under physiological conditions (such as in the human body) and has therefore received a great deal of attention for use in drug delivery [49]. Figure 2.4 shows the chemical structure of PCL.

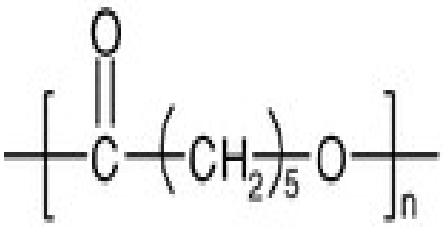

Figure 2.4 *The chemical structure of PCL* [63].

UNIVERSITY of the
WESTERN CAPE

Biodegradation of PCL is very slow in comparison to other polymers, therefore the polymer is also suited for long-term drug delivery of up to a year and beyond [64]. Drug release rates from PCL depends on the type of formulation; if it is nanospheres or nanocapsules, method of NP preparation, PCL content, NP size and percent of drug loaded in the NPs. Various drugs such as insulin, indomethacin and propranolol HCl have been encapsulated within PCL NPs using the w/o/w emulsion method (explained in section 2.9.2) [61]. Table 2.2 below summarises various drugs which have been encapsulated within PCL NPs.

http://etd.uwc.ac.za/

Table 2.2 *Tabular summary of selected studies formulating PCL NPs for drug delivery.*

Drug	Therapeutic target	PCL NP average size (nm)	Reference
Tamoxifen	Preferential tumour targeting and circulating drug reservoir	210.3 ± 24.8	[65]
Propranolol	Applying double emulsion technique to encapsulate low molecular weight and hydrophilic drug	250 ± 17.8	[4]
Clonazepam	Drug release behaviour can be modulated by introducing thermo sensitive polymers	45-210	[66]
Saquinavir	Higher intracellular saquinavir concentrations	271 ± 1.6	[67]
Taxol	Higher taxol loading	≤ 100	[68]
Insulin	Preservation of insulin's biological activity	358 ± 12	[69]
Docetaxel	Higher antitumor effect	87.5 ± 9.5	[70]
Indomethacin	Study the release behaviour and cytotoxicity	≤ 200	[71]
Vinblastine	Slow drug release up to 20 days	213 -227 ± 2	[72]

UNIVERSITY of the WESTERN CAPE

http://etd.uwc.ac.za/

2.6 Nanomedicine and treatment of CVDs

Nanomedicine offers an opportunity to improve the effectiveness of drugs used for the treatment of CVDs. Various types of NPs are currently being investigated for CVD treatment. The first study in this field was conducted by Labhasetwar and his group [73]. In 1997, the authors investigated the potency of a polymeric NP 2-aminochromone loaded as a model anti-proliferative agent in the treatment of restenosis by using an *ex-vivo* arterial model. They synthesised PLGA NPs and modified their surfaces using a cationic agent, didodecyldimethylammonium bromide. The *ex-vivo* model study demonstrated that the arterial uptake of surface coated NPs was 10-fold higher than that of the non-coated NPs [7].

The application of NPs in the treatment of hypertension continues to expand. PNPs were shown to prolong release of valsartan, thereby potentially decreasing therapeutic dose, frequency of dosing, and side effects [74]. The therapeutic use of isradipine, an antihypertensive agent, is hampered due to its rapid and intense vasodilator effect. However, isradipine in its NP form had shown initial slow release and a prolonged antihypertensive's effect, when given orally [75]. One of the widely used anti-hypertensives, nebivolol, presents with the problem of poor solubility and bioavailability and thus frequent dosing. Jana *et.al*, 2014 studied Eudragit RS 100® NPs encapsulating nebivolol. The *in-vitro* drug release data showed prolonged drug release with low initial burst release [76]. A study of nifedipine PNPs to investigate changes in the pharmacokinetic and pharmacodynamic properties of nifedipine following encapsulation showed that the NP nifedipine preparations represented sustained release forms with increased bioavailability, a less pronounced initial antihypertensive effect and a long-lasting action. This study also showed the potential to increase patient compliance through decreasing in frequency of administration [77][78]. Table 2.3 is a summary of other studies which have demonstrated the potential of NPs to increase bioavailability, and reduce

http://etd.uwc.ac.za/

the dose, and frequency of dosing of anti-hypertensive drugs. However, to the best of our knowledge, there are no *in-vivo* studies on propranolol delivery using PNPs.

Table 2.3 *NP-mediated drug delivery system for hypertension treatment* [79]**.**

Antihypertensive drug	**NP system**	**Animal model**	**Main therapeutic result**	**Reference**
Pitavastatin	PLGA	MCT-induced rat model	Pitavastatin-NP was more effective than pitavastatin alone in inhibiting cellular proliferation and inflammation *in-vitro*	[80]
NF-kB decoy	PEG-PLGA	MCT-induced rat model	The NP-mediated NF-B decoy delivery into lungs prevented monocrotaline-induced NF-kB activation, and attenuated inflammation and proliferation	[81]
Imatinib	PLGA	MCT-induced rat model	Suppressed the development of pulmonary hypertension and significantly inhibited proliferation after 24 hours of treatment	[82]
Beraprost	PLA and PEG-PLA	MCT-induced rat model	Sustained drug release and tissue targeting profiles	[83]

UNIVERSITY of the WESTERN CAPE
http://etd.uwc.ac.za/

Beraprost	PLGA	Sugen/hypoxia rat model	Beraprost NPs significantly improved the survival rate in the monocrotaline rat model. No infiltration of inflammatory cells, hemorrhage, or fibrosis was found in the liver, kidney	[84]
AntimiRNA-145	Liposome	Sugen/hypoxia rat model	Effective and low toxicity drug delivery	[85]

NF-kB, nuclear factor kappa B; MCT, monocrotaline rat model

UNIVERSITY of the
WESTERN CAPE

2.7 Emulsions

Emulsions are dispersions of one liquid phase in another immiscible liquid phase. They are made using a mechanical shear. Due to differences in attractive interactions between the molecules of the two liquid phases, an interfacial tension, σ, exists between the two liquids. The interfacial tension can be reduced significantly by adding amphiphilic surface-active molecules, or surfactants, that are highly soluble in at least one of the liquid phases [86][87][88].

Generally, emulsions are classified based on which liquid forms the continuous phase as shown in Figures 2.5 and 2.6:

- Water-in-oil (W/O) emulsions consisting of water droplets dispersed in oil.

- Oil-in-water (O/W) emulsions consisting of oil droplets dispersed in water.

http://etd.uwc.ac.za/

- Complex emulsions; for example, water-oil-water (W/O/W), consisting of water droplets dispersed in oil droplets that are in turn dispersed in water [88].

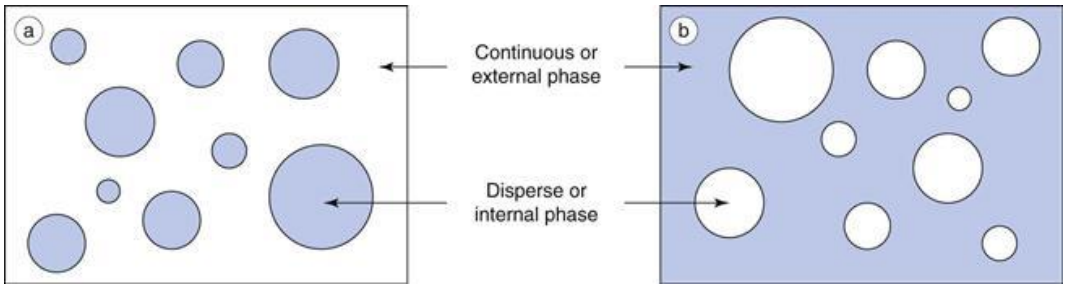

Figure 2.5 *Schematic representations of (a) an oil-in-water emulsion and (b) a water-in-oil emulsion. The shaded area represents the oil* [89].

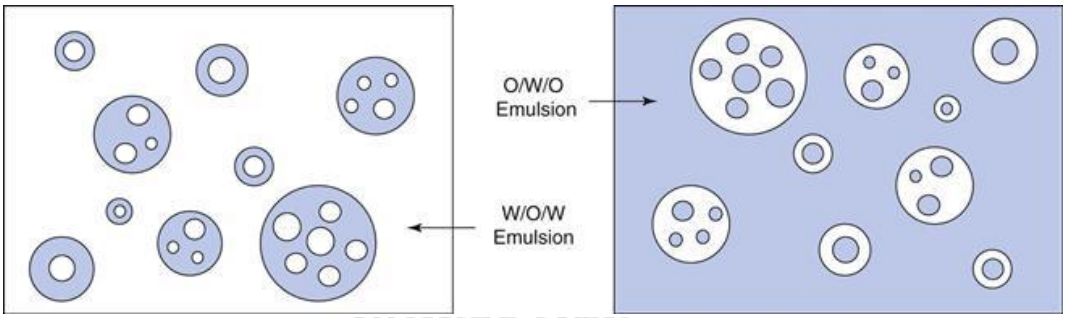

UNIVERSITY of the
WESTERN CAPE

Figure 2.6 *Schematic representations of a multiple w/o/w emulsion and o/w/o emulsion. The shaded area represents the oil* [89].

The upper liquid phase (e.g. hydrocarbon oil), has a mass density that is less than that of the lower liquid phase (e.g. water) (Figure 2.7). In the absence of a surfactant or other impurities, the system will return to this lowest energy configuration at thermodynamic equilibrium. To ensure that a stable emulsion persists over weeks or years, it is necessary to add a surfactant, which is usually soluble in the continuous liquid phase, but not highly soluble in the dispersed phase. Surfactants are chemical compounds which preferentially adsorb at interfaces, and as part of their structure, they possess non-polar hydrocarbon tails and polar or charged head groups. A system of classification of the tendency of surfactants to disperse in

http://etd.uwc.ac.za/

polar or non-polar liquids is referred to as the hydrophile–lipophile balance (HLB) [90]. HLB values range from 0 to 20 on an arbitrary scale. The lower the HLB, the more lipophilic the compound and vice versa [90]. A numerical HLB scheme exists for classifying surfactants in terms of their relative solubility in aqueous and oily liquid phases. The HLB of an emulsifier is an expression of the amounts of hydrophilic and lipophilic groups in the compound. An emulsifier that is lipophilic in character is assigned a low HLB number (below 9.0), and one that is hydrophilic is assigned a high HLB number (above 11.0). Those in the range of 9-11 are intermediate. The functions of emulsifiers might well be classified by HLB, emulsifiers with HLB values in the range (4-6) are W/O emulsifiers and those in the range of 8-18 are used as O/W emulsifiers [91][92].

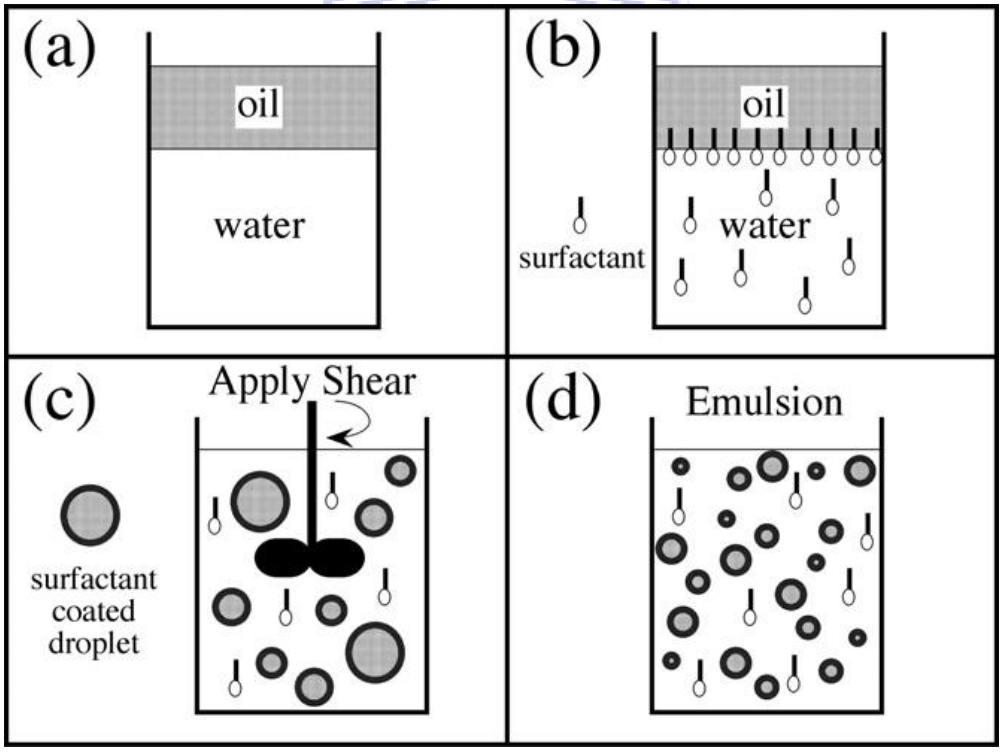

Figure 2.7 *Mechanism of stabilization of two emulsion phases by a surfactant [87],(a) Two immiscible liquids, such as oil and water, will phase separate into a layer of the less dense liquid on top of a layer of the more dense liquid below with a flat interface to minimize the interfacial and gravitational energies. (b) A surfactant, generally soluble in the continuous*

http://etd.uwc.ac.za/

phase, preferentially adsorbs on the oil–water interface and exchanges with monomers and micelles in solution. In this example, the surfactant is soluble in the water phase, so a direct emulsion is anticipated. (c) Shear is applied to the system, causing the oil to break up into droplets that are coated with surfactant and are inhibited from coalescing due to the interfacial repulsion. As the emulsion is sheared, larger oil droplets are stretched, undergo a capillary instability, and rupture into smaller droplets. (d) After the shear has been stopped, the emulsion can persist for many years, and a fraction of the shear energy applied is stored in the greater surface area of the droplets.

2.7.1 Surfactants used in the stabilization of NP drug delivery systems

Surfactants can be categorised in several ways. The most accepted classification is based on the ionic character of the head, with subgroups based on the nature of the tail. The four basic groups of surfactants are defined as follows:

Anionic surfactants: The polar head group of anionic surfactants carries a negative charge. These surfactants are used in the majority of industrial applications, including pharmaceutical formulations (sulfosuccinates), soaps (carboxylates), and detergents (alkylbenzene sulfonates). An important, widely used surfactant belonging to this category is sodium dodecyl sulfate (SDS) [93].

Cationic surfactants: This category includes surfactants, which have a positively charged, mostly amine–containing head group. They are also known to be less biodegradable and more toxic than other groups of surfactants. As a consequence, they are used mainly in two cases, i.e., as antiseptic agents against bacteria and fungi [93][94].

Zwitterionic surfactants: These contain both positively (e.g., amine groups) and negatively charged (e.g., carboxyl) head groups, such that the net charge is equal to zero. Examples are betaines, sulfobetaines and substances of biological origin, such as amino acids and

http://etd.uwc.ac.za/

phospholipids. Because of the low potential for irritation and their biocompatibility, zwitterionic surfactants are widely used as emulsifiers for food, dermatological products and in many pharmaceutical applications [93].

Nonionic surfactants: The head group of nonionic surfactants is not charged. They derive water solubility from the presence of highly hydrophilic polar groups, such as polyethylene oxide, fatty acid ethoxylates, sorbitan ester ethoxylates or sugars. As they are more biocompatible than ionic surfactants, their most widespread use is in pharmaceutical applications. Examples of surfactants used in cosmetics and drug delivery formulations are sorbitan esters and their ethoxylated derivatives (Spans, Tweens) [93][94].

2.8 Emulsion Stability Mechanisms

Adsorbed surfactants stabilise emulsions via two main mechanisms: steric stabilisation and electrostatic stabilisation. Steric stabilisation arises from a physical barrier to contact and coalescence. For instance, high-molecular-weight polymers can adsorb on the surface of dispersed phase droplets and extend significantly into the continuous phase, providing a physical barrier for particle contact. As polymer coated particles approach, the polymers are forced into close proximity and repulsive forces arise, keeping particles apart from each other [88]. Electrostatic stabilisation of emulsions is based on the mutual repulsive forces that are generated when electrically charged surfaces approach each other. In an electrostatically stabilised emulsion, an ionic or ionisable surfactant forms a charged layer at the interface. [88]. In general, electrostatic stabilisation is significant only for oil-in-water emulsions since the electric double-layer thickness is much greater in water than in oil. Stable w/o emulsions result from the encapsulating effect of rigid films formed on the water droplets by solid particles or high molecular weight molecules. Both electrostatic and steric forces can prevent aggregation or coalescence and hence stabilise emulsions [95][96].

http://etd.uwc.ac.za/

Prior to emulsification, an emulsifier is added to a continuous phase or organic solution. Common examples of surfactants are polyvinyl alcohol (PVA), polyvinyl pyrrolidone, solutol, polysorbate, poloxamer, carbopol, polyethylene glycol (PEG), SDS, proteins, carbohydrates, lecithin, and PEG-lipids (e.g., PEG-ceramide, *d*-α-tocopheryl polyethylene glycol 1000 succinate (TPGS). It is important to note that the type and concentration of surfactant affect the NP quality, drug encapsulation efficiency, drug release, pharmacokinetics, and cellular uptake/interaction. Therefore, a surfactant should be selected in consideration of the intended functionality and quality of NPs [97].

2.8.1 Polyvinyl alcohol (PVA)

PVA (Figure 2.8) is the most commonly used emulsifier in the formulation of PCL and PLGA polymeric NPs. A fraction of PVA remains associated with the NPs despite repeated washing as PVA forms an interconnected network with the polymer at the interface [98]. PVA is a biodegradable polymer, and its degradability is enhanced through hydrolysis because of the presence of hydroxyl groups on the carbon atoms as shown in Figure 2.8. Moreover, it is water-soluble and has a hydrophilic nature [99]. PVA is partially crystalline upon formation, and is characterised by properties such as chemical resistance, water solubility, and biodegradability. The similarity in physical properties makes it compatible with human tissues. PVA has been widely developed for biomedical applications due to its biocompatible property and has a structure that can absorb protein molecules, and has no toxic effects [99].

UNIVERSITY of the
WESTERN CAPE

http://etd.uwc.ac.za/

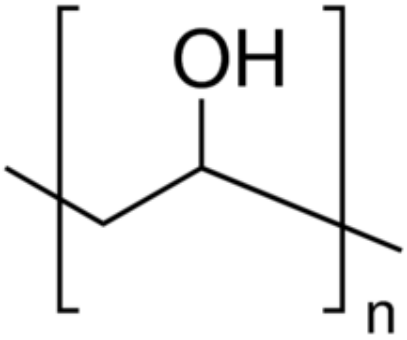

Figure 2.8 *Structural formula of PVA* [99].

2.8.2 D-α-tocopheryl polyethylene glycol succinate

D-α-tocopheryl polyethylene glycol succinate (Vitamin E TPGS or simply TPGS) is a water-soluble derivative of natural Vitamin E, which is designed by esterification of Vitamin E succinate with PEG. Figure 2.9 shows the chemical structure of TPGS. Intrinsically, TPGS possesses the advantages of PEG and Vitamin E in the application of many drug delivery devices, owing to its ability to extend the half-life of the drug in plasma and enhance the cellular uptake of the drug. Typically, TPGS has the amphiphilic structure of a lipophilic alkyl tail and a hydrophilic polar head and has an HLB value of 13.2 [100][101]. The United States-Food and drug administration (FDA) has approved TPGS as a safe pharmaceutical adjuvant used in drug formulation. TPGS has been used as an absorption enhancer, emulsifier, solublizer, additive, permeation enhancer and stabiliser [102][103]. During the past decade, Feng's group has been dedicated to the study of the various uses of TPGS in nanomedicine, including TPGS-based prodrugs, micelles, liposomes, TPGS-emulsified PLGA NPs and NPs of TPGS-based copolymers, which can significantly enhance the solubility, permeability and stability of the formulated drug and realise sustained, controlled and targeted drug delivery [104]. TPGS has proved to be an efficient emulsifier for synthesis of NPs of biodegradable polymers, resulting in high drug encapsulation efficiency, high

http://etd.uwc.ac.za/

cellular uptake *in-vitro* and high therapeutic effects *in-vivo* [104]. For example, TPGS may have more than 77 times higher emulsification efficiency compared with the traditional emulsifier, PVA [104][100]. TPGS was also used as a surfactant to emulsify PLGA, PCL, PLA-TPGS, and PLGA-PEG and NPs. TPGS as a surfactant can be as low as 0.15%-0.06% in concentration [105][100].

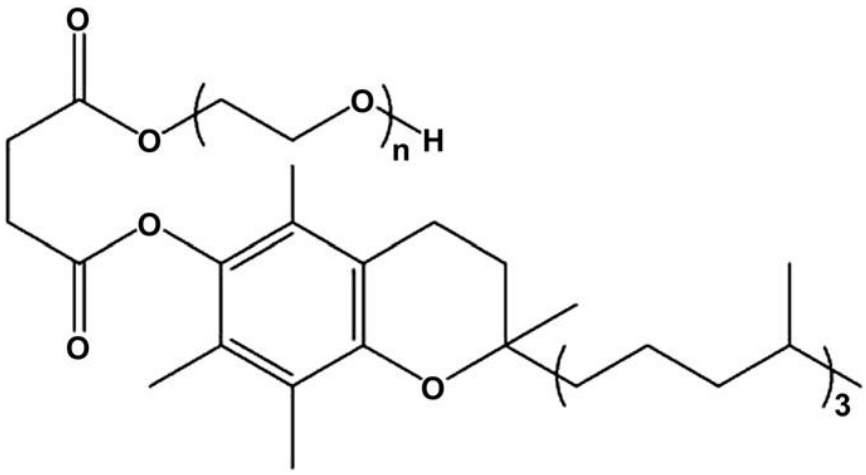

UNIVERSITY of the
WESTERN CAPE

Figure 2.9 *Chemical structure of TPGS* [100].

2.8.3 Span 80

Span 80, also known as sorbitan monoleate, is a fatty acid ester of anhydrosorbitol. Span 80 is a good oil soluble emulsifying agent with HLB value of 4.3 (Figure 2.10). Span 80 has been used to stabilise emulsions [106]. In a study by Ahmed *et.al,* 2014 in an attempt to improve the physical stability of the formed NPs and prevent particle aggregation, Span 80 was added to the organic phase at a concentration of 0.25% w/v. Results showed that the addition of Span 80 to the organic phase improved the physical stability of the nanosuspensions, showing no visible aggregates upon storage for one week in the

http://etd.uwc.ac.za/

refrigerator. However, the mean particle size of the NP increased upon addition of Span 80 compared to particles prepared without the addition of Span 80 [107].

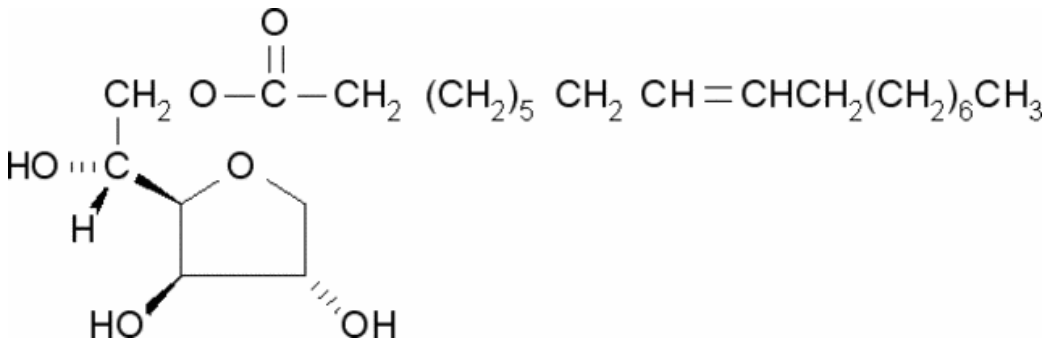

Figure 2.10 *Chemical structure of Span 80* [107].

UNIVERSITY of the
WESTERN CAPE

2.9 Methods for the formulation of polymeric NPs

Several methods have been developed for preparing PNPs, i.e. the emulsification-solvent evaporation method, solvent displacement method, salting-out method, emulsification-solvent diffusion method and the double emulsion solvent evaporation method [108][109]. The selection of an appropriate method for the preparation of NPs depends on the physicochemical character of the polymer and the drug to be loaded [110].

2.9.1 The emulsion-solvent evaporation method (EEM)

This method is one of the most commonly used methods for the preparation of NPs, because it is relatively simple and allows efficient encapsulation of several types of compounds [110]. The method is based on two steps as shown in Figure 2.11. Briefly the first step requires emulsification of the polymer solution which is formed from polymer dissolved in a solvent into an aqueous phase which usually contains a stabiliser. In the second step, the organic solvent is evaporated by increasing the temperature under reduced pressure or by continuous

http://etd.uwc.ac.za/

stirring; this leads to the precipitation of the polymer as NPs of a few hundred nanometres in diameter. The NPs are collected by ultracentrifugation and washed with distilled water to remove stabiliser residue or any non-encapsulated drug and lyophilised for storage [111] [108]. The NP size can be controlled by adjusting the stirring rate, type and amount of surfactant, viscosity of organic and aqueous phases and temperature [108][110]. Polymers that have been used in this method include PLA, PLGA, ethyl cellulose (EC), cellulose acetate phthalate and PCL [110]. This method is used to encapsulate primarily water-insoluble drugs and hydrophobic molecules, since the drug is dissolved in an organic phase in which the polymer is also dissolved [2][49] such that as NP formation proceeds, the interfaces formed during emulsification and evaporation of the organic solvent involve stages like adsorption and polymer aggregation that enable entrapment of a larger amount of the drug into the nanostructure [112].

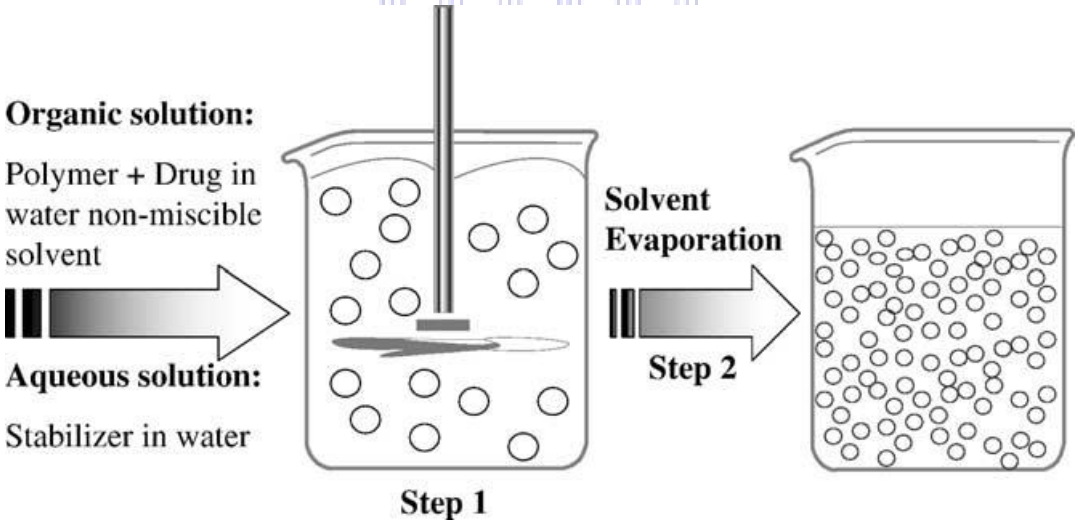

Figure 2.11 *Schematic representation of the EEM* [108].

2.9.1.1 The mechanism of formation of PNPs by EEM

The mechanism of formation of polymer NP by EEM has been studied by Desgouilles and co-workers in 2003 [111] and has been discussed by Vauthier and [110] Ponchel, 2016 [112].

http://etd.uwc.ac.za/

Desgouilles *et al*. expected that the number of the NPs that are formed after the evaporation of the solvent depended on the mechanism that governed the transition from the emulsion droplet state to the NP state. This mechanism is actually unknown, but two hypotheses could be proposed: In the first hypothesis, each emulsion droplet produces one NP. The emulsion droplets, which are stabilised by surfactants, are perfectly stable during the solvent evaporation stage; thus, the formation of a NP resulted from single volume shrinkage of the initial emulsion droplet [111]. On the contrary, in the second hypothesis, emulsion droplets could fuse together during the solvent evaporation step to form one NP from two or more emulsion droplets [111]. Desgouilles *et.al in* 2003 study was mainly based on the measure of the variation of the emulsion and NP surface charge and size during the solvent evaporation process. Two different models were proposed for NP formation with two polymer types (ethyl cellulose (EC) and PLA) (Figure 2.12). In the EC model, after shrinkage of the emulsion droplets as the direct consequence of solvent evaporation, coalescence occurred before stable and solvent-free NPs were obtained (Figure 2.12 A). On the contrary, in the PLA model, only limited or no aggregation and coalescence occurred so that one PLA NP was created from one or only a few of the PLA emulsion droplets (Figure 2.12 B). The data obtained show the importance of the polymer/solvent pair in the final NP architecture and mechanism of formation [111][112].

UNIVERSITY of the
WESTERN CAPE

http://etd.uwc.ac.za/

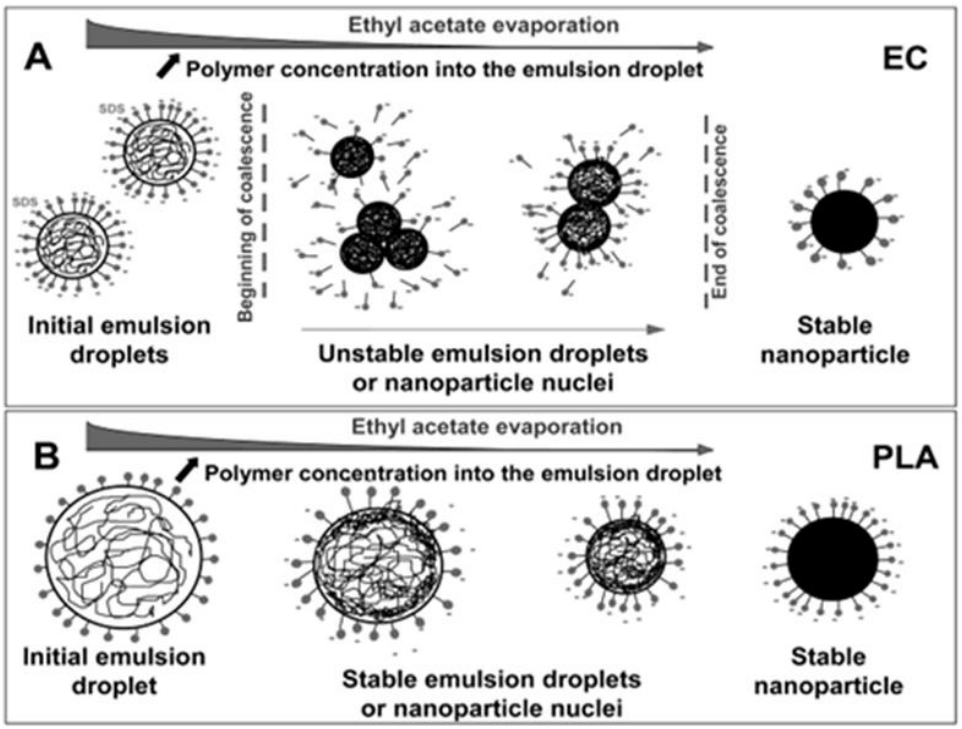

Figure 2.12 *Description of the possible mechanisms of formation of the NPs by emulsion solvent evaporation EEM using solutions (A) of EC in ethyl acetate and (B) of PLA in ethyl acetate* [111].

UNIVERSITY of the
WESTERN CAPE

2.9.2 The double emulsion and solvent evaporation method

Numerous groups have described the double emulsion ($W_1/O/W_2$) method in the manufacture of NPs that could successfully encapsulate water-soluble drugs. This method is known as the double, or multiple, emulsion-solvent evaporation method, (Figure 2.13), and is now the protocol that is best suited for encapsulating hydrophilic drug compounds in NPs [115]. However, when the aim is to incorporate hydrophilic drugs like peptides, proteins, and vaccines into polymeric NPs, low encapsulation efficiencies are reported with the utilisation of the single emulsion method [113][112]. The double emulsion-solvent evaporation method is a modification of EEM which adds a third step. Briefly, the first step involves an aqueous phase of deionised water (W_1) in which a fixed amount of hydrophilic drug is dissolved. After that, the drug solution is added to a unique organic phase (O) that consists of a polymer

http://etd.uwc.ac.za/

solution in an appropriate organic solvent, or combination of solvents. Once the W_1 and O phases are mixed, a second stage begins in which the two phases are subjected to vigorous stirring until a primary water-in-oil emulsion is achieved. Commonly, nanosized polymer droplets are induced by sonication or homogenisation [117]. In the third step, the primary water-in-oil emulsion is poured into a second aqueous phase (W_2), prepared as a solution that contains a stabiliser such as PVA or poloxamer. This second emulsion is further emulsified under smoother mixing and stirring conditions for a short time. In the fourth step, the organic solvent is evaporated under the same conditions as in the single-emulsion technique (i.e., continuous magnetic stirring at room temperature or under reduced pressure). Finally, the NPs are usually recovered by centrifugation, washed with distilled water to eliminate or remove additives such as surfactants, and then lyophilised in the presence of cryoprotectants [112][114]. Drugs can be restrained on the PNP surface after a polymerisation reaction or can be encapsulated on the PNP structure during a polymerisation step.

UNIVERSITY of the
WESTERN CAPE

The main problem with trying to encapsulate hydrophilic drugs is the fast diffusion of the molecule into the outer aqueous phase during emulsification, which leads to poor drug loading and low encapsulation efficiency [114][2]. Thus, to avoid drug diffusion into the organic phase and improve encapsulation efficiency, the immediate deposit of a polymer membrane during the first water-in-oil emulsion is critically important. Song *et.al*, 1997. were able to accomplish this by dissolving a high concentration of a high molecular weight PLGA polymer into the oil phase of an 80:20% dichloromethane/acetone solution [114]. Additionally, by increasing the concentration of the stabiliser in the inner aqueous phase to increase viscosity of the primary emulsion resulting in decreasing drug diffusion into the organic phase [115].

http://etd.uwc.ac.za/

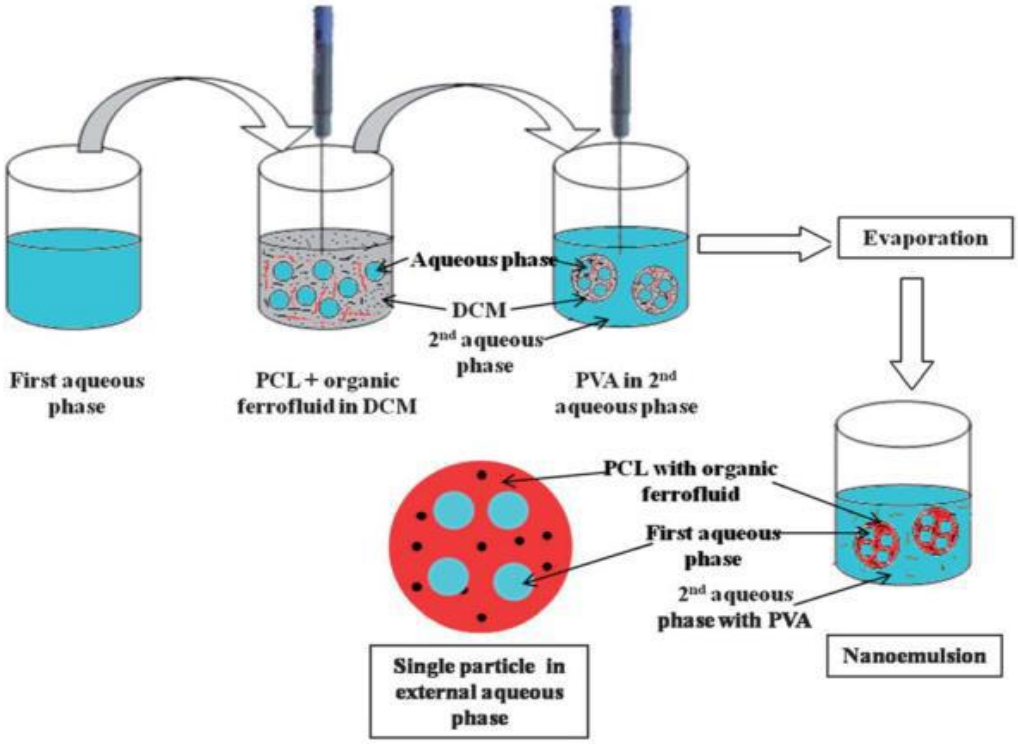

Figure 2.13 *A typical process of double emulsion formation* [116].

UNIVERSITY of the
WESTERN CAPE

2.9.3 The emulsion solvent diffusion method

This is another widely used method to prepare NPs [117]. The process is shown in Figure 2.14 and involves the formation of an o/w emulsion in a partially water-soluble solvent (such as propylene carbonate or benzyl alcohol), which contains the polymer, and an aqueous phase containing a stabiliser such as PVA [108]. The subsequent addition of water to the system causes the diffusion of the solvent into the external phase, leading to the formation of nanospheres or nanocapsules. Finally, the solvent is eliminated by evaporation or filtration [117][108]. Generally, this technique is assumed as a supplementary method to prepare hydrophobic drug-loaded NPs and offers several advantages, such as high encapsulation efficiencies, no requirement for homogenisation, and ease of scale up. Disadvantages include the high volume of water to be eliminated from the suspension and the potential leakage of

http://etd.uwc.ac.za/

water-soluble drugs into the saturated-aqueous external phase during emulsification, thereby reducing encapsulation efficiency [118][116].

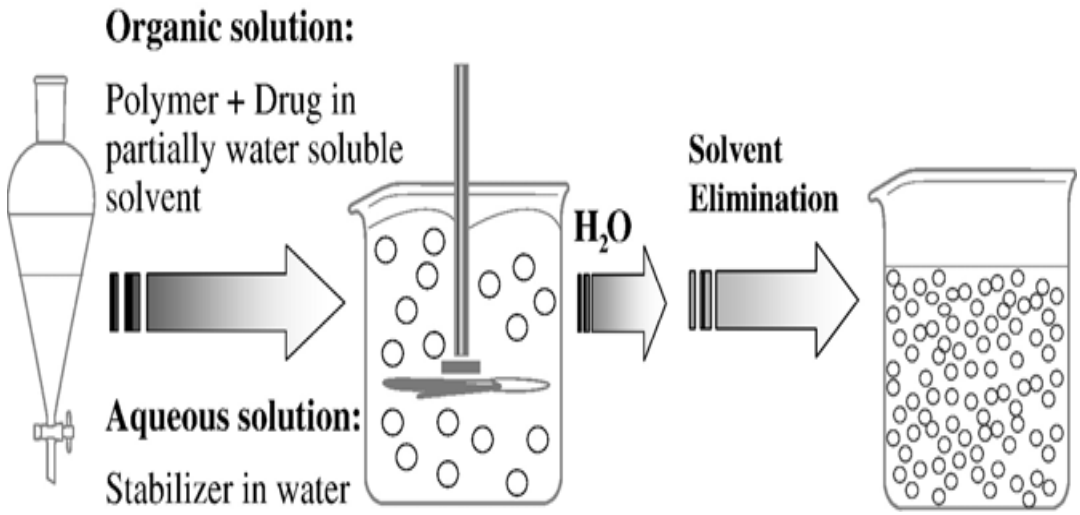

Figure 2.14 *Schematic representation of the emulsion-solvent diffusion method* [108].

2.9.4 The solvent displacement / nanoprecipitation method

Nanoprecipitation, also called the solvent displacement method, is one of the commonly used methods for the synthesis of hydrophobic drug-loaded PNPs, which was firstly developed by Fessi *et.al*. in the late 1980s [60][116]. It is based on spontaneous emulsification of the organic internal phase containing the dissolved polymer and drug into the aqueous external phase (Figure 2.15). The procedure involves the drop-wise addition of a solution of polymer in a water-miscible organic solvent such as acetone or methanol to an aqueous solution. Due to the spontaneous diffusion of the water-soluble solvent (acetone or methanol), an interfacial turbulence is created between two different liquid phases leading to the formation of NPs [119][116]. The nanoprecipitation method is well suited for lipophilic drugs because of the miscibility of the solvent with the aqueous phase, however, it is not an efficient means of encapsulating water-soluble drugs [108]. In addition, traditional nanoprecipitation is still

http://etd.uwc.ac.za/

currently limited inside laboratories due to its drop-wise operation, and the difficulties of extraction, of NPs [116].

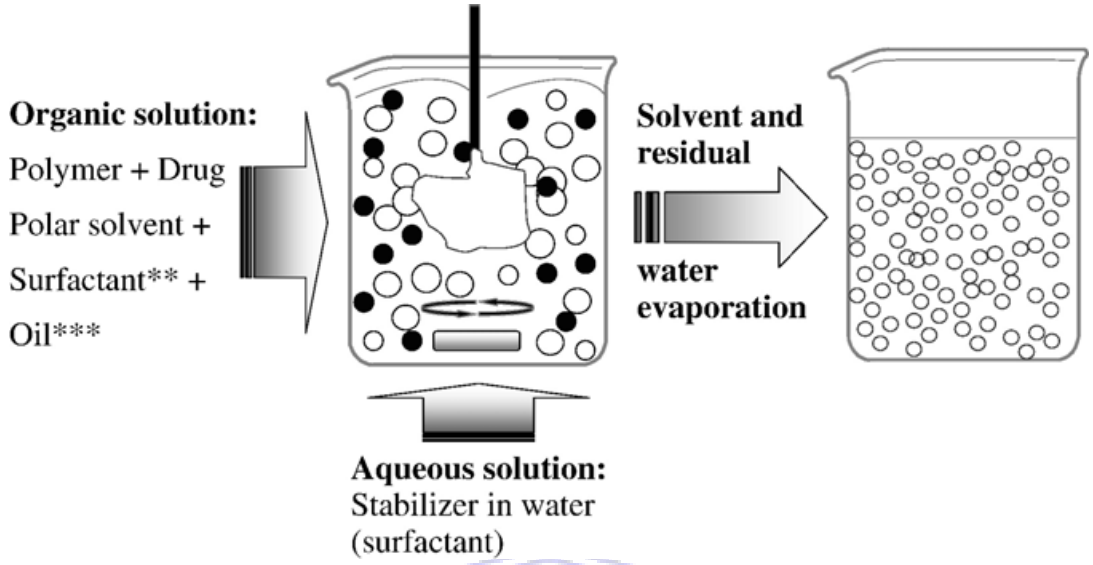

Figure 2.15 *Schematic representation of the solvent displacement technique* [108]

UNIVERSITY of the
WESTERN CAPE

2.9.5 The salting out method

Salting out is based on the separation of a water-miscible solvent from an aqueous solution [108][120]. To prepare NPs by the salting out method as shown in Figure 2.16, the polymer and drug are initially dissolved in an organic solvent which is subsequently emulsified into an aqueous gel containing the salting out agent (i.e. electrolytes, such as magnesium chloride and calcium chloride, or non-electrolytes such as sucrose) [116] and a colloidal stabiliser such as polyvinylpyrrolidone or hydroxyethylcellulose [108]. The salting out agent is present at a high concentration to prevent the diffusion of organic solvent into water. This o/w emulsion is diluted with a sufficient volume of water to enhance the diffusion of solvent into the aqueous phase, thus inducing the formation of NPs (Figure 2.16). Salting out does not require an increase of temperature and therefore may be useful when heat sensitive compounds are to be encapsulated. The main disadvantage of this method is its exclusive

http://etd.uwc.ac.za/

application to lipophilic compounds and the extensive NP washing steps to remove the salts that are involved which may lead to NP loss and the leaching out of the drug [121].

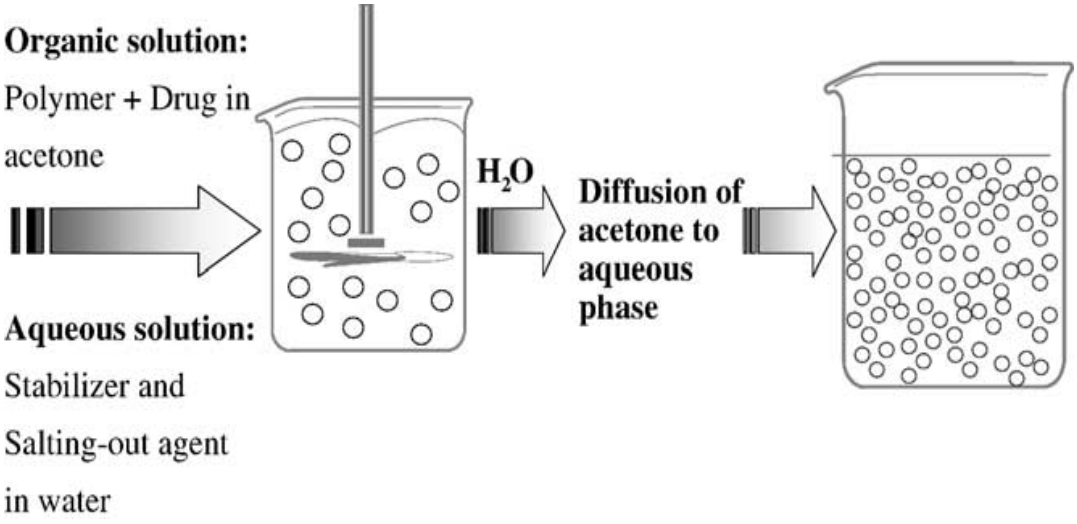

Figure 2.16 *Schematic representation of the salting out method, the polymer and drug solution is added to a surfactant solution containing a high concentration of salts then diluted with water to produce NPs* [108].

UNIVERSITY of the
WESTERN CAPE

2.10 Characterization of nanoparticles

NPs are generally characterised to determine their size, shape and zeta potential. For determining particle size and shape, advanced microscopic techniques such as scanning electron microscopy (SEM), transmission electron microscopy (TEM) and atomic force microscopy (AFM) are used. The average particle diameter, size distribution and charge influence the physical stability as well as the *in-vivo* distribution of the NPs and are therefore important properties to measure.

2.10.1 Determination of average particle size

Currently, the fastest and most reliable method of determining NP size is by use of photon-correlation spectroscopy (PCS) also referred to as dynamic light scattering (DLS) (Figure

http://etd.uwc.ac.za/

2.17). Using DLS, particle size is determined based on shining a monochromatic light (laser) onto a suspension of particles undergoing Brownian motion which causes a Doppler shift of incident laser light. When the light hits the moving particle a causes change in the wavelength of the incoming light. This change in the wavelength is related to the size of the particle [122]. It is possible to extract the size distribution and give a description of the particle's motion in the medium, measuring the diffusion coefficient of the particle and using the autocorrelation function [123].

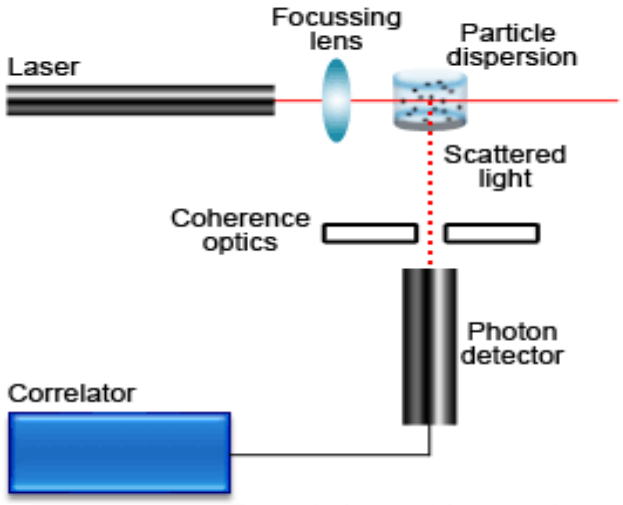

Figure 2.17 *Schematic of a dynamic light scattering instrument* [118].

2.10.2 Determination of particle shape and surface morphology

2.10.2.1 Scanning electron microscopy (SEM)

SEM is often used to study the surface morphology and shape characteristics of NPs [124]. The technique offers several advantages in morphological and sizing analysis; however, it provides limited information about the size distribution and true population average [123]. For SEM characterisation, the suspension of NPs is mounted on a sample holder then dried

http://etd.uwc.ac.za/

completely, followed by a coating with a conductive metal, such as gold, using a sputter coater. The sample is then scanned with a focused fine beam of electrons. An electron beam is generated by an electron gun and passes through the electromagnetic lenses of a column and across the surface of a sample. Electrons interact with atoms on the surface of the sample, producing various signals that can be detected to create an image, providing information about the sample size topography and composition [110] [123].

2.10.2.2 Transmission electron microscope (TEM)

TEM is a high spatial resolution structural and chemical characterization tool [124]. The sample preparation for TEM is complex and time consuming because of its requirement to be ultra-thin for electron transmittance. The NP dispersion is deposited onto support grids or films. To make NPs withstand the instrument vacuum and facilitate handling, they are fixed using either a negative staining material, such as phosphotungstic acid or derivatives, uranyl acetate, etc. The surface characteristics of the sample are obtained when a beam of electrons is transmitted through an ultra-thin sample, interacting with the sample as it passes through [124].

UNIVERSITY of the
WESTERN CAPE

2.10.3 Measurement of particle zeta potential (ZP)

Particles in aqueous media carry an electric charge; the development of this charge at the particle surface affects the distribution of ions around it and results in an increase in the concentration of counter ions [125]. The area over which this layer extends is referred to as the electrical double layer covering the particle surface. This layer has two separate parts: an inner region commonly called the stern layer (strongly bound ions) and an outer (diffuse) region (loosely associated ions). As particles move in solution due to an applied voltage or Brownian motion, the ions move with it as well. A boundary exists at some distance from the

http://etd.uwc.ac.za/

particle in which ions do not move and this is referred to as the slipping plane The potential that exists at the slipping plane is called the ZP (Figure 2.18) [126][125].

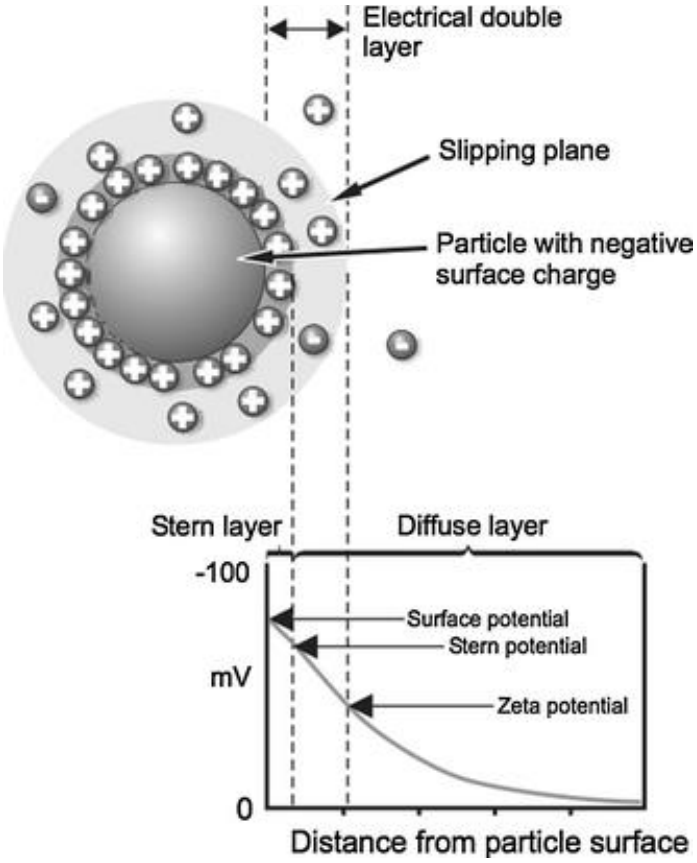

Figure 2.18 *Schematic showing the electrical double layer that surrounds a particle in an aqueous medium and the position of the slipping plane. The ZP is the electrical potential at the slipping plane* [125]

NP stability is usually assessed through measurement of the ZP of NPs. High ZP values, either positive or negative, should be achieved in order to ensure stability and avoid aggregation of the particles [110][123]. The ZP of NPs is measured by using PCS; a voltage is applied across a pair of electrodes at either end of a cell containing the particle dispersion. Charged particles are attracted to the oppositely charged electrode. The particles move in an

http://etd.uwc.ac.za/

electrical field of known strength in the interference pattern of two laser beams and produce scattered light which depends on the speed of the particles; from this the ZP can be recorded [127]. NPs with a ZP above ± 30 mV have been shown to be stable in suspension, as the surface charge prevents aggregation of the particles. The ZP also can be used to determine whether a charged active material is encapsulated within the centre of the NP or on the surface [39].

2.11 Determination of the kinetics of drug release from NPs

One of the central applications of PNPs is the sustained and controlled delivery of drugs. Several factors, such as solubility of drug, desorption, drug diffusion, particle matrix degradation or erosion, can affect drug release [118][34].

The commonly used methods for drug release assessment can be classified under four categories, including membrane diffusion techniques, sample and separate methods, continuous flow techniques and *in situ* techniques. Table 2.4 summarises the main advantages and limitations of each method [34][110].

UNIVERSITY of the
WESTERN CAPE

http://etd.uwc.ac.za/

Table 2.4 *The major potential and limitations of commonly used methods for drug release assessment* [34]

Technique	Examples	Advantages	Limitations
Membrane diffusion techniques	Dynamic dialysis • Reverse dialysis • Modified United States pharmacopeia (USP) dissolution apparatus I • Side-by-side dialysis	•Are easy to conduct •Provide in-process isolation of free drug from NPs • Offer possibility of changing the bulk medium • Are cost effective	Drug release is governed by diffusion through two barriers • Drug diffusion to donor compartment is often governed by partitioning phenomenon • Size and charge of membrane impacts the extent and rate of drug diffusion • Investigation of drug membrane binding affinity is required
Sample and separate techniques	Isolation of the drug molecules through: • Filtration • Ultrafiltration • Centrifugation or ultracentrifugation	Enable direct investigation of the *in-vitro* release • Are easy to conduct	Additional separation steps are required • Incomplete particle isolation is possible • Premature drug release can occur • Change of bulk medium is not possible • A small amount of nanocarriers is removed after each sampling (inappropriate for small volumes)
In situ	Direct measurement of free drug	Enable direct measurement	Are only applicable for a narrow range of drug cargos

http://etd.uwc.ac.za/

methods	concentration through • Polarography • Spectroscopy	of the free drug within the medium • Require no additional separation steps	
Continuous flow techniques	USP apparatus IV or its modifications	Enable direct investigation of the *in-vitro* release • Require no additional separation steps • Are easy to conduct with full-automated instruments	• Instrument is costly • Are difficult in setup • Filter clogging is possible • Build-up of high pressure can occur • Adsorption of the drug to the filter is possible • Keeping a constant flow rate is difficult • Drug release depends on the flow rate (type of the pump and the filter) • Require high rapidness in replacing release medium (in case of nonautomated instruments)

UNIVERSITY of the
WESTERN CAPE

http://etd.uwc.ac.za/

2.11.1 Drug release mechanisms

Drug release from carriers is influenced by several factors including the composition (drug, polymer, and additives), their ratio, physical and/or chemical interactions among the components, and the preparation methods. According to the mechanism by which a drug escapes a carrier, drug release can be classified into four categories (diffusion, solvent, chemical reaction, and stimuli controlled release) as briefly summarised in Figure 2.19 [128].

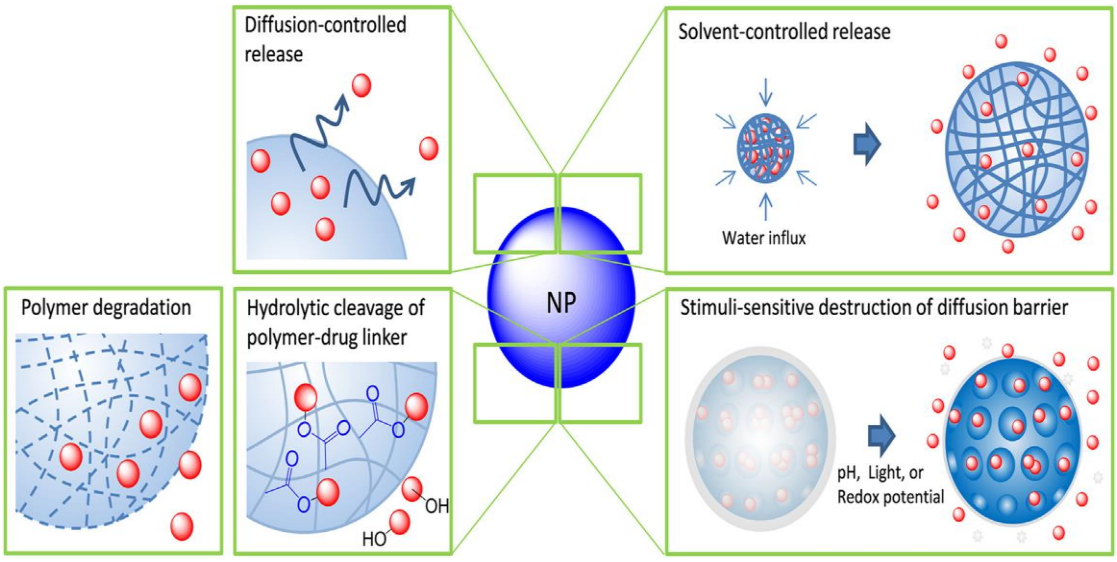

WESTERN CAPE

Figure 2.19 *Schematic of drug release mechanisms from NPs* [128]

In general, the drug release rate depends on: (1) drug solubility; (2) desorption of the surface-bound or adsorbed drug; (3) drug diffusion through the NP matrix; (4) NP matrix erosion or degradation; and (5) the combination of erosion and diffusion processes. Hence, solubility, diffusion, and biodegradation of the particle matrix, govern the release process [2].

In the case of nanospheres, where the drug is uniformly distributed, drug release occurs by diffusion or erosion of the matrix. If the diffusion of the drug is faster than matrix erosion, then the mechanism of release is largely controlled by a diffusion process. The rapid, initial

http://etd.uwc.ac.za/

release, or burst, is mainly attributed to a weakly bound or adsorbed drug to the relatively large surface of NPs [128].

2.11.2 Modelling drug release

The release of a drug product proceeds *via* a series of processes through which a drug is freed from its enclosing matrix, and dissolves to form a homogenous phase, in order to be subjected to the pharmacokinetic processes of absorption, distribution, metabolism and excretion. Advantage can be taken of drug release kinetics in order to produce a formulation with desired release characteristics, translating to optimum bioavailability and efficacy. Prediction of these desired release kinetics can be done by model-dependent methods of release profile analysis *via* mathematical modelling [129]. Thus, various phenomena – such as water diffusion into the polymer enclosing the drug, drug dissolution and diffusion or swelling, dissolution and degradation of the polymer – may be involved in drug release [130].

UNIVERSITY of the
WESTERN CAPE

Drug release kinetics involved in drug release can be described with suitable mathematical models to estimate drug release from a formulation as well as to elucidate mechanisms involved in drug release [131]. It is relevant to mention that there is no universally acceptable model for release of all drugs, and release data are usually fitted to various models in order to assess goodness of fit prior to selection of the best model [132]. When modelling drug release, some equations serve to describe the release profile while other equations can be used to predict the mechanism of drug release in addition to describing the release profile. Equations and models used to describe the release profile are referred to as empirical. Conversely, semi-empirical models describe the shape of the curve and also offer explanations for the underlying drug release mechanism. Examples of semi-empirical models of drug release employed in this study are the Weibull, and Korsmeyer-Peppas models [133].

http://etd.uwc.ac.za/

To describe the drug release rate from different drug delivery system, a large number of models were developed. Some of the important models are described herewith:

The zero order rate equation (Eq.1) describes NP systems where the drug release rate is independent of its concentration [134].

$$C = k_o t \qquad \text{(Eq.1)}$$

Where C is the concentration of the drug at time (*t*) and k_o is the zero-order release rate constant.

The first order (Eq.2) describes drug release from a system where the release rate is concentration dependent [134].

$$\text{Log}C = \log C_0 - kt / 2.303 \qquad \text{(Eq.2)}$$

UNIVERSITY of the
WESTERN CAPE

Where C is the amount of drug released in time 't', C_0 is the initial amount of the drug in the solution and k is the first order release constant.

Higuchi described the release of drugs from porous, insoluble matrices as a square root of a time dependent process based on Fickian diffusion as shown in Eq.3 [135].

$$Q = Kt^{1/2} \qquad \text{(Eq.3)}$$

Where Q is the amount of drug released in time 't' per unit area, K is the Higuchi dissolution constant.

The Hixson-Crowell cube root law (Eq.4) describes the release from systems where there is a change in surface area and diameter of particles [135].

http://etd.uwc.ac.za/

$$Q_0^{1/3} - Qt^{1/3} = KHC\ t \qquad \text{(Eq.4)}$$

Where Q_0 is the initial amount of drug in the dosage form, Q_t is the remaining amount of drug in the dosage form at time 't' and K_{HC} is a constant incorporating the surface volume relation.

The Korsmeyer-Peppas model is appropriate in situations where the release mechanism is not well understood, or where more than one mechanism is involved, such as a combination of active diffusions (Fickian transport) and Type II transport (non-Fickian, controlled by relaxation of the polymer chains). Korsmeyer-Peppas proposed the values of the release exponent (*n*) that characterised three different mechanisms (Fickian, anomalous, or Type II transport). According to Korsmeyer and Peppas, $n < 0.43$ indicates that release is governed purely by classical Fickian diffusion, while $n > 0.85$ reflects Type II transport, involving polymer swelling and relaxation of the polymeric matrix. Intermediate values of *n* ($0.43 < n < 0.85$) indicate anomalous transport kinetics, with a combination of the two diffusion mechanisms and Type II transport [136]. To evaluate the mechanism of drug release, data for the first 60% of drug release were plotted into Korsmeyer *et.al.*'s equation (Eq.5) as a log cumulative percentage of drug released vs. log time. The exponent (*n*) was calculated using the slope of the straight line [137] [135].

UNIVERSITY of the
WESTERN CAPE

$$Mt/M\infty = Kt^n \qquad \text{(Eq.5)}$$

Where ($Mt/M\infty$) is the fractional solute release, (*t*) is the release time, (K) is a kinetic constant characteristic of the drug/polymer system, and (*n*) is an exponent that characterises the mechanism of release of compounds. [138][137][135].

The Weibull model was first described by Weibull in 1951 and later modified by Langenbucher [139] to suit the release process. It usually gives a very good fit for most dissolution data; the equation for the Weibull model can be successfully applied to most release curves and is commonly encountered in dissolution studies [134] as the Eq.6.

http://etd.uwc.ac.za/

$$C = C_0 [1- e (t-Ti)^{\beta} / \alpha] \qquad \text{(Eq.6)}$$

Where, (C) is the amount of dissolved drug as a function of time (t); (C_0) is a total amount of drug being released. (Ti) is lag time before onset of the release process and is usually zero, (α) is a scale parameter that describes the time dependence, and the exponent of time, β, in the Weibull equations, can serve as an indicator of the release mechanism of a drug through a polymer matrix, according to the values below:

If the exponent $\beta \leq 0.75$, then the drug release mechanism is Fickian diffusion, and if $0.75 < \beta < 1$, then it is a combined release mechanism. An exponent value $\beta > 1$ is indicative of a complex release mechanism.

The model selection criteria for evaluating the goodness of fit of the release data are essential for the quantitative evaluation of drug release characteristics. Among the criteria, the most popular one in the field of release model identification is the coefficient of determination (Rsqr, r^2) [140].

UNIVERSITY of the
WESTERN CAPE

http://etd.uwc.ac.za/

CHAPTER 3

Formulation, development and characterisation of poly (ε-caprolactone) nanoparticles

3.1 Introduction

In this chapter, the methods used in the synthesis and characterisation of PCL NPs are presented. Firstly a study was performed to determine the formulation with the best physicochemical properties to be used for further experiments. The effect of different surfactants on NPs characteristics was also determined. Finally, the stability of NPs in aqueous media and in human serum albumin as well as the extent of albumin binding to NPs was assessed. The results obtained are presented and discussed as well.

UNIVERSITY of the
WESTERN CAPE

3.2 Aims

- To synthesise and characterise PCL NPs.
- To investigate the influence of surfactant type on the physiochemical characteristics of the NPs.
- To evaluate NP stability in aqueous media and in human serum albumin solutions.
- To assess the extent of albumin binding to NPs.

3.3 Hypothesis

It was hypothesised that:

i. The double emulsion (w/o/w) technique can produce nano-sized PCL particles and that the formulation variable (i.e. surfactant to polymer ratio) has a noticeable effect on the resultant NPs.

http://etd.uwc.ac.za/

ii. Surfactant type influences the physicochemical characteristics of PCL NPs and influences albumin adsorption onto the NPs.

3.4 Materials

3.4.1 Equipment and materials

The following equipment was used:
Analytical balance (Mettler®, model PE 6000, USA); Centrifuge (Centrifuge 5417, Eppendrof AG 22331, Hamburg, Germany); Fluorescence micro-plate reader (Synergy Mx, BioTek Instruments, USA); Freeze-dryer (Virtis, Freeze mobile model 125L; Malvern instruments, Ltd., UK); Probe sonicator (Sonoplus GM 2070, Bandelin, Germany); Ultra-sonic bath (Model 702 Voltage 2030v, 100W, LABOTEC, South Africa); pH meter (Basic 20, Lasec, South Africa); Rotary evaporator (Buchi, Labotec, South Africa); Scanning electron microscope (Auriga HR-SEM F50, Zeiss, South Africa); Sputter coater (Emitech K550X, England); Scientific balance (Ohaus®, model GA 110); Thermomixer (Comfort, Eppendrof, Germany); High speed homogeniser (IKA® T18 digital Ultra Turrax®, Germany); Vortex Mixer (Benchmark Scientific Inc, BV1000 vortex mixer, Taiwan).

UNIVERSITY of the
WESTERN CAPE

The following chemicals were used:
Poly (ε-caprolactone) polymer (average Mw ~ 14,000 g/mol, average Mn ~ 10,000 by GPC, flakes Sigma-Aldrich); Span 80 (clear, yellow viscous liquid, purity ≥ 60% and saponification value 145-160, Sigma-Aldrich); D-α-Tocopherol polyethylene glycol 1000 succinate (BioXtra, water soluble vitamin E conjugate, MP: > 36°C, solubility in H_2O: soluble 1 g/10 mL, clear to faintly turbid. Sigma-Aldrich); Polyvinyl alcohol (PVA) (average Mw 13,000-23,000 g/mol, 98% hydrolysed. Sigma Aldrich); Chloroform (analytical grade, AR Saarchem, Merck Chemicals, PTY Ltd); Distilled water (Millipore, Milford, MA, USA); D-

http://etd.uwc.ac.za/

(+)-Glucose (Mw: 180.16 g/mol MP: 150-152°C. Sigma- Aldrich); Human serum albumin (from human male AB plasma, USA, sterile-filtered. Sigma-Aldrich); PBS salts; Sodium hydroxide pellet (NaOH: 40.00g/mol B & M Scientific); Potassium dihydrogen phosphate (Mw 136.09g/mol) Merck, Germany.

3.5 Methods

3.5.1 Synthesis of PCL NPs

The emulsion-solvent evaporation technique was used to synthesize a double emulsion (w/o/w) PCL NPs [1]. Various concentrations of surfactant (PVA) and polymer (PCL) were investigated for their impact on NP size. The formulation variables are defined as surfactant/oil weight ratio: SOR (PCL polymer was considered the oil phase) [141].

The SOR(%) was calculated using Eq. 3.1 [141]:

$$\textbf{SOR(\%)} = \frac{\textbf{weight of surfactant}}{\textbf{weight of surfactant+weight of polymer}} \textbf{ x 100} \quad \text{(Eq. 3.1)}$$

UNIVERSITY of the
WESTERN CAPE

The mass of PVA ranged from 9 mg to 8 g and the PCL mass ranged from 50 to 250 mg, which gave a SOR (%) range of 15.25 to 96.97%. The NPs were synthesised by dissolving the amount of PCL in 5 mL of chloroform (concentration range: 10 to 50 mg/mL). To this organic phase, 1 mL of deionized water as internal phase was added drop-wise while stirring at 1200 rpm using a magnetic stirrer at room temperature. The emulsion was allowed to equilibrate by stirring for 15 min. The primary (w/o) emulsion was homogenised (IKA high speed homogenizer) at 3000 rpm for 2 min and thereafter it was added drop-wise to 100 mL of an aqueous solution containing the surfactant PVA (concentration ranging from 0.09 to 80 mg/mL). The emulsion was then sonicated using a probe sonicator (Sonoplus GM 2070, Bandelin, Germany); at intensity of 85% for 20 sec continuous and 20 sec pulse in an ice

http://etd.uwc.ac.za/

bath, to formulate the double emulsion (w/o/w). Subsequently, chloroform was removed by evaporation under reduced pressure using a rotavapor. To collect and wash the NPs, the resultant emulsion was then centrifuged at 20817 x *g* at 25°C for 1 h, the supernatant was discarded and the pellet (consisting of NPs), was re-suspended in the same volume with deionised water and re-dispersed by vortexing and sonication in a water bath sonicator for 5 min. This washing procedure was performed three times to remove excess surfactant and polymer before characterisation of the suspension for particle size, polydispersity index (PDI) and zeta potential (ZP). These properties were measured using Dynamic light scattering (DLS) techniques using a Malvern Zetasizer Nano ZS (Malvern instruments, Ltd., UK). Figure 3.1 is a schematic representation of the NP synthesis protocol.

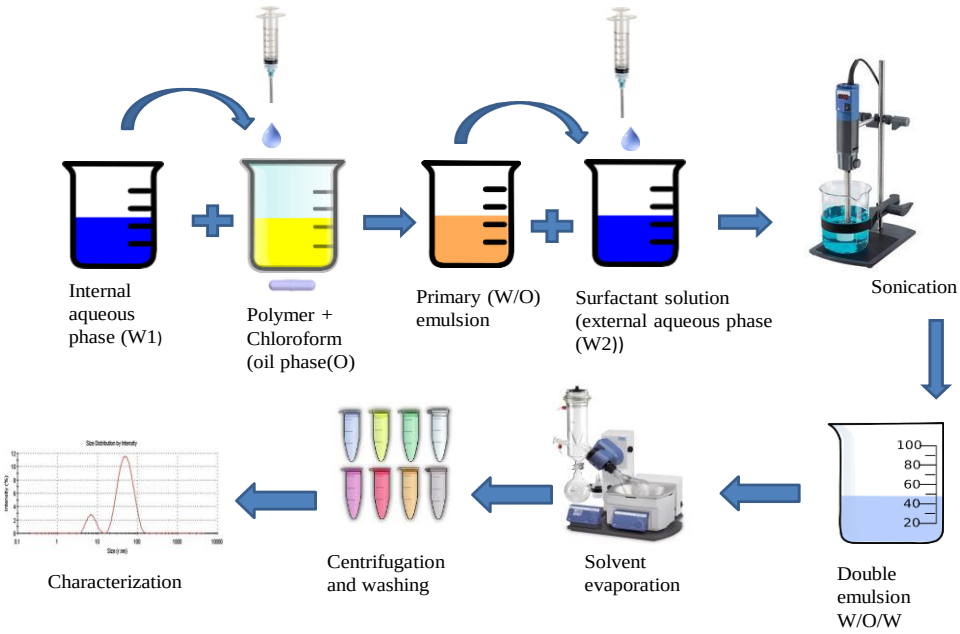

Figure 3.1: *Schematic representation of the double emulsion-solvent evaporation method for synthesis of PCL NPs.*

http://etd.uwc.ac.za/

3.5.2 Characterisation of particle size, PDI and ZP of the NPs

The z-average NP size (diameter) and PDI, after washing and re-suspension in deionized water, was measured using photon correlation spectroscopy techniques on a Malvern Zetasizer Nano ZS (Malvern instruments, Ltd., UK) equipped with DTS software version 7.11. Measurements were performed at 25°C using DLS at an angle of 173° to the laser beam. The ZP was measured by a laser Doppler anemometer coupled to the same instrument. A sample of 1 mL was taken for z-average size and PDI determination from each NP preparation after washing. It was then transferred to a 12 mm disposable plastic cuvette and placed into the instrument. The intensity-weighted mean value was measured and the average of three measurements was taken. For ZP characterisation, a disposable folded capillary cell was rinsed with distilled water using a 1 mL syringe prior to analyses as recommended by the manufacturer and 700 µL of NP solution was added to the cell. The samples were then analysed with a voltage of 4 mV at 25°C at an angle of 173° to the laser beam. The intensity-weighted mean value was measured and the average of three measurements taken.

UNIVERSITY of the
WESTERN CAPE

Statistical analysis (mean, SD, student t-test) was performed to compare the size, PDI and ZP readings across the various formulations. All readings were performed in triplicate using independently prepared samples.

3.5.3 Determining the influence of surfactant type on the physicochemical characteristics of the NPs

Span 80 and TPGS are also typically employed in the formulation of polymeric w/o/w NPs [142][143][100]. Therefore, we sought to determine the influence of surfactant type on the characteristics of the PCL NPs; in comparison to the characteristics of the PVA stabilised nanoparticles. The 33% SOR formula was taken to prepare the PCL NPs to evaluate the

http://etd.uwc.ac.za/

effect of surfactant type on the NP characteristics by using three different surfactants [144] [107].

The preparation of PCL NPs was achieved by the modified multiple emulsion method similar to that employed by Ubrich and co-workers in 2004 [4] and [146]. The method modification was based on the use of two surfactants; a hydrophobic surfactant for stabilization of the first emulsion and a hydrophilic surfactant for stabilization of the second emulsion.

In this study one surfactant with low HLB value, i.e. Span 80 (HLB = 4.3) was added to the organic phase (chloroform) at a concentration of 4.93 mg/mL, while the surfactants with higher HLB values were added in the aqueous phases. Those surfactants were TPGS (HLB = 13.2) at a concentration of 0.30 mg/mL, and PVA (HLB = 18) (0.25 mg/mL). These concentrations were used to maintain a SOR of 33%. Seven possible combinations according to the type of surfactant were incorporated into the emulsion phases (Table 3.1).

UNIVERSITY of the

3.5.3.1 Calculation of HLB values of surfactant mixtures

The HLB values of the surfactant mixtures were calculated according to the following equation:

$$\textbf{HLB mixture} = \frac{(\textbf{C1x HLB1})+(\textbf{C2 x HLB2})+(\textbf{C3xHLB3})}{\textbf{C total}} \qquad \text{(Eq. 3.2) [147]}$$

Where C1, C2, and C3 are the per cent of component proportion and HLB1, HLB2, and HLB3 are the HLB values for each component [147].

http://etd.uwc.ac.za/

Table 3.1: *Distribution of the surfactants in the double emulsion phases and the calculated HLB values of the surfactant mixture.*

Formulation	Inner aqueous phase (W1)	Oil phase (O)	Outer aqueous phase (W2)	HLB value of the surfactant mixture
SP	-	Span 80	PVA	10.75
ST	-	Span 80	TPGS	8.77
TT	TPGS	-	TPGS	13.20
TST	TPGS	Span 80	TPGS	8.78
PSP	PVA	Span 80	PVA	10.79
PST	PVA	Span 80	TPGS	8.82
TP	TPGS	-	PVA	17.99

UNIVERSITY of the
WESTERN CAPE

To synthesise the NPs, 50 mg of PCL and 24.63 mg (0.04 mL) of Span 80 [148] were dissolved in 5 mL chloroform to form the organic phase. A volume of 1 mL of deionized water was added drop-wise to this organic phase and homogenised at 10000 rpm for 2 min to form the primary emulsion (O/W), and then the emulsion was sonicated using a probe sonicator with an intensity of 85% in an ice bath for 1 min to decrease the emulsion droplet size. The first emulsion was thereafter poured drop-wise into 100 mL of 0.025% w/v PVA (or 0.03% w/v of TPGS in ST, TT and TST formulations) aqueous solution. This secondary emulsion was homogenised at 5000 rpm for 1 min and sonicated for 30 sec to obtain the w/o/w emulsion. Chloroform was evaporated under reduced pressure. The resulting NPs were

http://etd.uwc.ac.za/

isolated by centrifugation at 20817 x *g*, 25°C for 1 h and thereafter were washed three times with deionised water (as described in section 3.5.1). The supernatant was removed, and the pellet was re-suspended with water. In order to determine whether the samples were in the nano range prior to the freeze drying process a portion of each NP formulation was taken for z-average particle size, PDI, and ZP determinations (as described in section 3.5.2). The other portions were mixed with a specific amount of 10% (w/w) glucose as a cryoprotectant to prevent NP aggregation during the freeze drying process. After 72 h the freeze dried powder was weighed and stored in tightly closed vials in a fridge for future use.

Re-dispersion of lyophilised products was carried out by manually hand shaking them in a small glass vial with distilled water. A visual observation was done to investigate the formation of any aggregates or precipitates after shaking. Particle size and size distribution after re-dispersion of the sample was performed using a Zetasizer, [149][150].

UNIVERSITY of the
WESTERN CAPE

3.5.4 Determination of surface morphology of NPs

The shape (and size) of NPs was investigated based on the method published by [151] and [110]. A drop of the NP aqueous suspension was placed on carbon adhesive tape applied on an aluminium stub, and thereafter dried completely under a fume hood. The dried sample was coated with gold palladium for 30 sec using an Emitech K550X (England) sputter coater and viewed with the Auriga HR-SEM F50 (Zeiss, South Africa) with a voltage of 5 KV.

3.5.5 Assessment of NP stability

NPs constitute a relatively stable physical system due to their colloidal nature. Many variables can affect the stability of NPs. Generally, a colloidal suspension is stable and does not tend to separate as a result of slow deposition due to the mixing tendencies of diffusion and convection. However, some agglomeration can occur. The objective was to evaluate the

http://etd.uwc.ac.za/

stability of PCL NPs stored at different temperatures and in different media. The stability parameters studied were z-average NP size, PDI and ZP.

3.5.5.1 Evaluation of NP stability in aqueous solution

Two milligrams of the freeze dried NP powder were re-suspended in 2 mL of deionized water and evaluated for short-term stability. Z-average particle size and PDI were measured over 7 days. Samples were stored in glass vials at different temperatures, i.e. 4°C, 20°C and 37°C [152]. At time intervals of 1 h, 24 h and 7 days, the physical appearance of the NP suspension samples were visually observed for any sedimentation, and the z-average particle size and size distribution were measured using Malvern Zetasizer Nano ZS (Malvern instruments, Ltd., UK), at each time interval, as described in section 3.5.2. Experiments were performed in triplicate. Results of z-average, particle size and PDI were expressed as mean ± SD.

3.5.5.2 Evaluating NP stability in human serum albumin

To assess the NP stability in human serum albumin (HSA), the method described by Mirshafiee and co-workers in 2015 was used with some modification [153]. NP formulations at a concentration of 0.42 mg/mL were dispersed in 45% v/v HSA in phosphate buffered saline solution (PBS) pH 7.4 and incubated at 37°C, under gentle stirring (150 rpm). Z-average particle size and PDI were measured at four time points (i.e. 5 min, 30 min, 1 h, and 24 h), using DLS spectrometry on a Zetasizer Nano ZS. Measurements were performed within 2 min after sample removal from the incubator. All measurements were in triplicate. Results were expressed as mean ± SD.

3.5.6 Assessment of the extent of albumin binding to NPs

The extent of protein binding was determined for each NP formulation (SP, ST, TT and TST) using fluorescence quenching, as described by Li and co-workers in 2010 with slight

http://etd.uwc.ac.za/

modifications [148]. This method measures the fluorescence quenching ability of NPs on HSA. When the NPs bind to the HSA, only the fluorescence of the free HSA can be measured.

3.5.6.1 Quantification of albumin

Firstly, to quantify albumin, a calibration curve of HSA in PBS pH 7.4 was prepared over the concentration range 0-45% v/v. The excitation wavelength was 280 nm and the fluorescence spectra were acquired in the range of 300-500 nm. A plot of fluorescence intensity vs. concentration was made, and r^2 calculated. The calibration curve was generated in triplicate. Emission of HSA was measured by fluorescence spectrometry (Synergy Mx, BioTek Instruments, USA).

3.5.6.2. Assessment of extent of albumin binding to NPs

In saturation study to determine whether the NPs interfere with the albumin at 300-500 nm wavelength, 1 mg/mL of all NP formulations was prepared as stock solution, and serial dilutions were prepared (i.e. 0, 0.0625, 0.25, 1 mg/mL). PBS pH 7.4 was used as a blank. Fluorescence intensity was measured at 300-500 nm wavelengths.

To determine the extent of NP protein binding, the emission of HSA was measured at a constant concentration (10% v/v), in the presence of a range of NP concentrations (i.e. 0, 0.0625, 0.25, 1 mg/mL). The NP-protein solutions were incubated at 37°C in protein low-binding tubes (96 well plates). Emission of HSA was measured at a constant concentration of 10% v/v in the presence of increasing concentrations of NPs (0, 0.0625, 0.25, 1 mg/mL). The excitation wavelength was 280 nm and the fluorescence spectra were acquired in the range of 300-500 nm. At each time interval (30 min, 1 h, 6 h) the fluorescence intensity was measured by a fluorescence plate reader (Synergy Mx, BioTek Instruments, USA). Fluorescence

http://etd.uwc.ac.za/

intensity vs. wavelength was plotted. The area under the curve (AUC) was calculated in triplicate for each NP by using Graph Pad Prism version 6.01 software, (California, USA). The percentage protein binding was calculated using equation 3.2.

$$\textbf{Percentage protein binding} = \frac{\textbf{AUC protein} - \textbf{AUC protein+nanoparticle}}{\textbf{AUC protein}} \textbf{X 100} \quad \text{(Eq. 3.2)}$$

Statistical analysis

All experiments were performed in triplicate. Results shown are the mean ± SD. Comparison of means was performed using a one-way analysis of variance (ANOVA) (nonparametric) test and multiple comparisons. The significant difference considered when $p < 0.05$. All graphs were plotted using Graph Pad Prism version 6.01(California, USA).

UNIVERSITY of the
WESTERN CAPE

3.6 Results and discussion

3.6.1 Synthesis and characterization of PCL NPs

Eight NP formulations were synthesized using the double emulsion method over a SOR(%) range of 15.0 – 96.97%. Figure 3.2 shows the trends in z-average particle size of the NPs.

http://etd.uwc.ac.za/

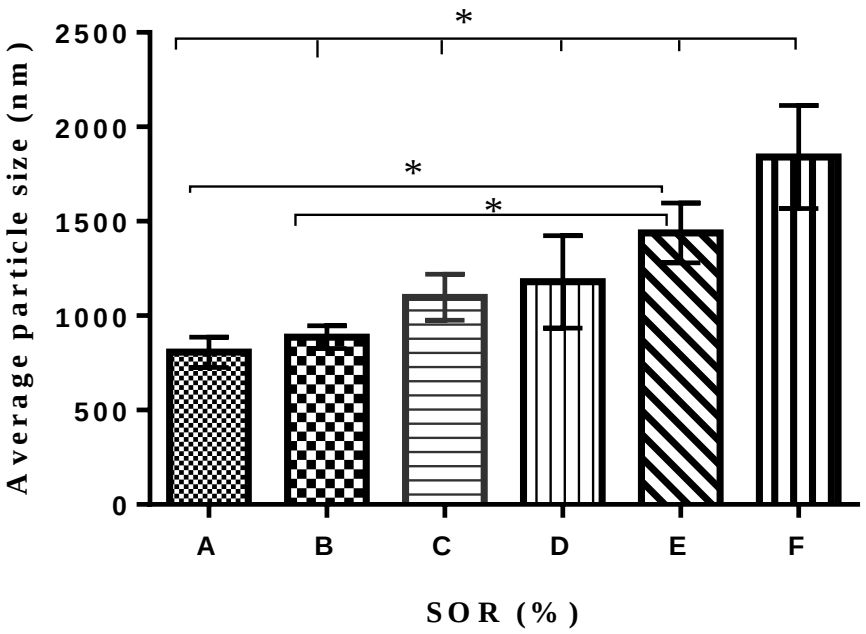

Figure 3.2: *Average (z-average) hydrodynamic particle size of PCL NPs at various SOR(%). Data for SOR(%) 15 and 25% are not shown, as the emulsion cracked. Data is the mean ± SD of three independently prepared samples. A = 33%, B = 50%, C = 66.60%, D = 88.80%, E = 94% and F = 96. 97%, (*) $p < 0.05$.*

UNIVERSITY of the
WESTERN CAPE

An increase in mean particle size was observed with increasing SOR(%). However in 15% and 25% SOR the double emulsion was separated and there was a precipitation observed after the addition of the first emulsion to the outer aqueous phase. NPs were obtained at SOR 33% and 50%, i.e. mean size was 806.5 ± 79.76 nm and 886.8 ± 59.91 nm, for SOR 33% and 50%, respectively. At SOR ≥ 66.60%, particles were no longer found in the sub-micron size range. There was a significant difference between the particle sizes of 96.97% SOR with all rest of SOR(%). The particle size of 94% SOR was significantly larger than the particle size of 33% and 50% ($p < 0.05$) while there was no significant difference ($p > 0.05$) in particle size between 33, 50, 66.60, and 88.8% SOR.

http://etd.uwc.ac.za/

PDI was measured and the size distribution was obtained for each NP formulation (Figure 3.3). The highest mean PDI values were obtained for SOR = 96.97% (0.45 ± 0.04) and the lowest values were 0.25 ± 0.02 and 0.31± 0.02, for SOR = 33% and 66.6% respectively.

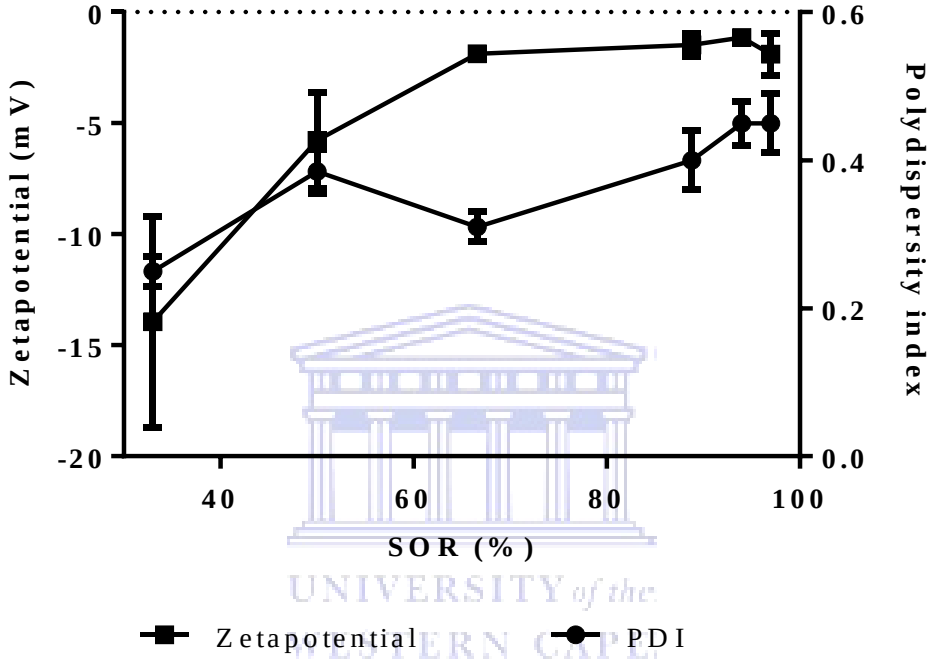

Figure 3.3: *PDI and ZP of PCL NPs prepared with different SOR(%) ratios (results shown as mean ± SD, n = 4 replicates).*

The ZP values for the formulations were all negative, and were in the range -1.15 ± 0.17 mV to -13.95 ± 4.75 mV (Figure 3.3). An increase (i.e. decrease in the negativity) in the mean ZP was observed as SOR(%) increased. The highest zeta potential values were observed for SOR 33% and 50% formulation i.e. -13.95 ± 4.75 mV and -5.78 ± 2.17 mV, respectively.

http://etd.uwc.ac.za/

Regarding the criteria used to select the optimised formulation, the PCL NPs produced with 33% SOR formulation were selected for further experiments because 33% SOR formulation had the lowest ($p < 0.05$) z-average particle size of 806.50 ± 79.76 nm with monodisperse size distribution 0.25 ± 0.02 and a ZP value of -13.95 ± 4.75 mV.

3.6.2 The effect of different surfactants on the physicochemical characteristics of 33% SOR PCL NPs

To investigate the effect of surfactant type on PCL NP characteristics, three different surfactants (Span 80, PVA, and TPGS) were included in the double emulsion phases as reported in section 3.5.3 to produce the four formulations SP, ST, TT, and TST, while for the other possible surfactant combinations, the resultant particle size was not in the submicron range.

UNIVERSITY of the
WESTERN CAPE

PVA is perhaps the most commonly used emulsifier. We have used a variety of emulsifying agents, including vitamin E-TPGS [145], PVA [154], and Span 80 [142]. Properly emulsified polymer NPs will appear as a homogenous, milky-white/opaque solution. A poor (or "broken") emulsion will show macroscopic heterogeneity or granularity, and it may even separate into two visually distinct layers in the tube. This generally indicates a failure to form NPs [155].

3.6.3 Characterisation of the physicochemical properties of NPs prepared with PVA, TPGS and Span 80 surfactants

Figures 3.4 and 3.5 show the z-average particle size, PDI and ZP of the PCL NPs stabilised by combinations of PVA, Span 80 and TPGS at SOR 33%. Figure 3.4 shows that the z-average particle size and PDI were significantly affected by the type of surfactant.

http://etd.uwc.ac.za/

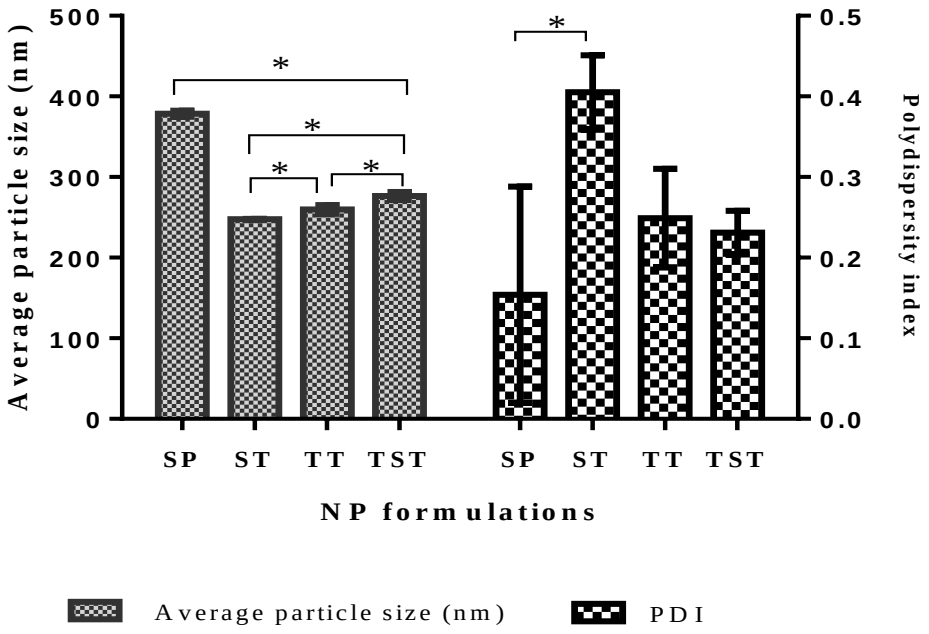

Figure 3.4 : *Z-average particle size and PDI of PCL NPs prepared with PVA, Span 80 and TPGS surfactants (results shown as mean ± SD; n=3. (*) p < 0.05).*

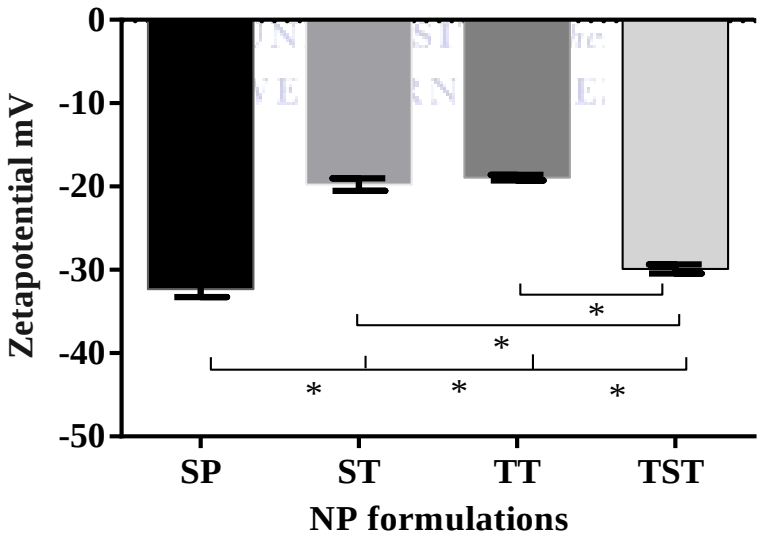

Figure 3.5: *ZP of PCL NPs prepared with PVA, Span 80 and TPGS surfactants (results shown as mean ± (SD); n=3(*) p < 0.05).*

http://etd.uwc.ac.za/

SP (Span 80, PVA combination) had the highest mean size of 378.50 ± 3.90 nm among the NP formulations ($p < 0.05$). This particle size was higher than that obtained by Ahmed *et.al*, 2014 [107]. This could be due to the different method that was used for the NP preparation, since they prepared PCL NPs containing atorvastatin calcium using Span 80 as emulsifier by the solvent displacement method. Ahmed *et.al*, stated that the mean particle size 182.33 ± 2.52 nm increased upon addition of Span 80 in the organic phase compared to particles prepared without the addition of Span 80 to 134.67 ± 1.53 nm. The larger particle size obtained by using PVA could be due to reported localised gelatinisation of PVA on the surface of the particles due to solvent-PVA interaction leading to decreased solvent migration and subsequent increase in particle size [107].

Another possible reason for the higher z-average particle size in the SP formulation could be the PVA surfactant which had been reported to give PVA results in particles with a higher mean size in comparison to TPGS stabilised NPs [145].

UNIVERSITY of the
WESTERN CAPE

A decrease in z-average size was observed for the other three NP formulations which were prepared with TPGS surfactants namely ST (Span 80, TPGS), TT (TPGS, TPGS) and TST (TPGS, Span 80, TPGS) 247.60 ± 0.60 nm, 259.80 ± 5.30 nm, and 276.30 ± 5.01 nm, respectively. This could be attributed to the greater effectiveness of TPGS in decreasing the interfacial tension between the organic and the aqueous phases and thus results in better emulsification which leads to smaller particle size. Similar results were obtained by Mu and Feng, 2003 [145]. They reported that TPGS at 0.03% (w/v) as an emulsifier in preparation of PLGA NPs resulted in smaller NPs with size range of 272.56 ± 169.5 nm.

In a study by Vandervoort and Ludwig, 2002, other polymers were tested as stabilisers [155]. These polymers were incorporated as such and in combination with PVA. Their aim was to

http://etd.uwc.ac.za/

study how the use of other polymers in the preparation of NPs would affect particle size and ZP value. The effect of the presence or absence of PVA during preparation as well as the effect of the concentration of the alternative stabilisers was evaluated. They found that NPs were obtained with most polymers when they were used in combination with PVA. Leaving PVA out of the formulation in most cases increased the size of the particles over 1 μm [156].

PDI was measured and size distribution was obtained for each NP formulation (Figure 3.4). PDI values were within the range of 0.15 ± 0.13 and 0.41± 0.05. PDI values obtained were below 0.45 which indicated good particle homogeneity.

Figure 3.5 show that PCL NPs had a negative ZP. ZP values were -32 mV or lower in all cases (-32.30 ± 0.96, -19.77 ± 0.74, -18.93 ± 0.32 and -29.90 ± 0.56 mV for SP, ST, TT, and TST, respectively). It is therefore expected that the NP dispersions would be stable. Zeta potential measurements showed a significant increase in negativity when TPGS and Span 80 surfactants were used together in NP formulation when each one was used alone.

UNIVERSITY of the
WESTERN CAPE

In summary, a small particle size with relatively mono-disperse size distribution was obtained when TPGS was used as an aqueous surfactant compared with Span 80 and PVA. This finding suggests that TPGS is more efficient in stabilising the emulsion formed during particle formation than Span 80 and PVA, which may be attributed to their different structures and HLB values. The HLB presented no trends in parameters as a function of the surfactant combination.

3.6.4 Evaluation of surface morphology of the NPs

Particle size measurements using DLS provided information on the hydrodynamic diameter only. DLS does not yield information about the shape and surface properties of the NPs;

http://etd.uwc.ac.za/

hence other techniques are usually applied for this purpose. SEM is often used to study particle size, shape and surface properties of NPs [124]. In this study, the investigation of shape and morphology was studied using a high resolution scanning electron microscopy (HR-SEM). Figure 3.6 shows SEM images of the prepared NPs.

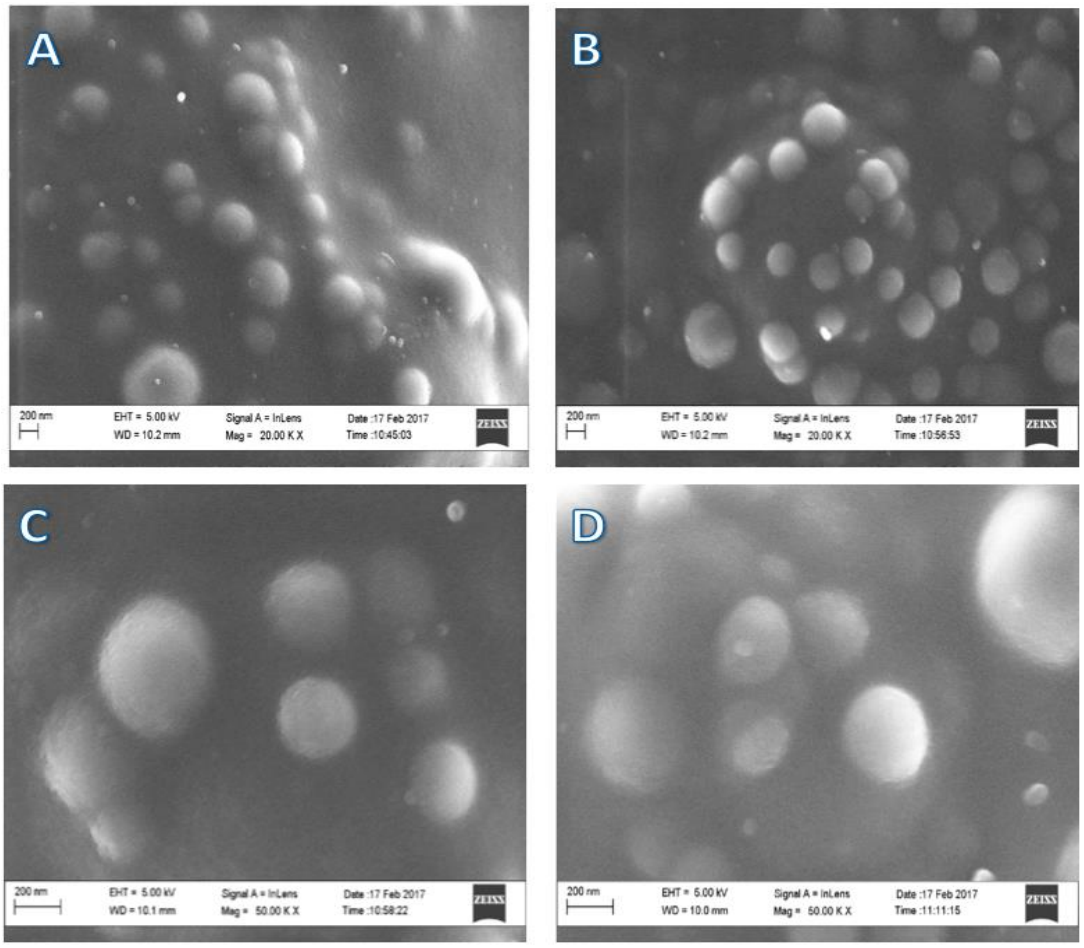

Figure 3.6: *HR-SEM images of PCL NPs (A) SP formulation, (B) ST formulation, (C) TST formulation, (D) TT formulation. A drop of nanosuspension was dispersed on the carbon adhesive tape applied on an aluminium stub and then left overnight to completely dry under a fume hood. The dried NPs were coated with gold palladium for 30 seconds using Emitech K550X (England) sputter coater and viewed with the Auriga HR-SEM F50 (Zeiss, South Africa) at a voltage of 5 KV. A scale-bar in nm, Extra high tension (EHT), Working distance (WD) and Magnification (Mag) is provided for each image.*

http://etd.uwc.ac.za/

SP NPs revealed a non-uniform particle size distribution of spherical like particles in the size range of ± 300 nm. From the SEM images it is interesting to note the contact among particles; these contacts can be attributed to PVA, which is sticky by nature and difficult to remove completely [157]. ST NPs showed more uniformity in size distribution of spherical like particles in a size range of less than 300 nm. TST and TT NP formulations showed relative uniformity in the particle size distribution of spherical like particles, and indicated little to no aggregation which could be a result of the effect of the TPGS surfactant which prevented the clumping of NPs.

The reported size distribution for all NP formulations after analysis using the Zetasizer NanoZS was smaller when compared with the sizes observed in the HR-SEM images. This is largely related to the different techniques used in the analysis of size. The Zetasizer NanoZs instrument uses dynamic light scattering (DLS) techniques to measure particles in solution undergoing Brownian motion and hydrodynamic size whereas in HR-SEM analysis, the sample requirement is smaller and must be completely dried under a fume hood prior to analysis [158]. However, we were successful in imaging PCL NPs that are spherical in shape, as most PCL NPs imaged using SEM as reported in the literature are spherical [159][160].

UNIVERSITY of the
WESTERN CAPE

3.6.5 Stability of the NPs in aqueous media

The objective was to evaluate the stability of the NPs when stored at different temperatures. The stability parameters studied were the physical appearance of the nanosuspensions, z-average particle size, PDI and ZP.

The physical appearance of the prepared SP, ST, TT, TST NP suspensions (1 mg/mL) did not change when samples were stored at 4°C, 20°C and 37°C for 7 days. Figures 3.7, 3.8 and 3.9

http://etd.uwc.ac.za/

show the influence of the storage temperature on PCL NPs, suspended in water on the average particle size, PDI and ZP as a function of time.

A

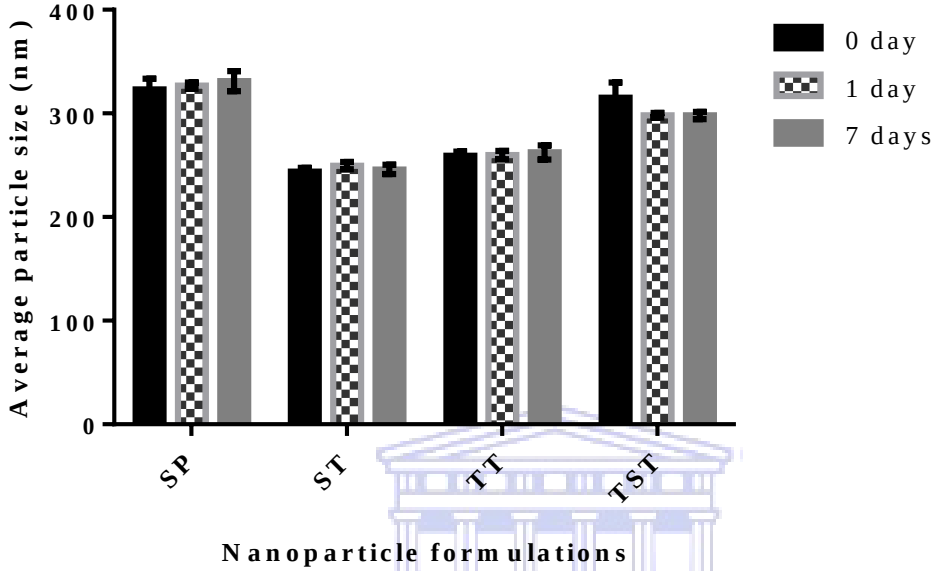

UNIVERSITY of the
WESTERN CAPE

B

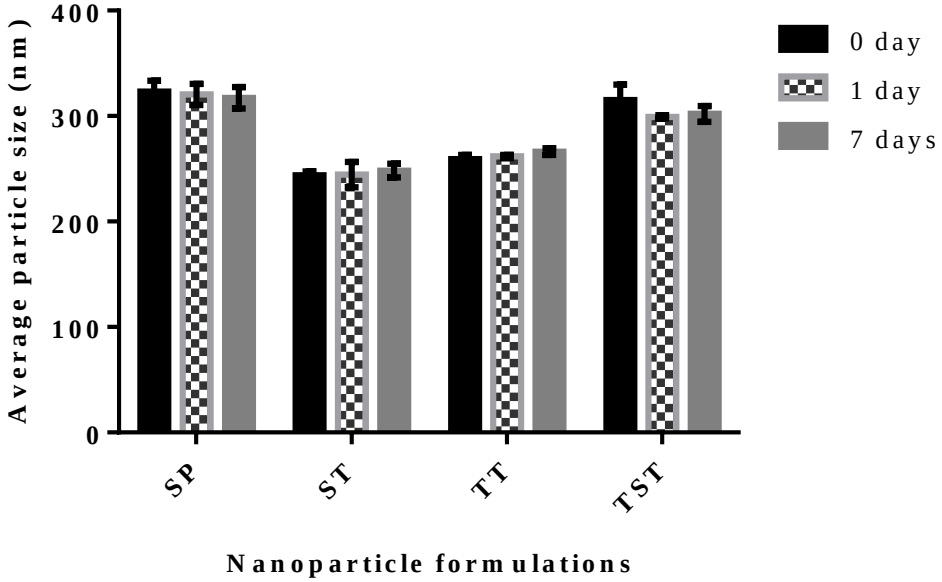

http://etd.uwc.ac.za/

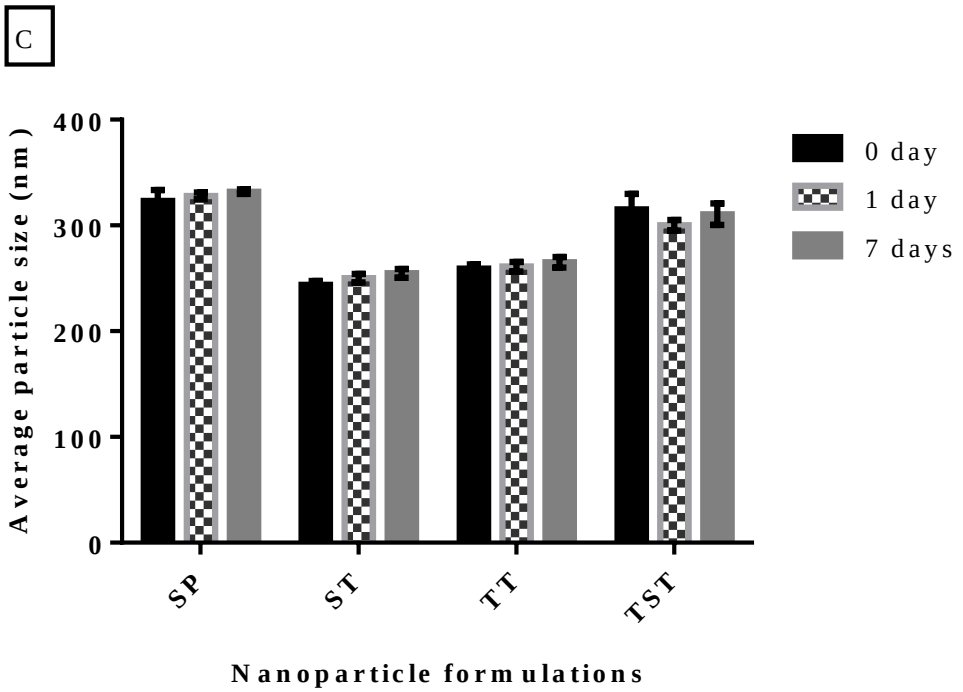

Figure 3.7: *Trends in the z-average particle size of SP, ST, TT, and TST NPs over seven days, (A) at 4°C, (B) at 20°C and (C) at 37°C, in aqueous media. Results shown as mean ± SD; n= 3.*

UNIVERSITY of the
WESTERN CAPE

http://etd.uwc.ac.za/

a

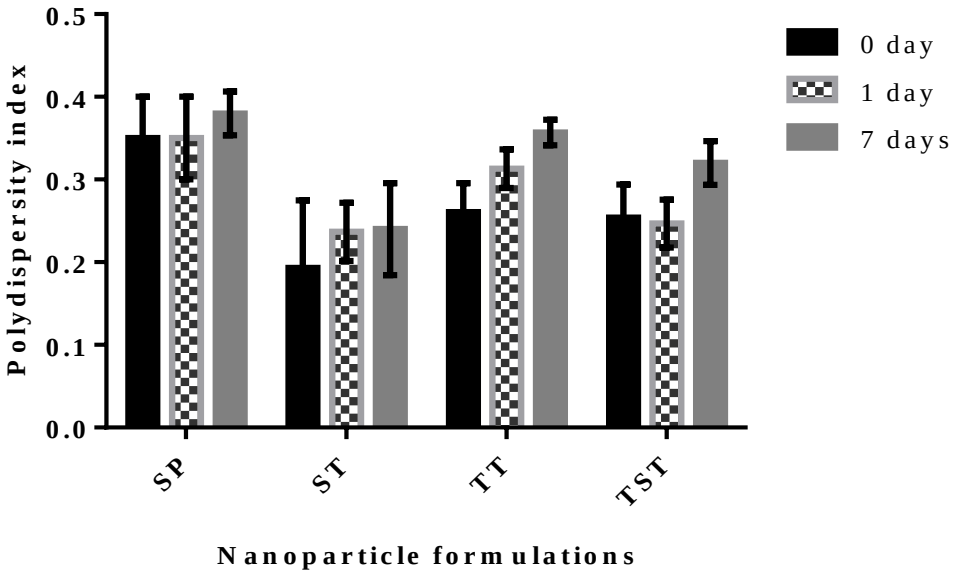

b

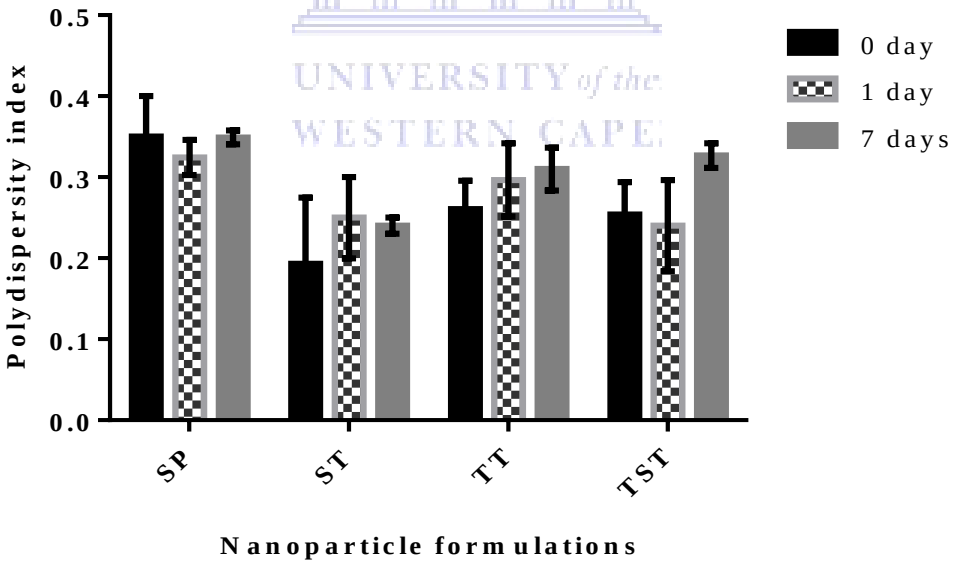

UNIVERSITY of the
WESTERN CAPE

http://etd.uwc.ac.za/

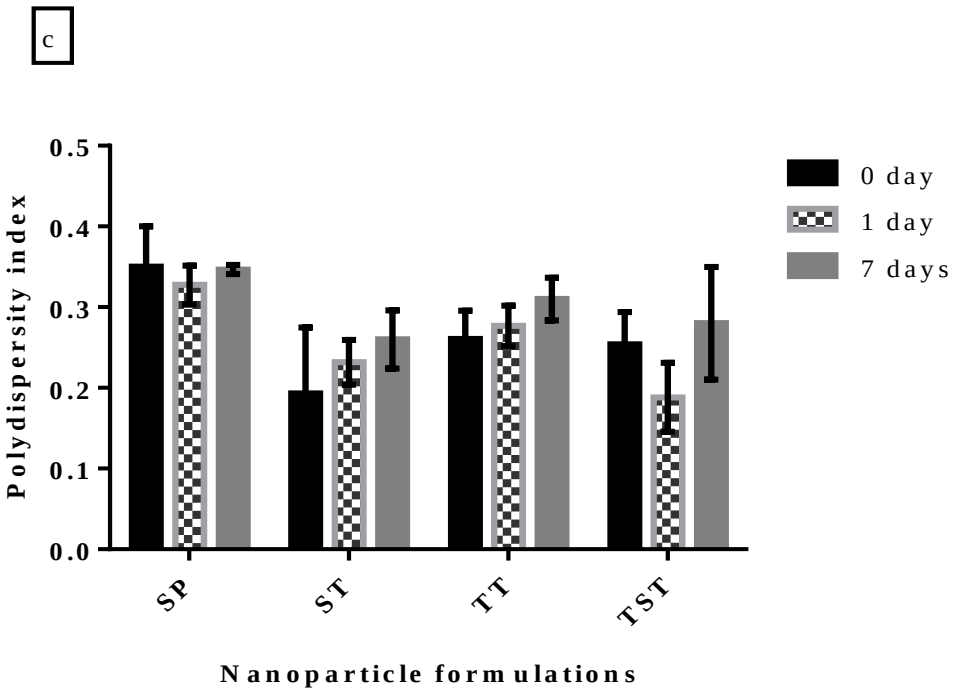

Figure 3.8: *Trends in the PDI of SP, ST, TT, and TST NPs over seven days, (a) At 4°C, (b) at 20°C and (c) at 37°C, in aqueous media. Results shown as mean ± (SD); n=3.*

UNIVERSITY of the
WESTERN CAPE

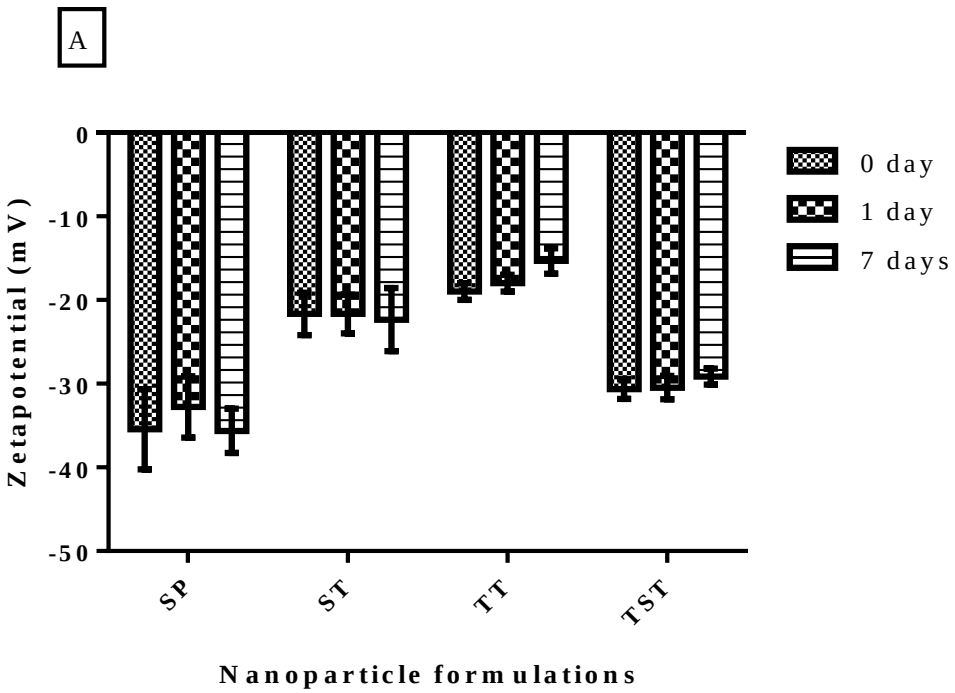

http://etd.uwc.ac.za/

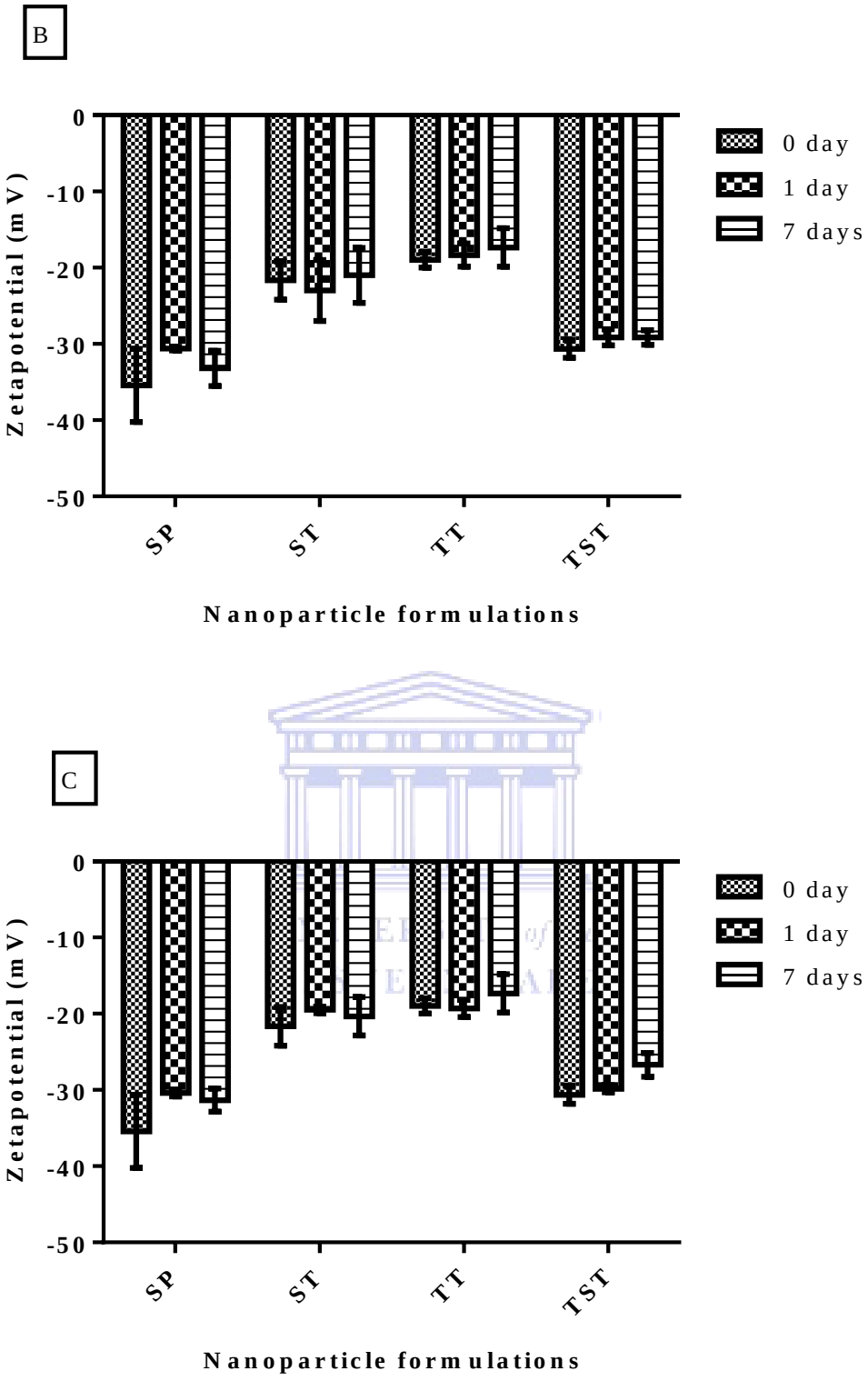

Figure 3.9: *Trends in the ZP of SP, ST, TT, and TST NPs over seven days, (A) at 4°C, (B) at 20°C and (C) at 37°C, in aqueous media. Results shown as mean ± (SD); n=3.*

http://etd.uwc.ac.za/

The z-average particle diameter (Figure 3.7 a, b, c), for SP NPs (Span 80, PVA) prior to the stability study (i.e. day 0) was 323.3 ± 10.4 nm and after 7 days was 331.2 ± 9.7, 317.3 ± 10.1 and 331.9 ± 2.2 nm when stored at 4°C, 20°C and 37°C respectively. For ST NPs (Span 80, TPGS) at day 0, the average size was 243.90 ± 3.60 nm and 245.9 ± 4.5, 284.3 ± 6.6 and 254.8 ± 4.2 nm after storage at 4°C, 20°C and 37°C respectively over seven days. However the average size of TT NPs (TPGS, TPGS) at day 0 was 259.3 ± 4.1 nm and 262.4 ± 6.8, 266.3 ± 3.3 and 265.0 ± 5.0 nm after storage at 4°C, 20°C and 37°C respectively over 7 days. There was no increase in the mean particle size in TST NPs (TPGS, Span 80, and TPGS) after 7 days when stored at 4°C whereas the size was 315.1 ± 14.9 nm at day 0, and after 7 days it was 298.0 ± 3.4, 302.0 ± 7.4 and 310.7± 10.1 nm at 4°C, 20°C and 37°C, respectively. All the formulations remained stable throughout the seven days of the experiment, with no major changes in particle size. These findings are in agreement with previous studies of the size of polymeric NPs [161] and [162].

UNIVERSITY of the
WESTERN CAPE

The PDI, which provides an indication of the size distribution of the particles, can also be used to assess stability. Factors that influence polydispersity include the properties of the solution, the thermodynamics of the system, and the method of preparation [163]. High PDI values (PDI > 0.4) are indicative of heterogeneity in the diameters of the suspended particles, while changes with time are due to the formation of particle populations that have diameters different to those of the initial particles, due to processes of aggregation, disintegration, or degradation. PDI values smaller than 0.4 are considered ideal, since this is indicative of a narrow particle size range [163]. The polydispersity values obtained were all below 0.4 (Figure 3.8 a, b, c), indicating good particle homogeneity.

The results demonstrated that the ZP values of the formulations remained fairly low (around −35 mV) during the 7 days (Figure 3.9 A, B, C), indicating that there was no tendency of

http://etd.uwc.ac.za/

aggregation with time, and that the formulations were stable. The negative values reflect the presence of carboxylic groups at the polymer extremities, since PCL is polyester [161].

3.6.6 Evaluating NP stability in human serum

NP exposure to biological fluids in the body results in protein binding to the NP surface, which forms a protein coating called the "protein corona"[164]. To evaluate the influence of both surfactant type and concentration on NP interaction with plasma proteins, HSA was chosen for the binding studies.

To simplify studies of protein–NP interactions, NPs were incubated with HSA at 37°C under gentle stirring and then characterised using DLS at four time points (i.e. 5 min, 30 min, 1 h, and 24 h). DLS measurements confirmed that NP exposure to HSA solutions significantly increased the NP diameters, as shown in Figure 3.10.

UNIVERSITY of the
WESTERN CAPE

http://etd.uwc.ac.za/

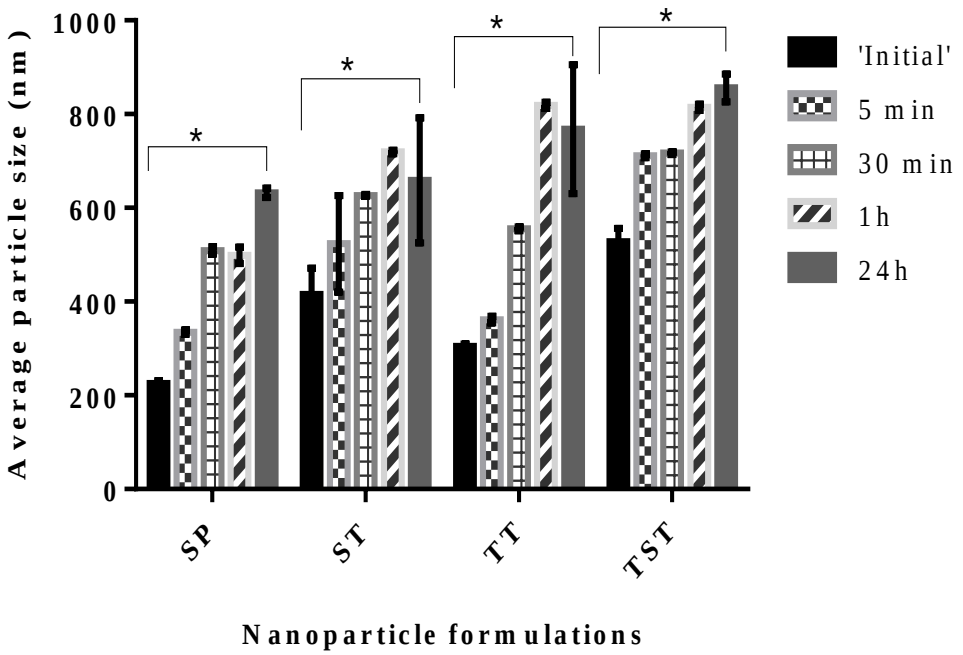

Figure 3.10: *Trends in z-average particle size of SP, ST, TT, and TST NPs over 24 h at 37 °C in HSA solution. Results shown as mean ± SD; n= 3. (*) p < 0.05.*

UNIVERSITY of the
WESTERN CAPE

NPs (SP, ST, TT and TST) exposed to HSA had an increase in particle size after incubation with HSA, likely due to the amount of proteins bound to their surfaces. The z-average particle size of SP changed from 252.83 ± 5.06 nm to 631.83 ± 9.88 nm after 24 h and the change in particle size was significant ($p < 0.05$) from initial to 24 h as shown in Figure 3.9. For ST, TT and TST the z-average particle size changed significantly ($p < 0.05$) from 415.63 ± 55.80 nm to 658.63 ± 133.12 nm, 304.73 ± 4.52 nm to 767.93 ± 137.75 nm and 527.73 ± 28.50 nm to 855.90 ± 29.29 nm respectively from initial to 24 h. However, the change in particle size for ST, TT and TST NPs became insignificant ($p > 0.05$) between the time points 1 h and 24 h.

Colloidal stability of NPs in the presence of proteins can be assessed by DLS studies through monitoring NP size [165]. The results of this study showed that the interaction between NPs

http://etd.uwc.ac.za/

and proteins depends on the type of stabilising surfactants and their concentration changes. As reported in a study by Wizen and co-workers in 2016. In this study, they show that the interaction between NPs and proteins strongly depends on the type of stabilizing surfactants and their (small) concentration changes. The reaction between human serum albumin and polystyrene NPs stabilized by an ionic or non-ionic surfactant-sodium dodecylsulfate or Lutensol AT50, respectively-was monitored. It was found that the amount of surfactant molecules on the surface significantly determines the protein binding affinity and adsorption stoichiometry [166].

3.6.7 Assessment of the extent of albumin binding to NPs

3.6.7.1 Standard curve determination for quantification of HSA in PBS

Fluorescence quenching was used to measure the adsorption of fluorescent proteins on the surface of NPs [167]. In our study, the concentration of HSA used (10% v/v) was determined from a HSA calibration curve in PBS pH 7.4 prepared over the range (0-45% v/v). Beer Lambert's law states that the relationship between concentration and fluorescence is directly proportional. However, beyond a certain concentration, the linear relationship no longer exists [168]. In order to ensure that the concentration of HSA used was within the range where the linear relationship exists, a series of dilutions were performed and the fluorescence was measured.

UNIVERSITY of the
WESTERN CAPE

As shown in Figure 3.11, a progressive increase in HSA concentration leads to a proportional increase in fluorescence. Thus a linear relationship was established for HSA (r^2 = 0.9915, Y= 947.6X+19942). The concentration of HSA used falls within this range and the results obtained for the protein binding of the NPs are thus assumed to be valid.

http://etd.uwc.ac.za/

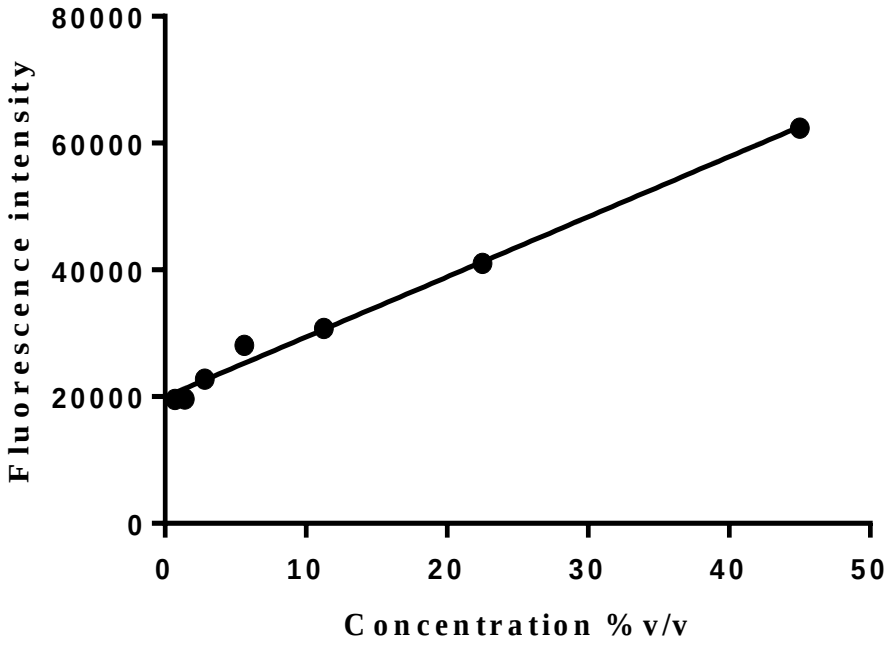

Figure 3.11: *Linear relationship between HSA concentration and fluorescence intensity*

To determine whether the NPs interfere with the HSA at the wavelength (300-500 nm), serial dilutions of NPs (0.0625-1 mg/mL), were made in PBS. It was found that all NP concentrations were close to PBS fluorescence, as shown in Figure 3.12.

http://etd.uwc.ac.za/

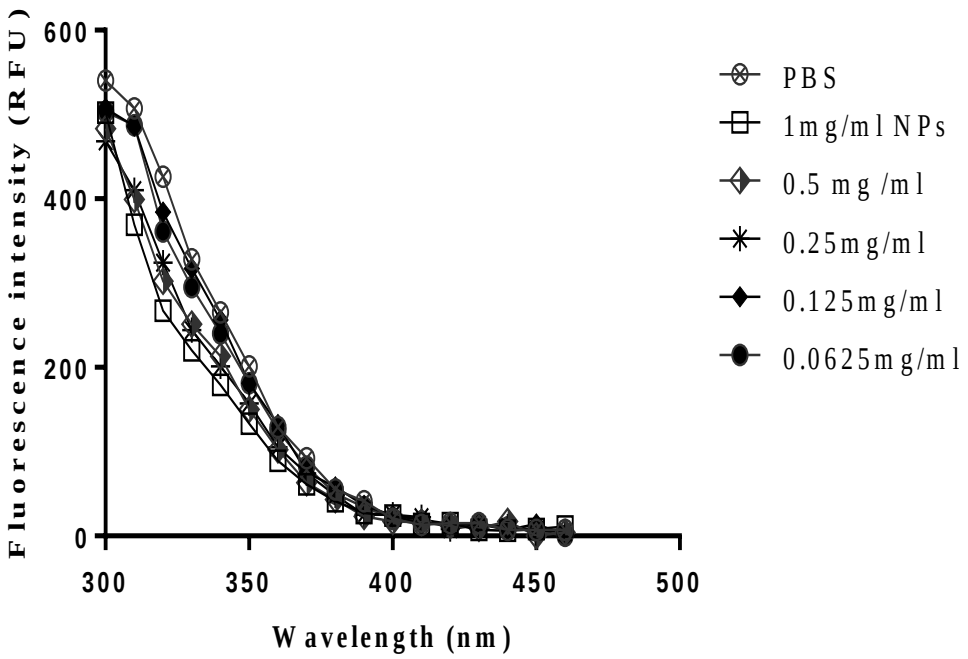

Figure 3.12: *Fluorescence intensity of serial dilutions from NP stock solution -1 mg/mL in PBS pH 7.4.*

UNIVERSITY of the WESTERN CAPE

3.6.7.2 Determination of the extent of albumin binding to NPs

As shown in Figure 3.13, after 30 min incubation at 37°C it was found that the type of surfactant has a significant effect on the mean percentage of protein binding, whereby Span 80 stabilized NP formulations and had a higher % protein binding than TPGS stabilized NPs.

http://etd.uwc.ac.za/

A

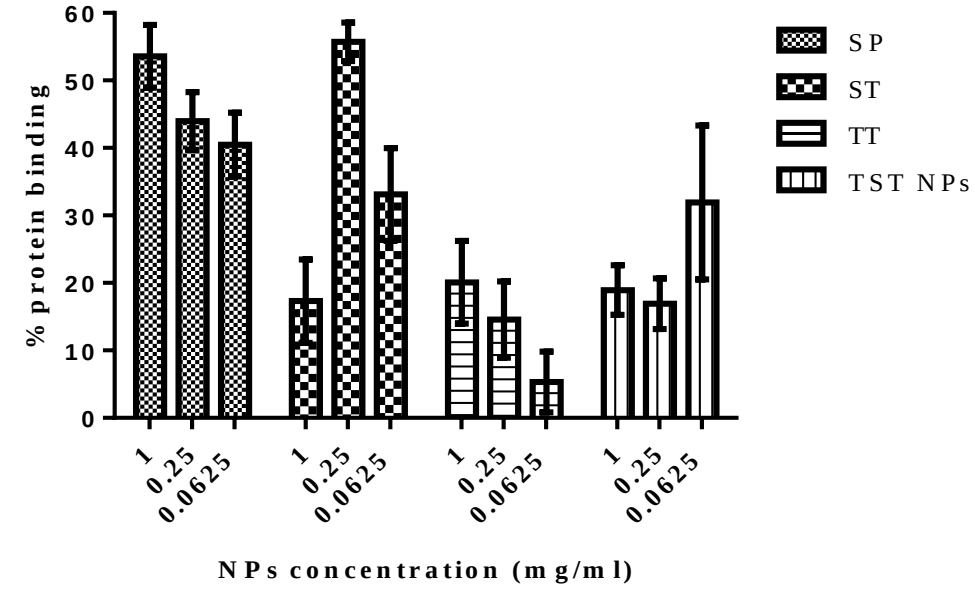

B

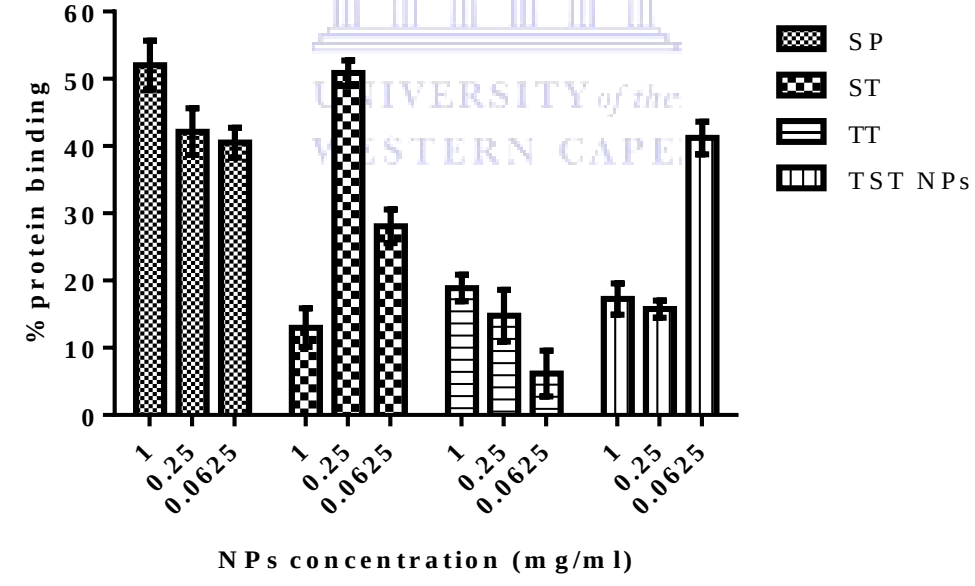

UNIVERSITY of the WESTERN CAPE

http://etd.uwc.ac.za/

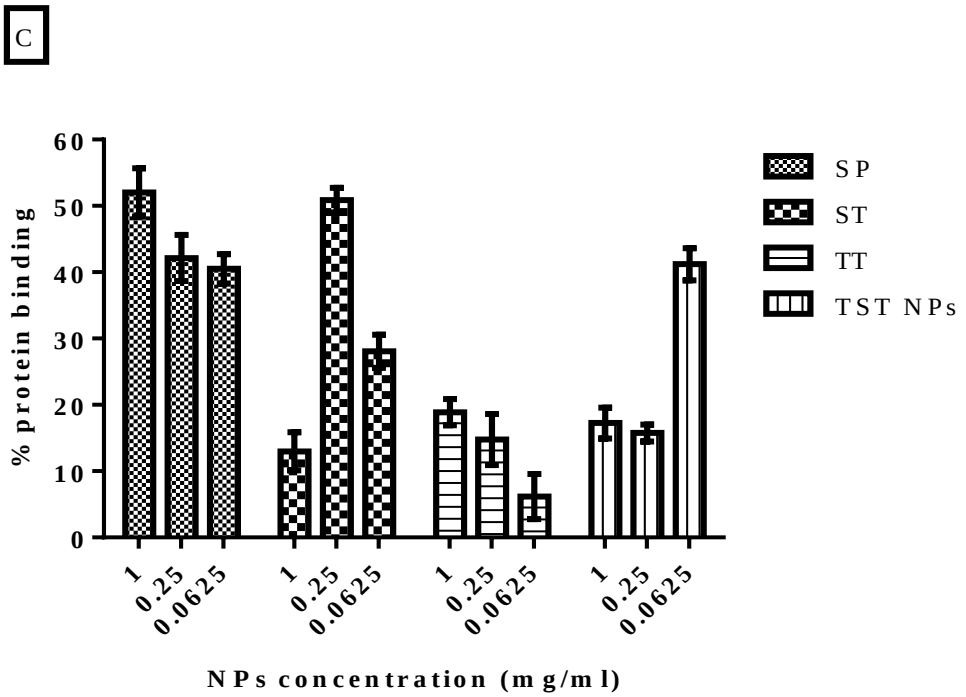

Figure 3.13: *Percentage of protein binding of SP, ST, TT and TST NPs at three concentration levels (1, 0.25, 0.0625 mg/mL NPs); over, (A) at 30 min, (B) at 1 h and (C) at 6 h incubation periods at 37° C in 10% (v/v) HSA.*

UNIVERSITY of the
WESTERN CAPE

Within each NP formulation, there was a difference in the influence of NP concentration on the mean percentage of protein binding at 30 min, namely in SP NPs, as the NP concentration increases there was an increase in % protein binding, where the highest ($p < 0.05$) mean percentage of protein binding occurred with 1 mg/mL SP NPs (53.56 ± 4.66%), then 0.25 mg/mL(43.99 ± 4.28%) and 0.0625 mg/mL(40.50 ± 4.72%) which may be due to the fact that more NPs were available for protein binding. For the ST NPs the highest ($p < 0.05$) mean % protein binding occurred at a concentration of 0.25 mg/mL(55.73 ± 2.81%), whereas 1 mg/mL and 0.0625 mg/mL had % protein binding of 17.31 ± 6.18% and 33.10 ± 6.85% respectively. With respect to the TT NPs, as the NP concentration increased the % protein binding also increased, i.e. 20.09 ± 6.14%, 14.57 ± 5.66%, and 5.33 ± 4.52% for 1 mg/mL, 0.25 mg/mL and 0.0625 mg/mL respectively. A minor decrease ($p > 0.05$) in mean % protein

http://etd.uwc.ac.za/

binding was observed as the NP concentration was increased for TST NPs, i.e. 18.45 ± 3.69%, 16.92 ± 3.74% and 31.91 ± 11.41% for 1 mg/mL, 0.25 mg/mL and 0.0625 mg/mL respectively. It could be speculated that with higher NP concentration less protein binding was observed due to saturation of surface of NPs occurring with the same amount of HSA used. Hence, some of the NPs surfaces became free from HSA.

In summary, the highest percent protein binding was observed with SP and ST NPs, thereafter a decrease in percent protein binding occurred with TT and TST NPs, which could be explained by the process that likely takes place during the interaction of HSA and surfactant at the particle surface. Most likely the surfactant-HSA interaction at the NP surface also consists of electrostatic and hydrogen bonding interactions. In this approach SP NP showed a high binding affinity to HSA which could be attributed to the Span 80 and PVA combination. The decrease in percent protein binding in TPGS stabilized NPs i.e. ST, TT and TST, was likely due to the TPGS which contains a long hydrophilic PEG chain. It is known that PEG chains attached to a surface increase the blood circulation $t_{1/2}$ of nanocarriers by reducing unspecific protein interactions [166]. Unlike pure PEG, TPGS contains an alkyl chain and may therefore prefer binding to hydrophobic pockets of HSA; this could be the reason for the percent protein binding which was observed in TPGS NPs. There was no significant difference in the mean percent of protein binding as the incubation time extended to 1 and 6 h, for all NP formulations; this could be the result of protein saturation on the NP surface.

It can be concluded that the type of available groups on particle surfaces have a significant effect on the protein binding properties of NPs.

http://etd.uwc.ac.za/

CHAPTER 4

Preparation and Characterisation of Propranolol-HCL loaded PCL NPs

4.1 Introduction

This chapter focuses on the methods of preparation and characterisation of propranolol loaded PCL NPs, as well as the quantification of propranolol loading in NPs. The effect of surfactant type on propranolol loading is investigated. Finally determination of kinetics of propranolol release from NPs is investigated. The results obtained are presented and discussed.

4.2 Aims

- Preparation and characterisation of propranolol loaded PCL NPs.
- To investigate the effect of surfactant type on the loading of propranolol in PCL NPs.
- To determine the kinetics of release of propranolol from PCL NPs.

UNIVERSITY of the
WESTERN CAPE

4.3 Hypothesis

It was hypothesised that surfactant type modulates the encapsulation efficiency and kinetics of release of propranolol from PCL NPs.

4.4 Materials

4.4.1 Equipment and Materials

The following equipment was used:

Analytical balance (Mettler®, model PE 6000); Centrifuge (Centrifuge 5417, Eppendrof AG 22331, Hamburg, Germany); Freeze-dryer (Virtis, Freeze mobile model 125L); Malvern

http://etd.uwc.ac.za/

instruments, Ltd.,UK); Probe sonicator (Sonoplus GM 2070, Bandelin, Germany); Ultra-sonic bath (Model 702 Voltage 2030v, 100W, LABOTEC, South Africa); pH meter (Basic 20, Lasec, South Africa); Rotary evaporator (Buchi, Labotec, South Africa); Scientific balance (Ohaus®, model GA 110); Thermomixer (Comfort, Eppendrof, Germany); UV-visible spectrophotometer (UV spectra were recorded on a Cintra® 2.2 GBC Scientific Equipment Pty. Ltd. UV/visible spectrophotometer); Magnetic stirrer, multi positions-Multistirrer series, VELP Scientifica®, USA connected with fixed heating circulator, (Julabo®, USA); High speed homogeniser (IKA® T18 digital Ultra Turrax®, Germany); Infrared (FTIR) (Perkin Elmer Spectrum 400 FT-IR Spectrometer). The analysis of the spectra conducted used Spectrum software version 6.3.5); Differential scanning calorimeter (DSC) (Perkin Elmer differential scanning calorimeter DSC7 connected with a Perkin Elmer thermal analysis controller TAC7/DX and Perkin Elmer thermal analysis gas station.); Vortex Mixer (Benchmark Scientific Inc. BV1000 vortex mixer, Taiwan);

UNIVERSITY of the
WESTERN CAPE

The following chemicals were used:

Poly (ε-caprolactone) polymer (average Mw ~ 14,000 g/mol, average Mn ~ 10,000 by GPC, flakes, Sigma-Aldrich); Span 80 (clear, yellow viscous liquid, purity ≥ 60% and saponification value 145-160, Sigma-Aldrich); D-α-Tocopherol polyethylene glycol 1000 succinate (BioXtra, water soluble vitamin E conjugate, MP: > 36°C, solubility in H_2O: soluble 1 g/10 mL, clear to faintly turbid. Sigma-Aldrich); Poly (vinyl alcohol) (average Mw 13,000-23,000, 98% hydrolysed, Sigma-Aldrich); Propranolol-HCL (≥ 99% TLC, powder, Sigma-Aldrich); Chloroform (analytical grade, AR Saarchem, Merck Chemicals, PTY Ltd); Distilled water (Millipore, Milford, MA, USA); D-(+)-Glucose (Mw: 180.16 g/mol mp:150-152° C Sigma-Aldrich); PBS salts; Sodium hydroxide pellet (NaOH: 40.00 g/mol B & M Scientific); Potassium dihydrogen phosphate (Mw 136.09 g/mol) Merck, Germany.

http://etd.uwc.ac.za/

4.5 Methods

4.5.1 Preparation of propranolol loaded PCL NPs

Propranolol loaded PCL NPs were prepared using the double emulsion procedure used to synthesise empty PCL NPs, as described in section 3.5.3 with modification. To prepare SP, ST, TT and TST propranolol loaded NPs, the inner aqueous phase was prepared by weighing and dissolving 20 mg of propranolol- HCl [4] in 1 mL of water and then, to prepare the organic phase, 50 mg of PCL polymer was weighed and placed in a test tube, then 5 mL solvent (chloroform) containing (4.93 mg/mL) of Span 80 was transferred into the polymer test tube, then vortexed until all the polymer was completely dissolved (~ 10 min). This step was excluded in the TT formulation synthesis since it does not contain Span 80. The rest of the procedure as described in section 3.5.3 with an additional step, the outer aqueous phase pH was adjusted to 10 (it was important for the outer aqueous phase to have pH 10 i.e. above the pKa of propranolol in order to decrease the aqueous solubility of propranolol in the outer phase). Thereafter the NPs were characterised for z-average particle size, PDI and ZP using the DLS technique and using a Malvern Zetasizer Nano ZS (Malvern instruments, Ltd., UK). Then the NPs were freeze dried as described in section 3.5.3.1.

4.5.2 Characterisation of propranolol loaded NPs

The z-average particle size, PDI and ZP of the propranolol loaded PCL NPs were analysed by DLS using a Malvern Zetasizer Nano ZS (Malvern instruments, Ltd., UK). The procedure used to characterize the empty, i.e. non-propranolol loaded PCL NPs described in section 3.5.2 was used.

http://etd.uwc.ac.za/

4.5.3 Quantitation of propranolol loading in NPs

For the quantitation of encapsulated propranolol in PCL NPs, a UV-visible spectrophotometric (UV-vis) method was used, based on the measurement of absorbance of propranolol at 290 nm in a mixture of solvents (methanol: water: chloroform) at a ratio of 7:2:1. It should be noted that, after dissolving PCL-propranolol loaded NP samples in methanol, a precipitant was observed, which was likely due to the PCL polymer. Therefore it was necessary to dissolve NPs in a mixture of solvents since propranolol dissolves in methanol and water and PCL dissolves in chloroform. The water in this solvent mixture was a supernatant of empty NPs, where the suspension of empty NPs was centrifuged and the supernatant and used as part of the solvent mixture to prevent the excipients from interfering in the quantification of propranolol. The UV-vis method was validated (section 4.5.4.2) according to the International Council on Harmonisation (ICH) guidelines for validation of an analytical procedure to determine linearity, accuracy and precision [169].

UNIVERSITY of the
WESTERN CAPE

4.5.3.1 Determination of drug loading

Propranolol was extracted from the NPs by continuously sonicating the freeze-dried NPs (1 mg/mL) in methanol: water: and chloroform with a ratio 7:2:1 [170] at intensity of 85% for 5 min. The sample was analysed by DLS using a Malvern Zetasizer Nano ZS to confirm that the NPs were destroyed. The sample was then centrifuged at 3000 rpm for 45 min, and thereafter the supernatant was collected and analysed for propranolol concentration using a validated UV-vis method described in section 4.5.3.2.

The theoretical percentage of drug loading (DL *theoretical*), actual percentage of drug loading (DL *actual*), and encapsulation efficiency (EE%) were calculated using equations 4.1, 4.2 and 4.3, respectively [171].

http://etd.uwc.ac.za/

$$\mathbf{DL}_{\textit{theoretical}}\ \mathbf{(\%)} = \frac{\textbf{Mass of drug added to formulation (mg)}}{\textbf{Mass of drug incorporated (mg)+mass of polymer +surfactant+glucose (mg)}}\ \mathbf{x100} \qquad \text{(Eq. 4.1)}$$

$$\mathbf{DL}_{\textit{actual}}\ \mathbf{(\%)} = \frac{\textbf{Mass of drug encapsulated in NPs (mg)}}{\textbf{Mass of NPs (mg)}}\ \mathbf{x\ 100} \qquad \text{(Eq. 4.2)}$$

$$\textbf{Encapsulation efficiency (EE\%)} = \frac{\textbf{DLC actual}}{\textbf{DLC theoretical}}\ \mathbf{x100} \qquad \text{(Eq. 4.3)}$$

4.5.3.2 Validation of UV-vis analytical procedure for quantitation of propranolol in NPs

Analytical method validation is an important regulatory requirement in pharmaceutical analysis. Method validation provides documented evidence, and a high degree of assurance that an analytical method employed for a specific test is suitable for its intended use.

A stock solution of propranolol-HCL (200 µg/mL) was prepared in a mixture of solvents, mixed in the ratio 7:2:1 of methanol, water, and chloroform respectively. A calibration curve was constructed by measuring the absorbance at 290 nm of solutions of five different concentrations of the propranolol solution (10, 20, 30, 40 and 50 µg/mL) by dilution with the methanol: water: and chloroform mixture with a ratio 7:2:1. Two calibration curves were made, one with propranolol in solvent (methanol, water, chloroform), and another using the NP supernatant after break-up of the NPs (in case the propranolol absorbance in pure solvent was differed from that in the presence of excipients used to synthesise the NPs).

Standard solutions were freshly prepared each day by appropriate dilution of the stock solutions with the solvent mixture (methanol: water: chloroform). Concentrations over the range 10–50 µg/mL were prepared. The complete procedure was repeated over three consecutive days. The absorbance of these diluted solutions were measured with a UV-vis spectrophotometer (UV-vis spectra were recorded on a Cintra® 2.2 GBC Scientific

http://etd.uwc.ac.za/

Equipment Pty. Ltd. UV-vis spectrophotometer); model spectrophotometer at 290 nm using methanol: water: chloroform as a blank. Linearity was determined by plotting propranolol concentration against absorbance using Graph Pad Prism version 6.01 Software.

A calibration curve was made with propranolol in methanol, water, chloroform. The water part in this mixture was NP supernatant after break-up of the NPs (in case the propranolol absorbance in the pure solvent was different from that in the presence of excipients used to synthesize the NPs).

Accuracy was assessed by analysing standard samples in triplicate at three different concentrations levels covering the linearity range, and comparing the measured value to the true value. Deviation of the concentration determined by the measured and the actual values was calculated as a percentage (% RSD) [172]. Precision was determined with standard samples in triplicate at three different concentration levels covering the entire linearity range. The precision was calculated by intraday (reproducibility) and inter-day (intermediate precision) and reported as % RSD.

UNIVERSITY of the
WESTERN CAPE

4.5.4 Differential Scanning Calorimetry (DSC): Thermo analytical analysis of the NPs

DSC was used to analyse the thermal behaviour of different samples and the physical status of the drug inside the NPs. DSC analysis provided an indication of whether the encapsulation of propranolol occurred by chemical interaction or not, as well as the form of drug inside the NPs. DSC was calibrated using indium as the standard. Samples of the drug, individual components of the NPs and drug loaded NPs, were analysed using DSC. Samples (2-5 mg) were accurately weighed and heated in sealed aluminium pans and an empty pan was used as a reference. The samples were scanned from 50 to 300°C at a scanning rate of 10°C/min. Nitrogen was used for purging the sample holders at a flow rate of 20 ml/min. Analysis was

http://etd.uwc.ac.za/

conducted, firstly with samples of pure polymer and propranolol-HCL pure drug, then loaded NPs were analysed and compared for possible drug-polymer interactions.

4.5.5 Fourier Transform Infrared spectroscopy (FTIR) analysis of NPs

FTIR analysis was conducted to verify the possibility of the interaction of chemical bonds between drug and polymer. The FTIR spectrum was performed by using a PerkinElmer 1600 USA spectrophotometer with a resolution of 2 cm^{-1}. Samples of pure drug, polymer, surfactants, and drug loaded formulations were scanned in the spectral region between 4000 and 400 cm^{-1} by taking an average of three scans per sample. Solid powder samples were used and pressed at 15000 psig. For the analysis of the data, the spectrum GX series model software was used.

UNIVERSITY of the
WESTERN CAPE

4.5.6 Determination of kinetics of propranolol release from NPs

Propranolol release from the NPs was evaluated in PBS pH 7.4 using the modified sample and separation method described by [173] and [174]. Freeze dried NPs suspended in PBS (20 mg/mL) were placed in separate tubes; each tube representing a time point over the range 0.5 – 48 h. The nanosuspensions were incubated at 37°C under mild agitation (using a Magnetic stirrer, multi positions-Multistirer series, VELP Scientifica®, USA connected with fixed heating circulator, Julabo®, USA). At specific time intervals (0.12, 0.25, 0.50, 1, 3, 6, 24 and 48 h), the representative tube was removed from incubation and centrifuged at 20817 *x* g for 15 min, the supernatant was then analysed to assess the amount of drug released by measuring the UV absorbance at 290 nm using a UV-vis spectrophotometer (UV spectra were recorded on a Cintra® 2.2 GBC Scientific Equipment Pty. Ltd. UV-vis spectrophotometer).

http://etd.uwc.ac.za/

4.5.6.1 Validation of UV-vis assay of propranolol-HCL in PBS pH 7.4

The assay was validated in accordance with ICH requirements for precision, linearity, and accuracy, as performed in section 4.5.3.2. The calibration curve of the drug (10-50 µg/mL) was constructed to determine concentration from the absorbance at 290 nm with PBS 7.4 as blank, n=3. Precision and accuracy were calculated as mentioned in section 4.5.3.2.

4.5.6.2 Determination of the kinetics of drug release

The profiles of the release of biologically active compounds from NPs can provide important information concerning the mechanisms involved [136]. Kinetics of propranolol release were determined, then in order to analyse the drug release mechanism, *in-vitro* release data were fitted into a zero-order, first order, Higuchi, Hixon-Crowell cube root law, Korsmeyer-Peppas model and Weibull model [175] using DDSolver software. DDSolver is a menu-driven add-in program for Microsoft Excel written in Visual Basic for Applications. The DDSolver program was developed to facilitate the modelling and comparison of drug dissolution data [140].

UNIVERSITY of the
WESTERN CAPE

4.6 Results and discussion

4.6.1 Properties of the propranolol loaded PCL NPs

The z-average particle size, PDI and ZP for the propranolol loaded PCL NPs SP (PVA, Span 80), ST (Span 80, TPGS), TT (TPGS in W1 and W2) and TST (TPGS, Span 80 and TPGS) were analysed by DLS techniques using a Zetasizer Nano ZS. (Malvern Instrument, UK). Figure 4.1 shows that the z-average particle size and PDI were significantly affected by the type of surfactant.

http://etd.uwc.ac.za/

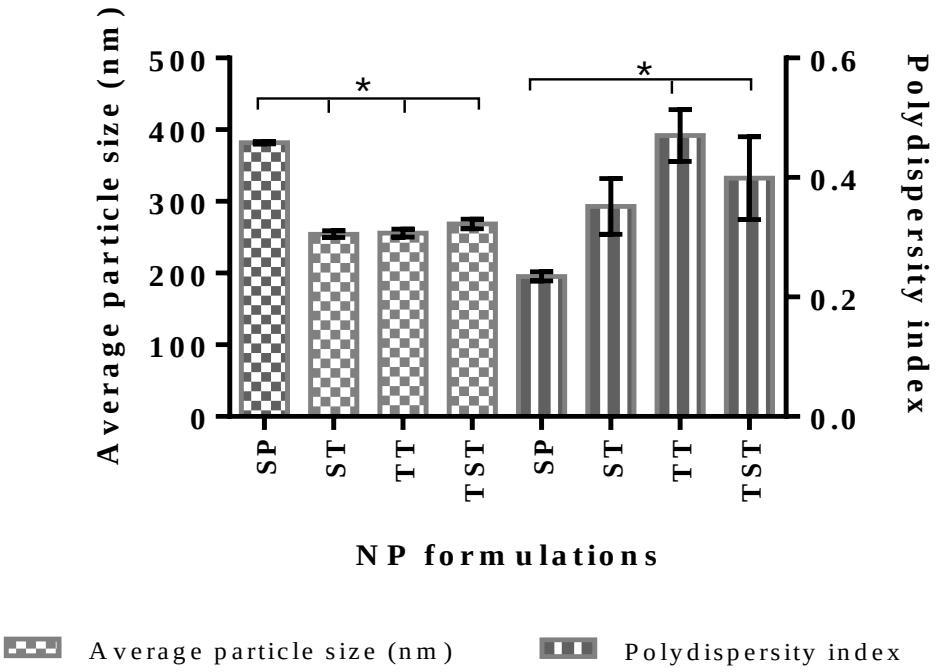

Figure 4.1 *Z-average particle size and PDI of propranolol loaded PCL NPs, SP (PVA + Span 80), ST (Span 80 + TPGS), TT (TPGS in W1 and W2) and TST (TPGS + Span 80 + TPGS). (Results shown as mean ± SD; n=3. (*) P < 0.05).*

UNIVERSITY of the
WESTERN CAPE

SP NPs had the highest mean size of 381.80 ± 1.56 nm among the NP formulations ($p < 0.05$). There was a decrease ($p < 0.05$) in NP mean size with the other three NP formulations which were prepared with TPGS surfactant namely ST, TT and TST, i.e. 254.40 ± 4.91 nm, 255.80 ± 5.37 nm, and 268.40 ± 6.65 nm, respectively. Similar results were obtained by [145] as they reported that TPGS at 0.03% (w/v) as emulsifier in preparation of PLGA NPs resulted in NP size of 272.56 ± 169.5 nm. It was shown that, in general, the size of NPs was smaller when fabricated with 0.03% (w/v) TPGS as emulsifier and that the PDI at this emulsifier concentration was narrower than those of the NPs fabricated at higher concentration.

In comparison with the empty PCL NPs, the size of propranolol loaded NPs were not significantly different from the empty NPs ($p > 0.05$), section 3.6.3 and Figure 3.4. These

http://etd.uwc.ac.za/

results are correlated with those observed by Verrachia *et.al*, 1995 [176]. Indeed these authors stated that propranolol in the internal phase acted as a surfactant. Since the particle size is related to a great extent to the stability of the first emulsion, the authors claimed that the drug can act as a surfactant by stabilising the first emulsion and consequently hampering the fast coalescence of the droplets. The chemical structure of propranolol-HCL, a hydrophilic molecule with a hydrophobic aliphatic chain, may confer a relative amphiphilic property to the drug which could behave as a surfactant [179]. Hence there was no significant increase in drug loaded particle size.

PDI was measured and the size distribution was obtained for each NP formulation (Figure 4.1). The PDI values were within the range of 0.23 ± 0.01 and 0.47 ± 0.04. The PDI values obtained were all below 0.5 (Figure 4.1), indicating good particle homogeneity.

Figure 4.2, shows that the propranolol loaded PCL NPs also possessed a negative ZP. ZP values were -57.43 ± 0.15, -43.97 ± 2.52, -30.23 ± 1.21 and -52.07 ± 1.24 mV for SP, ST, TT, and TST, respectively.

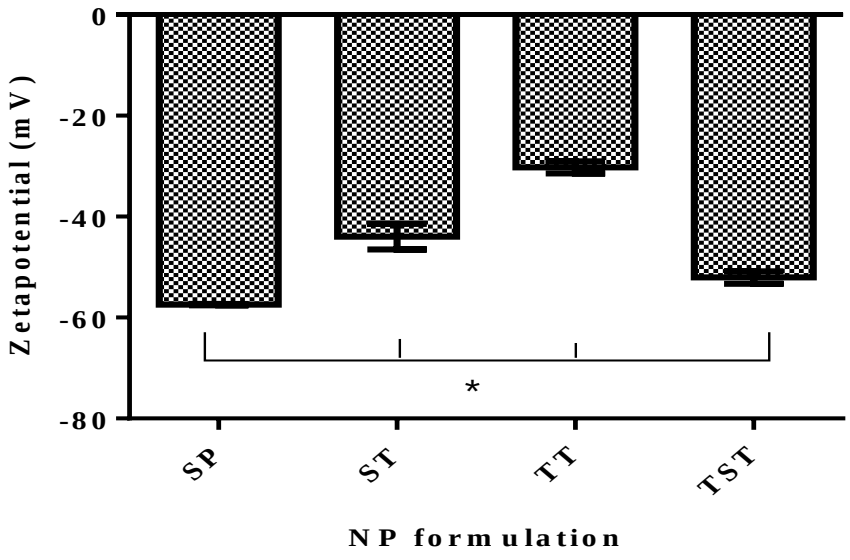

http://etd.uwc.ac.za/

Figure 4.2 *ZP values of propranolol loaded PCL NPs, SP (PVA + span 80), ST (span 80 + TPGS), TT (TPGS in W1 and W2) and TST (TPGS + span 80 + TPGS). Results shown as mean ± SD; n=3. (*) p < 0.05.*

In comparison with the empty PCL NPs obtained in Chapter 3 (section 3.6.3, Figure 3.5) the ZP values of propranolol loaded NPs were found to be significantly higher than empty NPs. The reason could be due to the presence of cationic groups of propranolol in the surface of NPs.

All four propranolol loaded formulations (SP, ST, TT, and TST) were freeze dried for 72 h. Using glucose as the cryoprotectant resulted in the formation of a white, brittle, crystalline material upon lyophilisation, and showed good redispersibility within a few minutes upon manual shaking. Z-average particles size was measured after redispersion of a specific amount of freeze dried NPs in 1 mL deionized water then dispersed using a vortex for 5 min. It was found that the particle size had not changed after the freeze drying process.

UNIVERSITY of the
WESTERN CAPE

In summary, a small particle size with a relatively monodisperse size distribution was obtained when TPGS was used as an aqueous surfactant compared with the Span 80 and PVA formulations. This finding suggests that TPGS is more efficient in stabilising propranolol loaded PCL NPs.

4.6.3 Quantitation of propranolol loading in NPs

4.6.3.1 Validation of UV-vis analytical procedure for quantitation of propranolol in NPs

Absorbance of various concentrations of propranolol-HCL, were measured and a graph was plotted with absorbance against concentration as shown by the calibration curve in Figure 4.3.

http://etd.uwc.ac.za/

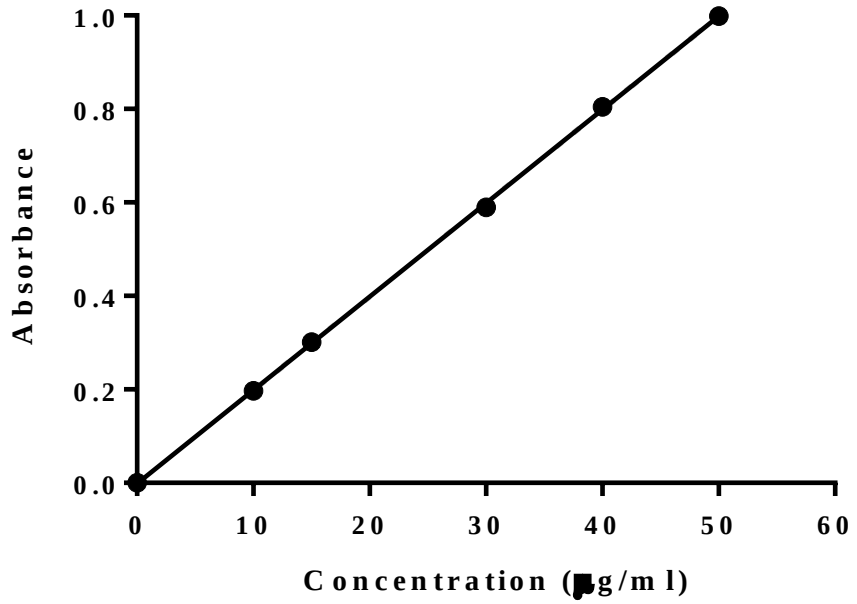

Figure 4.3 *Propranolol-HCL calibration curve in methanol: water: chloroform (7:2:1).*

Linearity was found in the range 10-50 µg/mL with correlation coefficient (r^2) 0.9998, indicating good linearity. Precision and accuracy data for propranolol assay are shown in Tables 4.1 and 4.2. The %RSD for the standard was less than 2%, indicating that the method was precise for the assay of propranolol.

UNIVERSITY of the
WESTERN CAPE

Table 4.1 *Intra-day and inter-day precision of the propranolol assay.*

Concentration (µg/mL)	Intra-day precision RSD (%)	Inter-day precision RSD (%)
10	0.47	0.47
30	0.32	0.03
50	0.17	0.15

http://etd.uwc.ac.za/

Table 4.2 *Accuracy and recovery data for quantification of propranolol.*

Given (µg/mL)	Found mean ± SD (µg/mL)	% Recovery	Accuracy (% Deviation)
10	9.68 ± 0.12	96.80	-3.20
30	28.12 ± 0.17	93.73	-6.27
50	49.27 ± 0.30	98.50	-1.45

The percent deviation was not more than 2%, thus displaying negative values because the concentration value results were smaller than the given values.

UNIVERSITY of the
WESTERN CAPE

4.6.3.2 Determination of propranolol loading and encapsulation efficiency in NPs

The double emulsion techniques for encapsulating hydrophilic drugs into PNPs generally suffer from low EE%, which is due to the drug rapidly penetrating from the inner aqueous phase to the external aqueous phase [148]. In order to improve the encapsulation of hydrophilic drugs, we used a modified double-emulsion solvent evaporation technique in which two surfactants were introduced into the emulsion process. The four NP formulations (SP, ST, TT, and TST) were characterised for propranolol EE%; the results are shown in Table 4.3.

http://etd.uwc.ac.za/

Table 4.3 *DL theoretical %, DL actual % and EE% of propranolol in the NP formulation results shown as mean ± SD; n=3.*

NP formulations	DL *theoretical* (% w/w)	DL *actual* (% w/w)	EE%
SP	5.80	0.44 ± 0.04	7.56 ± 0.64
ST	16.04	1.71 ± 0.09	10.68 ± 0.54
TT	20.00	3.15 ± 0.01	15.74 ± 0.56
TST	16.04	5.91 ± 0.19	36.85 ± 1.16

From the mass of the incorporated drug, polymer, surfactants and excipients, the theoretical drug loading (DL *theoretical*) of all NP formulations were calculated from Eq. 4.1, giving the results that are shown in Table 4.3. The EE% of the NPs was calculated from Eq. 4.3 based on the DL theoretical/actual drug loading (DL *actual*) ratios that are shown in Table 4.3.

UNIVERSITY of the
WESTERN CAPE

The lowest EE% was found in the SP formulation (7.56 ± 0.64%) and the higher EE% within the TPGS containing formulations (i.e. 10.68 ± 0.54%, 15.74 ± 0.56%, and 36.85 ± 1.16% for the ST, TT, and TST formulations respectively). TST formulation had the highest EE%. This formulation contains TPGS in the inner and the outer aqueous phase and Span 80 in the 'oily' phase. We speculate that this composition could result in the formation of stronger film around the particles that prevented leaching out of the drug.

In the literature, PNPs are usually prepared using PVA as emulsifier which has been found to have disadvantages including low emulsification efficiency, and difficulty in removing during the washing process [96]. However, we have found that the use of TPGS provides significantly higher encapsulation of propranolol than PVA.

http://etd.uwc.ac.za/

The low (less than 50%) drug EE% may be attributed to the water soluble nature of propranolol. This could have led to its rapid partitioning into the external aqueous phase and hence decreased entrapment into the NPs during polymer deposition. The large surface area of the NP geometry may have also contributed to loss of drug in the aqueous phase during preparation. Low drug incorporation efficiency of 14.5% of another water soluble drug, procaine hydrochloride, into PLGA NPs has also been reported by Govender *et.al,* 1999, [177]. Also, similar EE% values were observed by Niwa *et.al,* 1994.[142], who encapsulated a water soluble drug, nafarelin acetate, into PLGA NPs by the spontaneous emulsification solvent diffusion method. These researchers attributed the decreased drug encapsulation efficiency to the drug leakage in the aqueous phase which may apply to this study.

Increasing the pH of the external aqueous phase above the pKa of the propranolol is likely to result in a decreased degree of propranolol ionisation, therefore rendering propranolol less soluble in the aqueous external phase than in the inner aqueous phase. This may have therefore reduced the migration of drug into the external aqueous phase at pH 10, enhancing drug entrapment in the PCL NPs. Indeed, Jones and Pearce, 1995 showed that only 2% of propranolol (w/w) was entrapped in ethylcellulose particles prepared at pH 5 whereas an encapsulation efficiency of 50% was obtained at pH 10 [178]. This is the reason why a pH of 10 was selected for propranolol encapsulation (see section 4.5.1).

UNIVERSITY of the
WESTERN CAPE

4.6.5 Differential Scanning Calorimetry (DSC)

Any possible drug–polymer interaction(s) as well as the physical changes which occur in the drug or polymer can be studied using thermal analysis [179]. DSC is the most common thermal analysis technique in which the heat flow rate difference into a substance and reference is measured as a function of temperature, while the sample is subjected to a controlled temperature program. DSC experiments were carried out to define the physical

http://etd.uwc.ac.za/

state of the polymer and the drug in the formulation and to check for the possibility of any interactions between the drug and the polymer within the matrix.

Samples of the individual compounds, i.e. TPGS, PCL, propranolol, glucose and PVA, were determined as shown in Figure 4.4. Thereafter, propranolol loaded NPs (SP, ST, TT and TST) were also characterised with DSC and the results are shown in Figure 4.5. Span 80 was not included because it is a liquid, and it was not possible to analyse a sample in a liquid form using DSC.

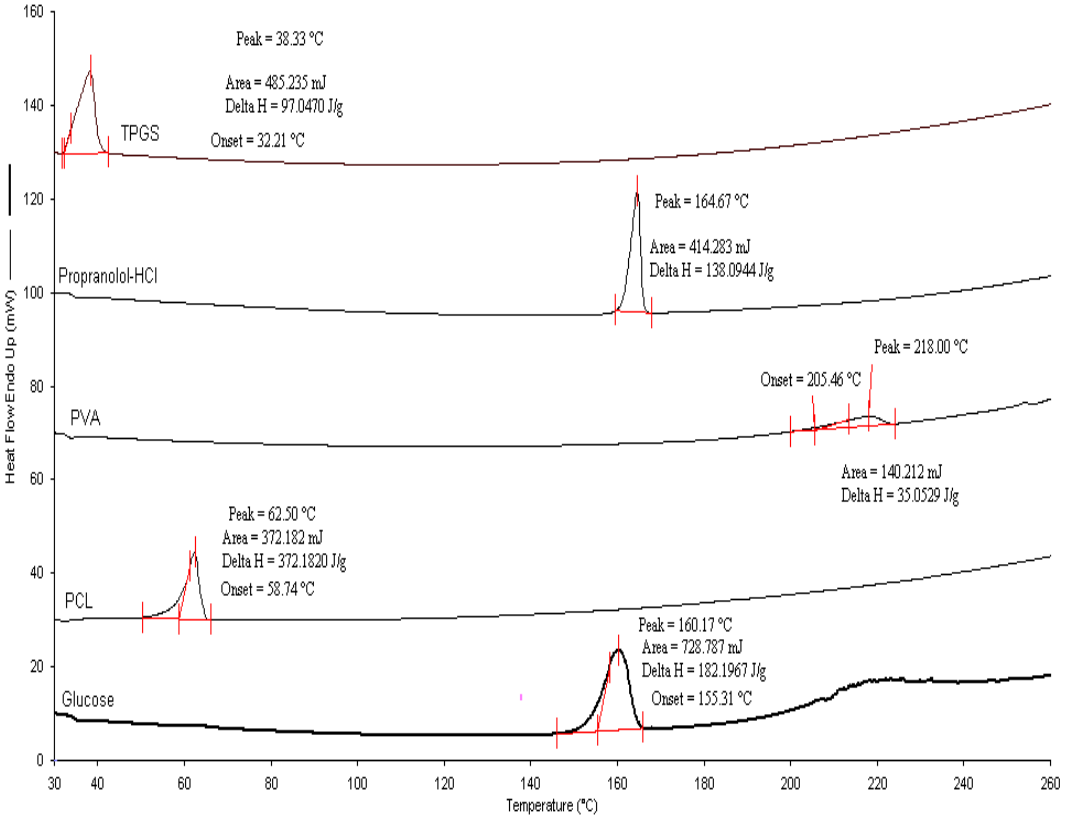

Figure 4.4 *DSC thermograms of individual compounds; (TPGS, PCL, propranolol, glucose and PVA).*

As observed in Figure 4.4, propranolol had a melting temperature of 164.67°C and a heat of fusion of 145.428 J/g. The semi crystalline polymer PCL was characterised by a melting peak

http://etd.uwc.ac.za/

at 62.50°C. Both these findings are well-known and were expected as observed by [146] and [4]. In the case of propranolol loaded NPs (Figure 4.5), a shift to much lower values of the drug's melting point with much wider peaks was observed due to a slower transition before reaching the melting point of the polymer. Values of 158.50°C, 149.00°C, 149.33°C, and 150.00°C for SP, ST, TT, and TST, respectively, were observed for the melting temperature of the drug loaded NPs. The drop in the melting temperature of the drug loaded NPs could be induced by interactions between propranolol HCL and the polymer as reported by [4].

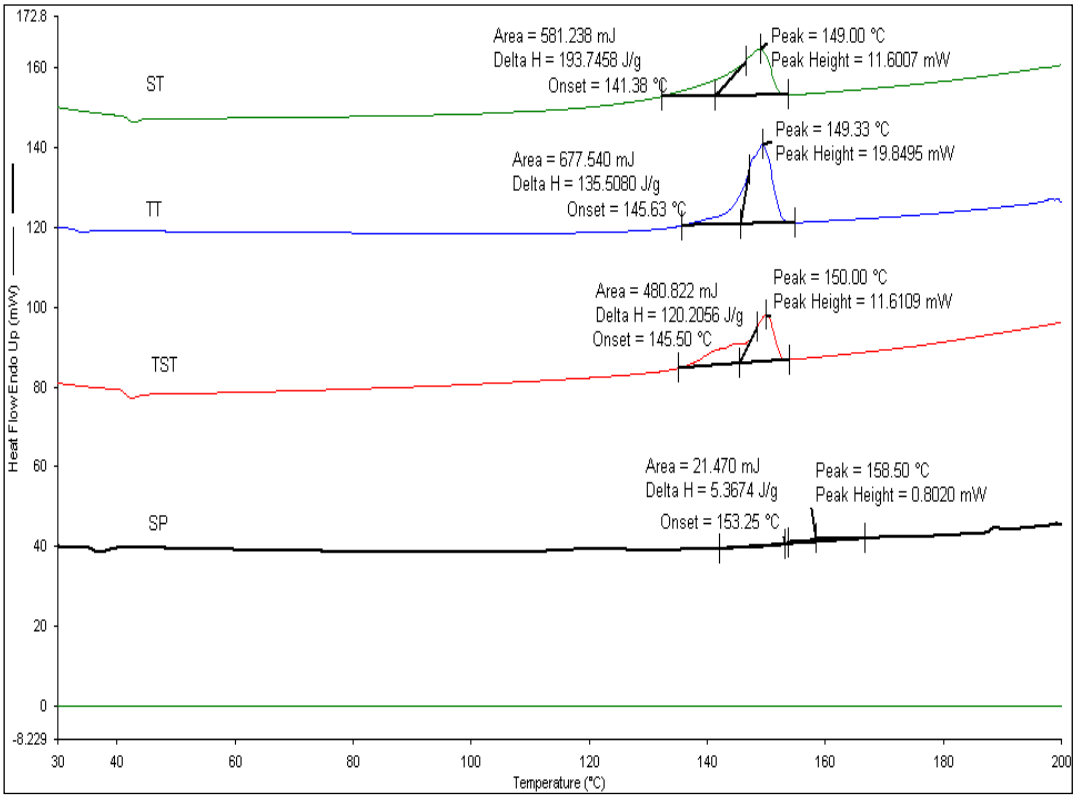

Figure 4.5 *DSC thermograms of propranolol loaded PCL NP formulations (SP, ST, TT and TST).*

http://etd.uwc.ac.za/

4.6.6 Fourier Transform Infrared spectroscopy (FTIR) of NPs (*Drug–polymer interactions)*

Using FTIR analysis, it is possible to obtain information about the occurrence of possible interaction(s) between substances involved in a nanocarrier system [179]. Generally, the interaction between drug and polymer is investigated through the band shifts exerted by the functional groups as well as through broadening in IR spectra compared to their individual spectra [179]. To confirm the presence of any interactions between propranolol and polymer, the FTIR spectra of propranolol loaded NP formulations were compared with pure drug and individual polymers.

As shown in Figure 4.6, the FTIR spectrum of propranolol showed a characteristic secondary amine –NH stretch at 3277.03 cm^{-1}, a C–H stretch at 2806.90 cm^{-1}, an aryl C=C stretch at 1579 cm^{-1}, an aryl O–CH2 asymmetric stretch at 1240 cm^{-1}, an aryl O–CH2 symmetric stretch at 1030 cm^{-1} and a peak at 797 cm^{-1} due to alpha-substituted naphathalene; this finding is in agreement with Srikanth *et. al*, 2012 [180].

UNIVERSITY of the
WESTERN CAPE

http://etd.uwc.ac.za/

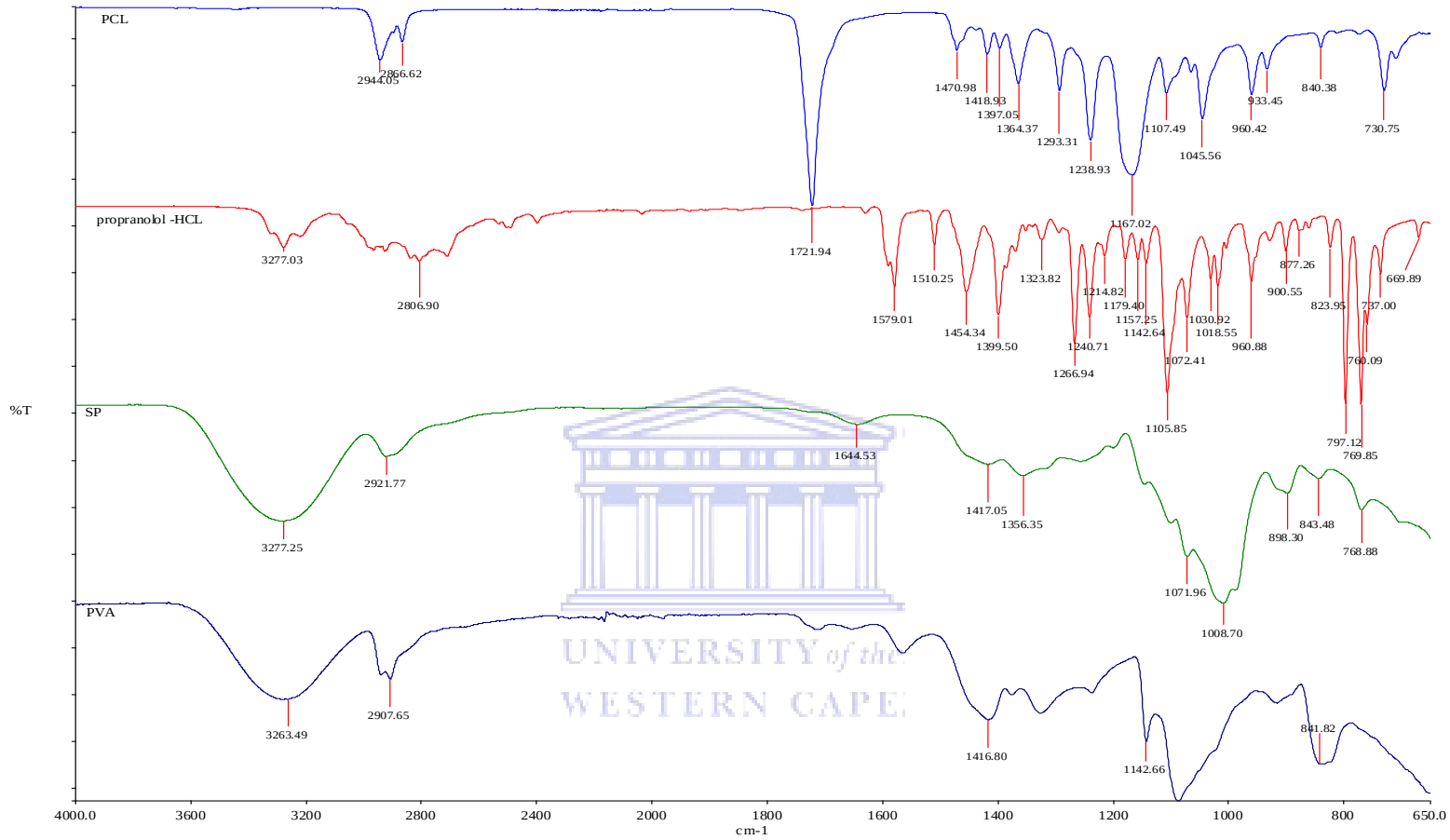

Figure 4.6 *FTIR spectra of PCL, propranolol-HCL, PVA and SP drug loaded NPs.*

http://etd.uwc.ac.za/

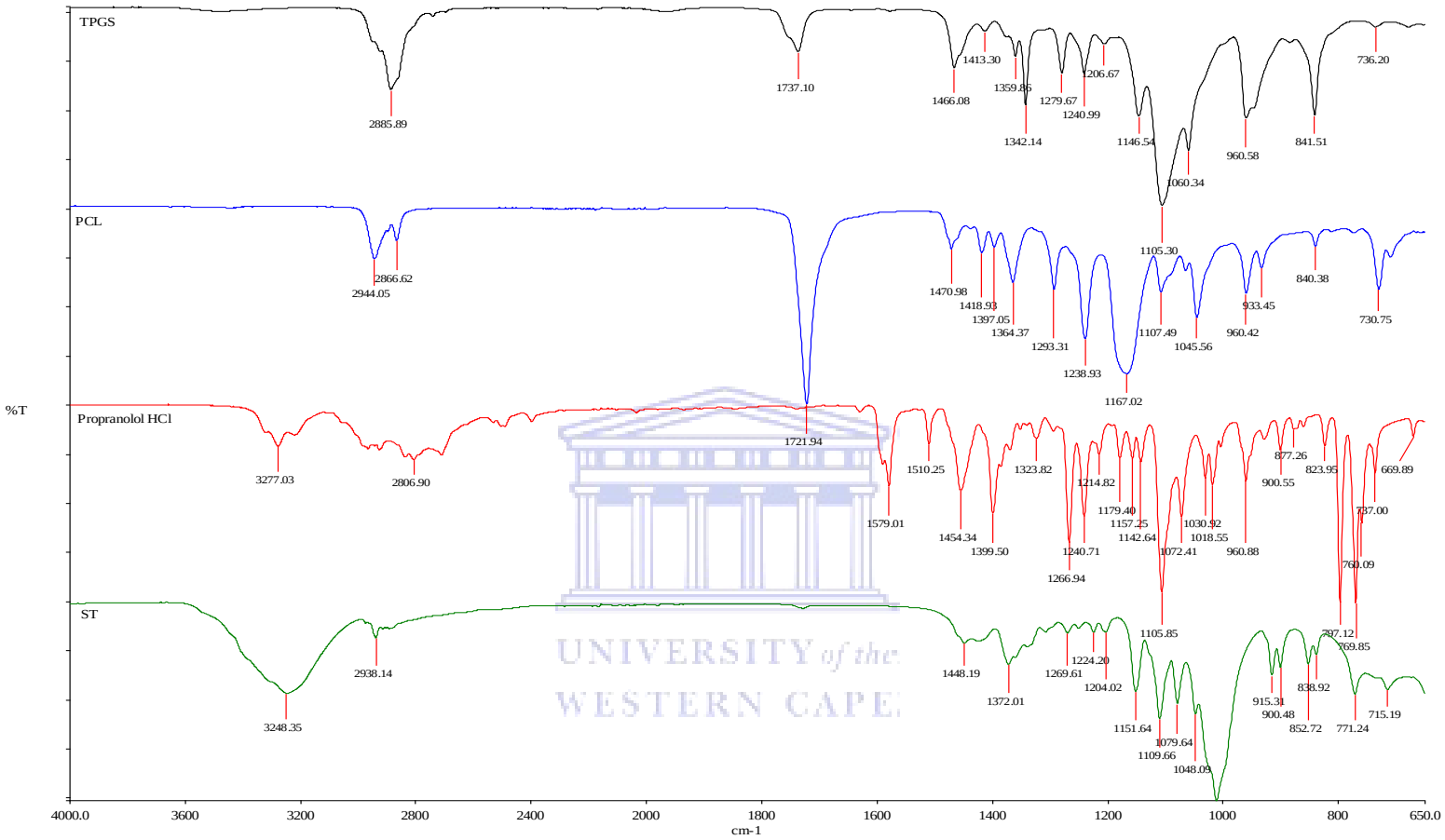

Figure 4.7 *FTIR spectra of PCL, propranolol-HCL, TPGS and ST drug loaded NPs.*

http://etd.uwc.ac.za/

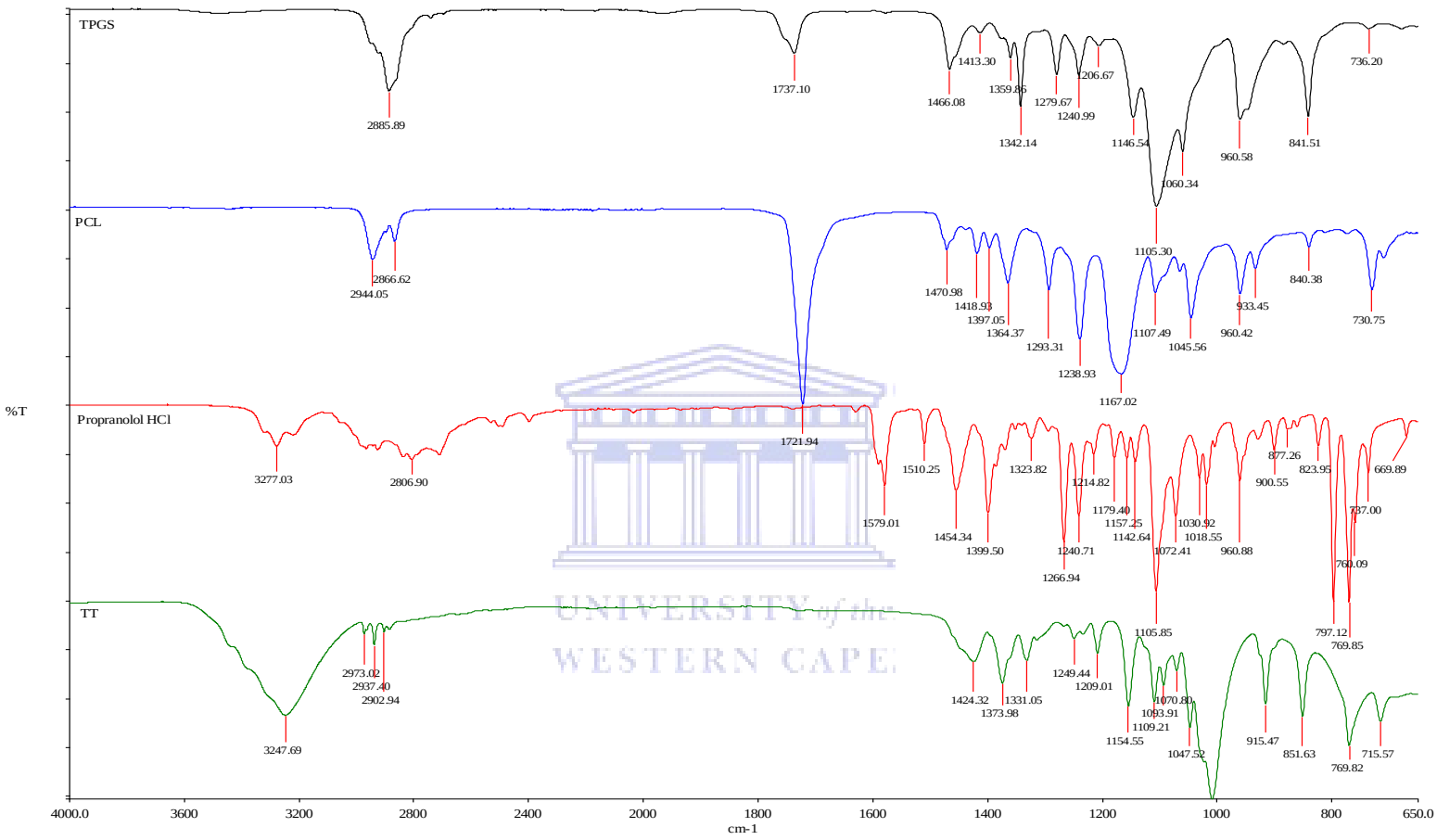

Figure 4.8 *FTIR spectra of PCL, propranolol-HCL, TPGS and TT drug loaded NPs*

http://etd.uwc.ac.za/

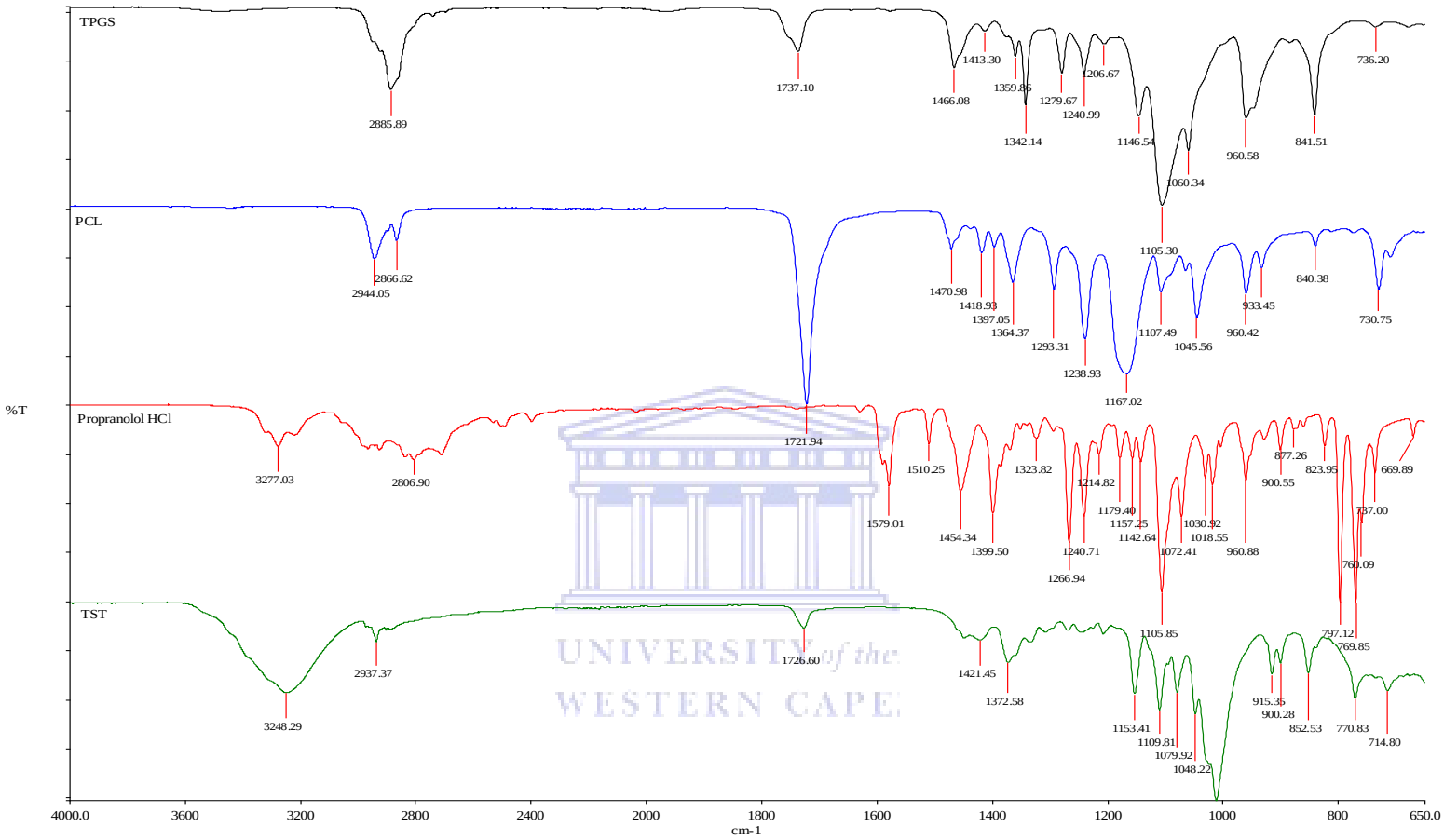

Figure 4.9 *FTIR spectra of PCL, propranolol-HCL, TPGS and TST drug loaded NPs.*

http://etd.uwc.ac.za/

A strong broad characteristic peak at 2944.05 cm^{-1}, corresponds to –C-H stretching and the strong characteristic peak at 1721.94 cm^{-1} corresponds to -C=O stretching for the pure polymer, PCL. PVA showed a strong broad characteristic peak at 3263.49 cm^{-1} corresponding to –O-H stretching and a peak at 2907.65 cm^{-1} which corresponds to –C-H stretching.

The FTIR spectra of the drug loaded SP formulation shows a strong broad peak at 3277.25 cm^{-1} due to the shifting of –OH in PVA spectra, and a –C-H peak at 2921.77 cm^{-1} which may have come from the shifting of 2907.65 cm^{-1} and 2944.05 cm^{-1} peaks for PVA and PCL, respectively. A new peak formed at 1644.53 cm^{-1} corresponding to -C=C stretching which may have come from the shifting of the 1579.01 cm^{-1} peak for propranolol.

The FTIR spectra of ST NP formulation (Figure 4.7) showed a strong characteristic peak at 3248.35 cm^{-1} due to –OH stretch and peak at 2938.14 cm^{-1} due to shifting of 2944.05 cm^{-1} for PCL. Furthermore, there was disappearing of –C=O peak at 1737.10 cm^{-1} and 1721.94 cm^{-1} for TPGS and PCL, respectively, and disappearing of –C=C peak at 1579.01 cm^{-1} for propranolol.

The FTIR spectra for the TT NP formulation (Figure 4.8) showed a strong broad characteristic peak at 3247.69 cm^{-1} due to –OH stretch and three new peaks formed at 2973.02 cm^{-1}, 2937.40 cm^{-1} and 2902.94 cm^{-1}which correspond to –C-H stretching, and the disappearing of C=O peak at 1721.94 cm^{-1} for PCL. Similar observations were noted for TST formulation (Figure 4.9), which showed a strong broad characteristic peak at 3247.69 cm^{-1} due to –OH stretch. The second peak corresponds to –C-H stretch at 2937.37 cm^{-1} due to shifting of 2944.05 cm^{-1} for PCL. The third peak corresponds to C=O at 1726.60 cm^{-1} due to

http://etd.uwc.ac.za/

shifting in the peak's intensity of 1737.10 cm^{-1} and 1721.94 cm^{-1} for TPGS and PCL. There was disappearing of the peak C=C at 1579.01 cm^{-1} for propranolol. This observation can be explained from the effect of adsorbed TPGS as surfactant onto the drug loaded NPs.

From the FTIR spectral results, it can be concluded that there was a significant drug to polymer interaction within the NPs, which suggests the encapsulation of propranolol into PCL nanoparticles with a chemical interaction. This finding was in agreement with the finding of Ubrich *et.al*, 2004, who reported a strong propranolol -PCL interaction [4].

4.6.7 Determination of propranolol release from NPs

4.6.7.1 Validation of UV-visible assay of propranolol-HCL

The calibration curve of the propranolol in PBS pH 7.4 was constructed and linearity (Figure 4.10) was found in the range 0.2-25 µg/mLwith correlation coefficient (r^2) 0.9989. Precision and accuracy data for propranolol assay are shown in Tables 4.4, and 4.5. The % RSD for the standard was less than 2%, suggesting that the proposed method was precise for the assay of propranolol.

UNIVERSITY of the
WESTERN CAPE

http://etd.uwc.ac.za/

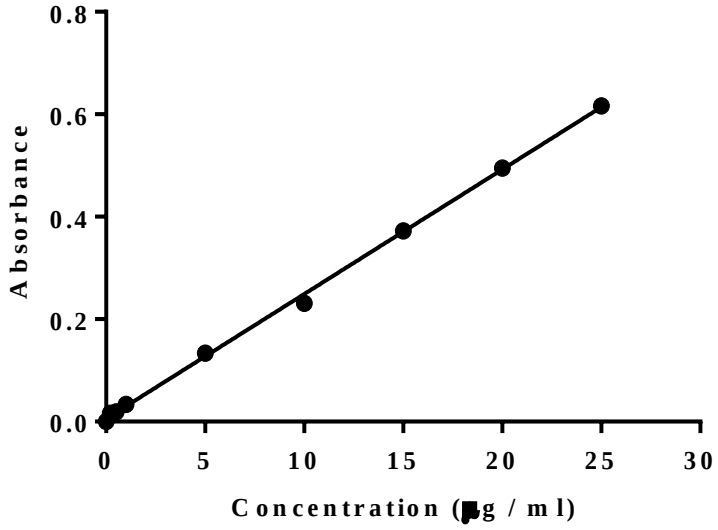

Figure 4.10 *Calibration curve of propranolol-HCL in PBS pH 7.4. Absorbance measured at 290 nm. Plot shown is the average of three runs.*

Table 4.4 *Intra-day and inter-day precision of the assay*

Concentration (µg/mL)	Intra-day precision RSD (%)	Inter-day precision RSD (%)
5	0.45	1.49
15	0.16	1.08
25	0.19	1.29

Table 4.5 *Accuracy and recovery data of the assay*

Given (µg/mL)	Found mean ± SD (µg/mL)	% Recovery	Accuracy (% Deviation)
5	4.58 ± 0.20	91.60	-8.40
15	15.01 ± 0.11	100.07	0.07

http://etd.uwc.ac.za/

25	25.03 ± 0.02	100.12	0.12

4.6.7.2 Determination of propranolol release kinetics from NPs

Drug release from a controlled release formulation often shows a biphasic release pattern and the PCL NPs were no exception (Figure 4.11). The first phase was a burst release (Figure 4.12) followed by a sustained release of propranolol. The reason for the burst release is possibly due to the release of the drug associated with the surface of the NPs [177].

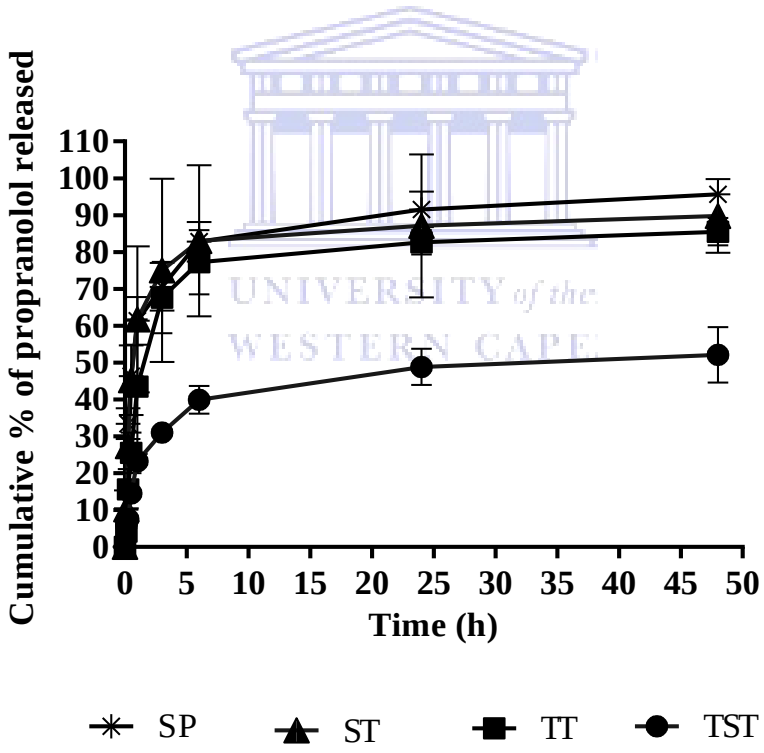

Figure 4.11 *In-vitro release of propranolol loaded NPs in PBS pH 7.4 at 37^0C over 48 h. Data shown are the mean ± SD of n=3.*

http://etd.uwc.ac.za/

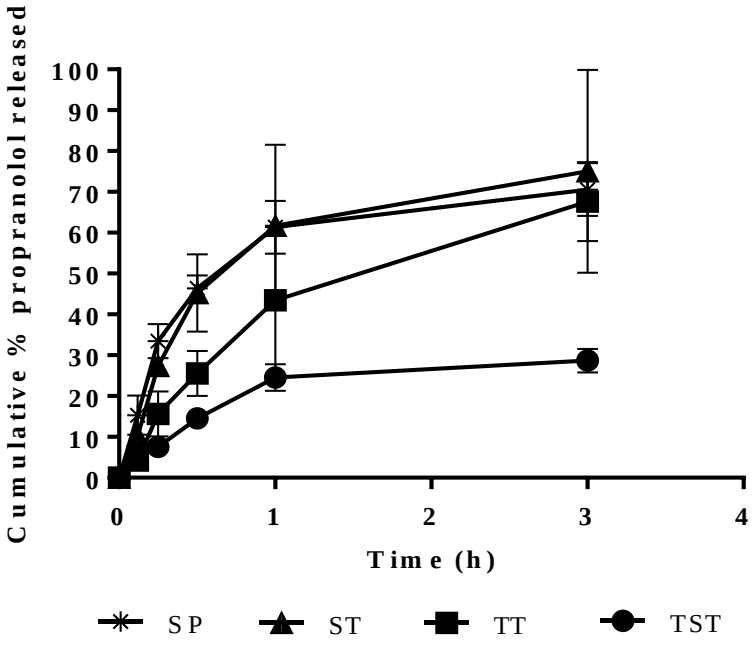

Figure 4.12 *The initial (burst) release of propranolol loaded NPs in PBS pH 7.4 at 37^0C over the first 3 h. Data shown are the mean ± SD, n=3.*

Propranolol release from NPs was found to be slow and spread over an extended period of time (48 h) and 95.66 ± 3.16%, 89.80 ± 10.01%, 85.50 ± 3.72%, and 52.14 ± 7.51% of encapsulated propranolol was released by the SP, ST, TT, and TST formulations, respectively. There was a significant difference between the % propranolol released with the TST formulation and the other three formulations ($p < 0.05$) whereas there was no significant difference in % drug released between the SP, ST, and TT formulations ($p > 0.05$). The reason could be attributed to the higher amine group's concentration of propranolol which could have interacted with TPGS and slowed down the drug release [4]. Indeed Ubrich *et.al,* 2004 compared the percent propranolol released between two NP formulations of 20 mg/mLand 60 mg/mLpropranolol concentrations used. They stated that the continuous drug released from NP60 may be attributed to the higher amine concentration in this NP60. Furthermore, it can be speculated that TPGS may have stabilised the particle surface more

UNIVERSITY of the
WESTERN CAPE

http://etd.uwc.ac.za/

efficiently and encapsulated more of the drug at the core, thereby slowing down the rate of release.

The incomplete *in-vitro* release of the drug, however, is not necessarily a disadvantage since it has been previously demonstrated that even a low and plateau release of nifedipine from PCL NPs still can yield a suitable biological activity *in-vivo* [77]. Furthermore, *in vivo*, the release from this biodegradable polymer could still be increased since there is also an enzymatic contribution to degradation of PCL. Indeed, Kedzierewicz *et.al*, 1998 have previously shown a dramatic increase in the release of a model compound in an esterase buffer medium when compared with the same free-esterase buffer medium [181].

When particles are prepared by the w/o/w method, water soluble drugs have been reported to exhibit a tendency to migrate to the aqueous medium, thereby concentrating at the surface of the particles and involving the burst effect [182][146]. Therefore, this might explain the observation made for propranolol in this study. Moreover, the burst release could also be explained by the imperfect encapsulation of the drug inside NPs, resulting from the unstable nature of the emulsion droplets during the solvent removal step. This potential instability may cause a part of the loaded drug to relocate at the NP surface, thereby being rapidly released. This effect has been reported by other research groups [183][182] and [146]. Furthermore, since PCL is a semi-crystalline polymer, water can easily penetrate the amorphous part of the polymer matrix thus facilitating the release of the water soluble drug by diffusion through pores that were created during the evaporation of the solvent from the polymer matrix [184]. Ha *et.al*, have shown that the degradation of PCL was very slow in an aqueous medium because of its semi-crystallinity and hydrophobicity [185]. This suggests that drug release was a result of diffusion and not the degradation of the polymer.

http://etd.uwc.ac.za/

Drug release from PCL NPs appeared to have two compartments with an immediate release of about 70.57 ± 6.47%, 75.03 ± 24.82%, 67.64 ± 9.68%, and 31.02 ± 1.42% for SP, ST, TT, and TST, respectively at the first three hours as shown in Figure 4.12. This was followed by a slower exponential release of the remaining drug over the next 42 hours. These findings were in agreement with Fonte *et.al*, 2012 [186] who prepared Insulin PLGA loaded NPs by the w/o/w method. The PLGA-NP after formulation released about 57% of the insulin in the first 2 h, and maintained a sustained release achieving 65% of insulin released after 48 h.

Among the four NP formulations and % propranolol release results, it could be concluded that TST formulation was more sustained in propranolol release over 48 h. This study therefore recommends that TST is the best NP formulation for delivery of propranolol.

UNIVERSITY of the
WESTERN CAPE

4.6.8 Determination of the mechanism of drug release

The release of drugs from PNPs is governed by various mechanisms, including desorption from the surface, diffusion through the pores or wall of the polymeric matrix, and disintegration, dissolution or erosion of the polymeric structure [187]. Identification of the mechanisms involved can be greatly assisted by the use of mathematical models [136].

The drug release data were fitted to various kinetic models using DDsolver software [140] in order to calculate the release constant and regression coefficients (r^2) as shown in Table 4.6.

http://etd.uwc.ac.za/

Table 4.6 *Kinetic release rate constants, correlation coefficient and diffusion exponent of various models (n=3).*

Formulation	Zero order		First Order		Higuchi model		Hixon-Crowell		Korsmeyer-Peppas			Weibull	
	r^2	K_0	r^2	K1	r^2	K_h	r^2	K_H	r^2	K	n	r^2	B
SP	0.808	0.277	0.966	0.015	0.924	5.023	0.943	0.003	0.991	7.639	0.504	0.995	0.370
ST	0.781	0.341	0.995	0.023	0.883	6.159	0.950	0.004	0.999	1.860	0.967	0.997	0.941
TT	0.847	0.295	0.988	0.012	0.931	5.184	0.969	0.003	0.992	1.471	0.909	0.987	0.603
TST	0.929	0.130	0.956	0.002	0.978	2.200	0.959	0.001	0.979	2.404	0.483	0.982	0.543

UNIVERSITY of the WESTERN CAPE

http://etd.uwc.ac.za/

4.6.8.1 Release profiles and kinetics at pH 7.4 for SP formulation

Among the models tested, the propranolol release profiles for the SP NP formulation was fitted to the Korsmeyer-Peppas model (r^2 = 0.991) (Figure 4.13). This model plots the logarithm of the cumulative percentage of drug release up to 60% versus the logarithm of time. In addition, the Weibull model (r^2 = 0.997), has been described for different dissolution processes and it is more useful for comparing release profiles of a matrix type drug release. The Korsmeyer-Peppas release exponent, *n*, for SP was 0.50. Such a value indicates that release of propranolol from the SP formulation was due to Fickian diffusion. This also seems to agree with the β value obtained from the Weibull model (β = 0.37) for propranolol release from SP NPs which was less than 0.75 and indicated that release of propranolol was by a diffusion mechanism.

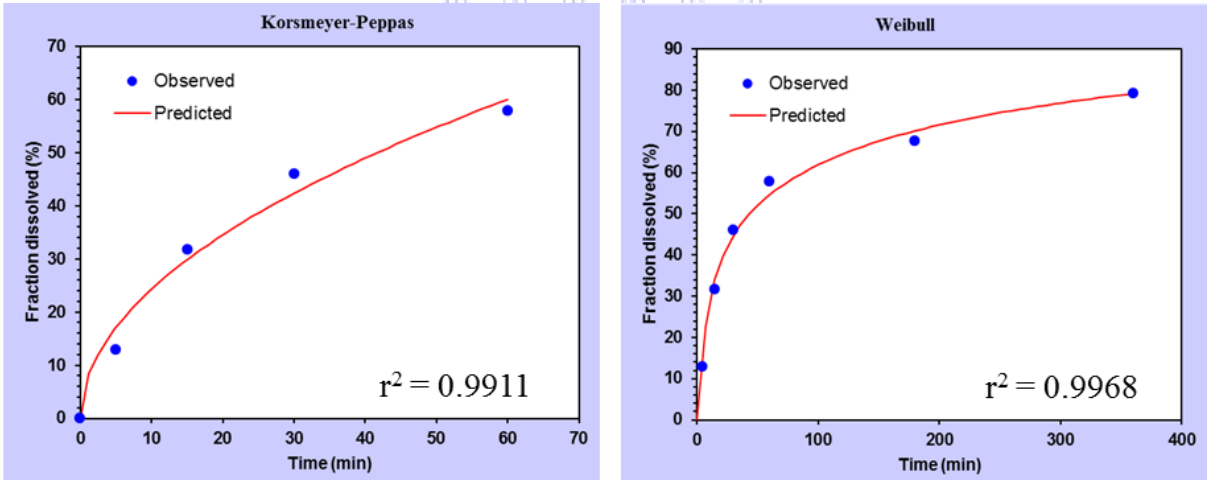

Figure 4.13 *Models of fit for in-vitro release of propranolol from SP NP formulation at pH 7.4. Data shown is the mean of n=3 replicates.*

4.6.8.2 Release profiles and kinetics at pH 7.4 for ST formulation

For release of the ST formulation, the plot showed relatively good r^2 values, with goodness of fit for the first order model, as well as the Korsmeyer-Peppas, and Weibull 1 models based on

http://etd.uwc.ac.za/

the regression coefficients (r^2 of 0.995, 0.999 and 0.997 respectively) (Figure 4.14). The Korsmeyer-Peppas release exponent for ST n = 0.967, indicated that release of the drug from the SP NPs at pH 7.4 was by super case-II transport, due to the polymer relaxation as a result of gel swelling, so-called super case-II transport [138], a confirmation of the inference drawn from the β value (β = 0.941) in the Weibull model of good fit, which suggested a combined release mechanism.

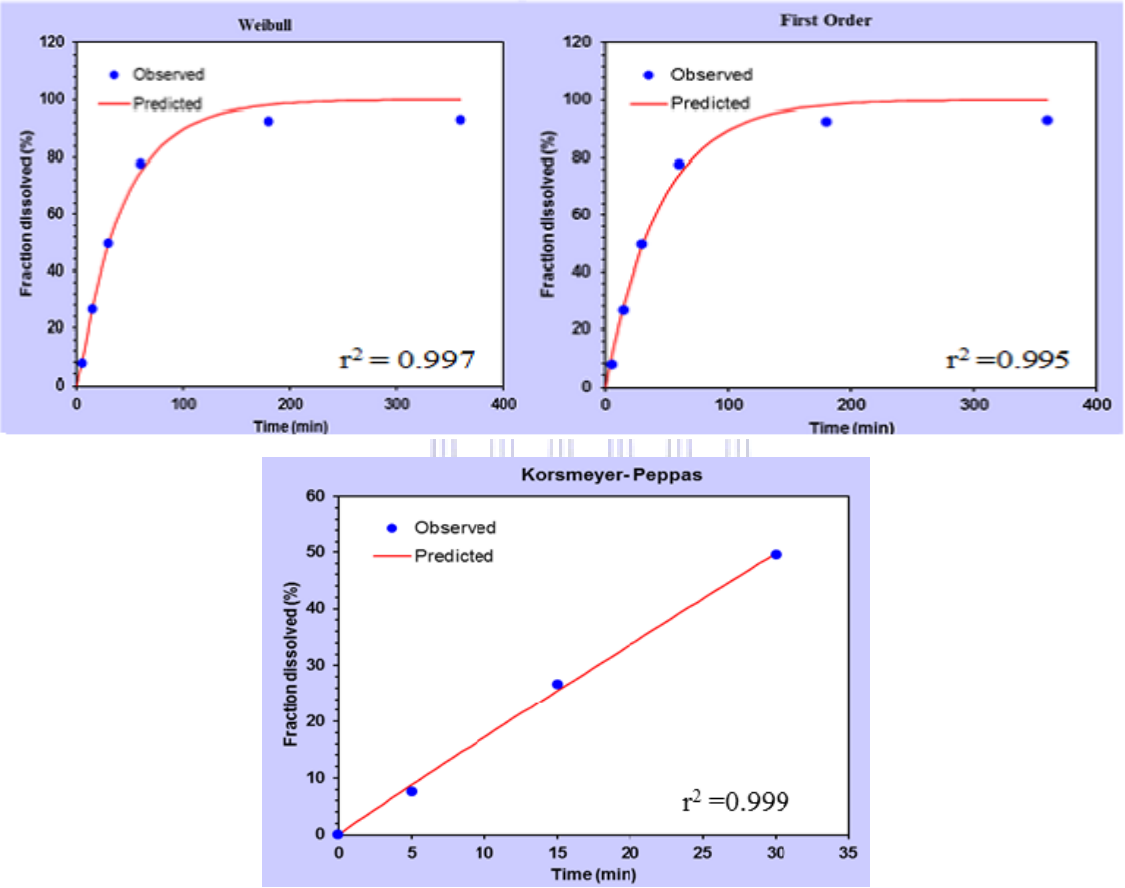

Figure 4.14 *Models of best fit for in-vitro release of propranolol from ST NP formulation at pH 7.4. Data shown are the mean of n=3 replicates.*

http://etd.uwc.ac.za/

4.6.8.3 Release profiles and kinetics at pH 7.4 for TT formulation

For the release of TT, the first order, Korsmeyer-Peppas and Weibull (r^2 of 0.988, 0.992, and 0.987 respectively) also met the required minimum r^2 value (i.e. 0.9800) for good model selection (Figure 4.15). The diffusion exponent n = 0.909 indicated super case II transport and the value of β for the Weibull model, implying that its release is by a complex mechanism.

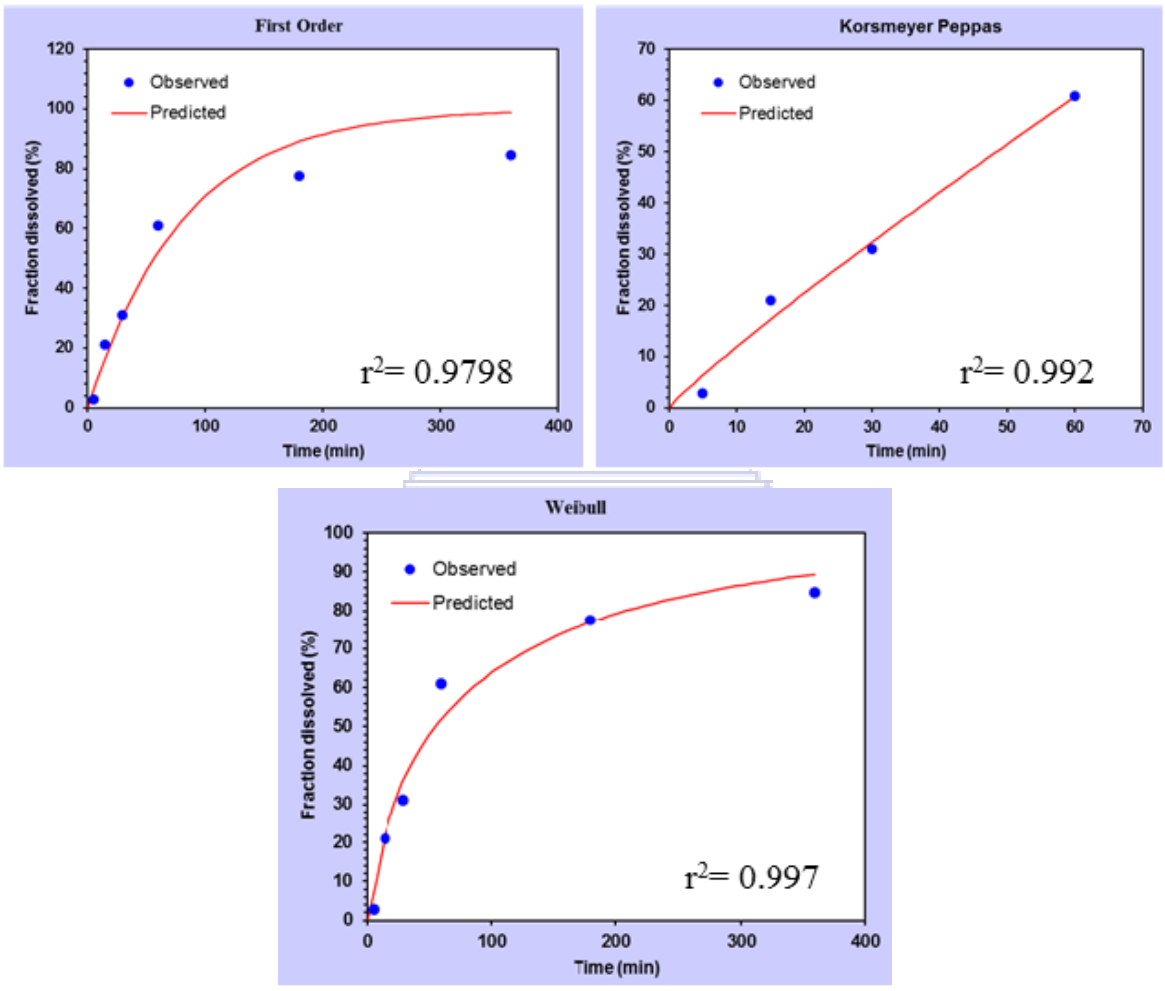

Figure 4.15 *Models of best fit for in-vitro release of propranolol from TT NP formulation at pH 7.4. Data shown is the mean of n=3 replicates.*

http://etd.uwc.ac.za/

4.6.8.4 Release profiles and kinetics at pH 7.4 for TST formulation

Formulation TST was fitted with the Higuchi, Korsmeyer-Peppas and Weibull models based on the regression coefficients (r^2 of 0.978, 0.979 and 0.982 respectively) (Figure 4.16). In Higuchi or square root kinetics, the drug diffuses at a comparatively slower rate as the distance for diffusion increases [188]. Thus the release of propranolol was proportional to the square root of time, indicating a diffusion controlled mechanism for TST formulation. The value of the Korsmeyer-Peppas release exponent for TST n = 0.483 and the time exponent obtained from Weibull model $\beta = 0.543$, which suggests that release of TST was via Fickian diffusion.

UNIVERSITY of the
WESTERN CAPE

http://etd.uwc.ac.za/

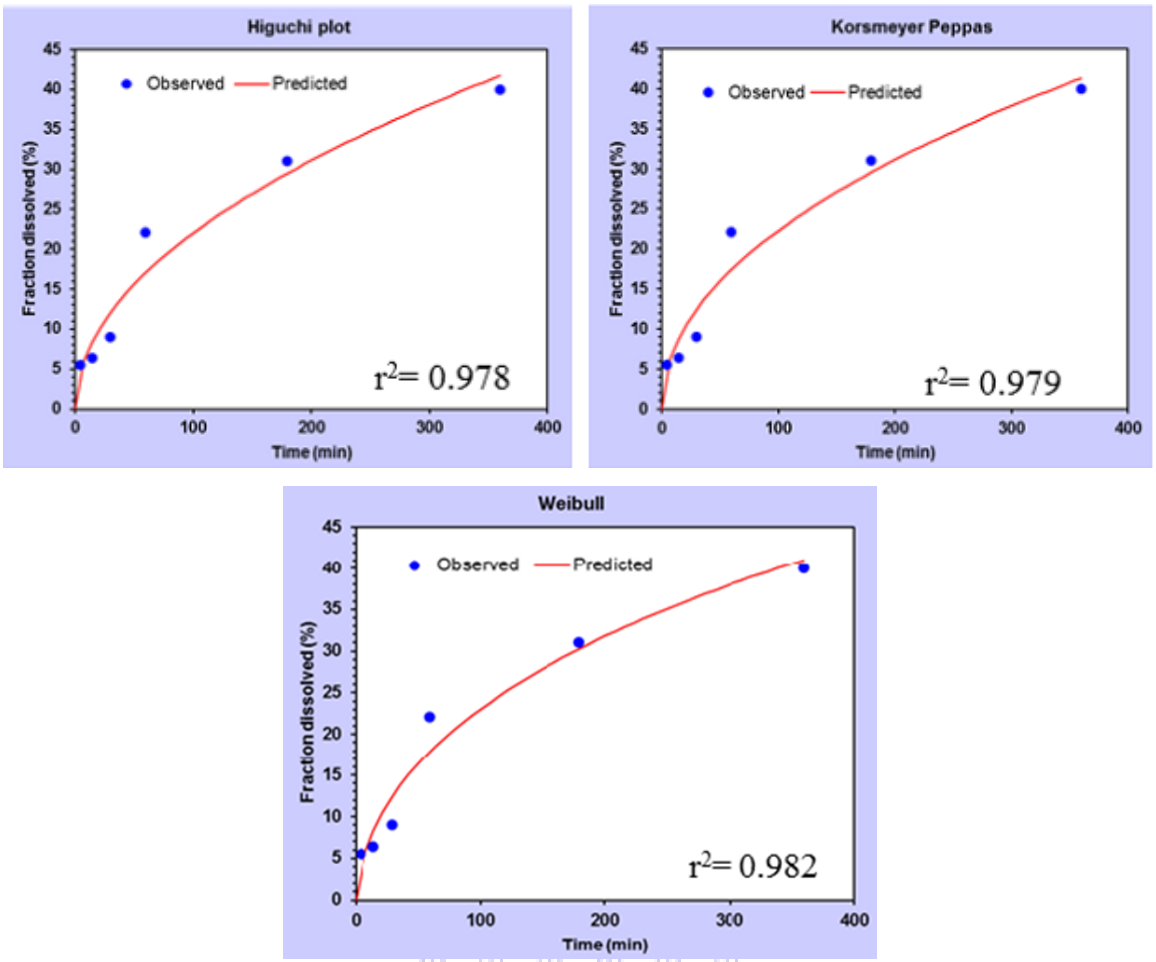

Figure 4.16 *Models of best fit for in-vitro release of propranolol-HCL from TST NP formulation at pH 7.4, n=3.*

UNIVERSITY of the
WESTERN CAPE

4.6.8.5 Summary of drug release fitting

The results of the curve-fitting study suggest that the Weibull and Korsmeyer-Peppas models are good mathematical models for describing propranolol release from PCL NPs at pH 7.4. Generally, the empirical models for the release description of propranolol at pH 7.4 differed in the various NP formulations. However, the release mechanisms were not Fickian diffusion in ST and TT formulations but ranged from combined to complex mechanisms that could all be described by super-case II transport. The release mechanisms were Fickian diffusion in SP and TST formulations. Furthermore, since PCL is a semi-crystalline polymer, the phosphate buffer solution can penetrate the amorphous part of the polymer matrix, thus facilitating the

http://etd.uwc.ac.za/

release of the drug by diffusion. The difference in the drug remaining in the matrix and the released drug in the phosphate buffer facilitates the release of the drug from NPs [189].

http://etd.uwc.ac.za/

CHAPTER 5

Conclusion and future recommendations

The objective of this study was to develop a NP drug delivery system for the delivery of the anti-hypertensive drug propranolol. The nanoparticle is intended to extend the short $t_{1/2}$ of propranolol, by providing sustained release of propranolol. To this end, several types of PCL based NPs were synthesised, and their physicochemical properties and drug release profiles were characterised. NPs were synthesised by the double emulsion solvent evaporation technique which is the most suitable method to synthesise NPs for a hydrophilic compound such as propranolol. Firstly, the optimum ratio of excipients was determined by synthesising the NPs using various surfactant/oil weight ratios (SOR%) of PCL polymer and PVA surfactant over SOR range 15-96.97%. It was hypothesised that the SOR% has an effect on NP properties.

UNIVERSITY of the
WESTERN CAPE

The z-average particle size of ratios ≤ 50% was found to be within the nano-size range, whereas at SOR% ≥ 66.60% particles were in the micron size range. PDI for all ratios was within 0.25 to 0.45 and suitable for drug delivery. ZP was negative and increased as SOR increased. Regarding the criteria used to select the optimised formulation, the PCL NPs produced with 33% SOR formulation were selected for further experiments as 33% SOR formulation had the lowest z-average particle size with monodisperse size distribution.

It was further hypothesized that surfactant type influences the physicochemical characteristics of PCL NPs. The effect of three surfactants, i.e. PVA, Span 80 and TPGS were investigated. NP formulations which were prepared with TPGS surfactant i.e. ST (Span 80, TPGS combination), TT (TPGS, TPGS) and TST (TPGS, Span 80 and TPGS) provided the smallest

http://etd.uwc.ac.za/

z-average particle size. PDI for all NP formulations were below 0.45 which indicated good particle homogeneity. ZP values were -32 mV or lower in all NP formulations which was an indication of stable colloidal dispersion. SEM images revealed PCL NPs that are spherical in shape.

Stability of NPs in aqueous media was characterized for seven days at three different temperatures; 4°C, 20°C and 37°C. All formulations showed good aqueous stability over the seven day experimental period (i.e. no significant changes in particle size, PDI and ZP). Furthermore, stability of NPs in HSA showed significant growth in particle size after incubation with HSA, and the surfactant type had no noticeable effect on HSA stability as all NP formulations showed an increase in mean particle size.

Assessment of the extent of albumin binding to the NPs indicated NP concentration on the protein binding among each NP formulation which concluded that the type of available groups on particle surface have significant effect on the protein binding properties of NPs. The maximum % protein binding occurred at the first 30 min of incubation and there was no significant difference as the incubation time extended.

It was hypothesised that surfactant type modulates the encapsulation efficiency and release kinetics of propranolol from NPs. From the results obtained, it was concluded that EE% was affected by surfactant type as PVA and Span 80 combinations (SP) had the lowest EE% and drug loading, whereas the TPGS containing NPs had higher EE% and drug loading. Interestingly, the formulation TST had the highest EE% and drug loading, indicating that the addition of TPGS to the inner/primary emulsion improved EE%. FTIR and DSC analysis indicated drug to polymer interaction within the NPs, which suggested that the encapsulation of propranolol into the PCL NPs also occurred through chemical interaction.

http://etd.uwc.ac.za/

Release of propranolol from the NPs was influenced by the type of surfactant. TST NPs containing TPGS in the inner and outer aqueous phases and Span 80 surfactants showed the slowest drug release rate. It is likely that TPGS may have stabilised the particle surface more efficiently and encapsulated more of the drug at the core particle thereby slowing down the rate of release. However, the mechanism of propranolol release from the NPs was not affected by the surfactant type. All NPs released propranolol predominantly through a diffusion mechanism.

All the objectives of the study were met. It was deduced that the TST formulation would be the best for the delivery of propranolol.

From the results, several areas for further research were noted to increase entrapment efficiency of the NPs. This includes modifying the TST formulation by incorporating PEG. This will reduce protein binding *in-vivo* and ensure extended propranolol $t_{1/2}$ as protein binding reduces the plasma residence time of the NPs. Protein binding studies *in-vitro* should also be performed on the PEGlyated particles. Sterilisation, long term stability and *in-vivo* studies in animals could further be performed to further characterise the delivery system (including efficacy and toxicity studies) for future clinical use.

http://etd.uwc.ac.za/

REFERENCES

[1] M. Iqbal, J.-P. Valour, H. Fessi, and A. Elaissari, "Preparation of biodegradable PCL particles via double emulsion evaporation method using ultrasound technique," *Colloid Polym. Sci.*, vol. 293, no. 3, pp. 861–873, 2015.

[2] K. S. Soppimath, T. M. Aminabhavi, A. R. Kulkarni, and W. E. Rudzinski, "Biodegradable polymeric nanoparticles as drug delivery devices," *J. Controlled Release*, vol. 70, no. 1, pp. 1–20, 2001.

[3] D. Allawadi, A. Kumar, N. Singh, S. Singh, and S. Arora, "Propranolol hydrochloride loaded nanospheres: Development and Characterization," *Int. J. Pharm. Sci. Res.*, vol. 4, no. 7, pp. 2639, 2013.

[4] N. Ubrich, P. Bouillot, C. Pellerin, M. Hoffman, and P. Maincent, "Preparation and characterization of propranolol hydrochloride nanoparticles: A comparative study," *J. Controlled Release*, vol. 97, no. 2, pp. 291–300, 2004.

[5] C. E. Astete and C. M. Sabliov, "Synthesis and characterization of PLGA nanoparticles," *J. Biomater. Sci. Polym. Ed.*, vol. 17, no. 3, pp. 247–289, 2006.

[6] I. Cicha, C. D. Garlichs, and C. Alexiou, "Cardiovascular therapy through nanotechnology–how far are we still from bedside?," *Eur. J. Nanomedicine*, vol. 6, no. 2, pp. 63–87, 2014.

[7] C. T. Sengel, "Delivery of nanoparticles for the treatment of cardiovascular diseases," *Glob Obes Diabetes Metab*, vol. 2, pp. 18–21, 2015.

[8] D. S. Celermajer, C. K. Chow, E. Marijon, N. M. Anstey, and K. S. Woo, "Cardiovascular disease in the developing world," *J. Am. Coll. Cardiol.*, vol. 60, no. 14, pp. 1207–1216, 2012.

[9] S. Mendis, P. Puska, B. Norrving, and others, *Global atlas on cardiovascular disease prevention and control*. World Health Organization, 2011.

[10] S. Wolfson and R. Gorlin, "Cardiovascular pharmacology of propranolol in man," *Circulation*, vol. 40, no. 4, pp. 501–511, 1969.

UNIVERSITY of the WESTERN CAPE

http://etd.uwc.ac.za/

[11] D. Yach, C. Hawkes, C. L. Gould, and K. J. Hofman, "The global burden of chronic diseases: Overcoming impediments to prevention and control," *Jama*, vol. 291, no. 21, pp. 2616–2622, 2004.

[12] S. Yusuf, S. Reddy, S. Ounpuu, and S. Anand, "Global burden of cardiovascular diseases: Part II: Variations in cardiovascular disease by specific ethnic groups and geographic regions and prevention strategies." *Circulation*, vol. 104, no. 23, pp. 2855–2864, 2001.

[13] A. Arora, N. Shafiq, S. Jain, G. K. Khuller, S. Sharma, and S. Malhotra, "Development of sustained release 'NanoFDC (Fixed Dose Combination)' for hypertension–an experimental study," *PloS One*, vol. 10, no. 6, pp. e0128208, 2015.

[14] F. Tesfaye, P. Byass, and S. Wall, "Population based prevalence of high blood pressure among adults in Addis Ababa: uncovering a silent epidemic," *BMC Cardiovasc. Disord.*, vol. 9, no. 1, pp. 39, 2009.

[15] W. B. Kannel, "Blood pressure as a cardiovascular risk factor: prevention and treatment," *Jama*, vol. 275, no. 20, pp. 1571–1576, 1996.

[16] T. D. Giles, B. J. Materson, J. N. Cohn, and J. B. Kostis, "Definition and classification of hypertension: an update," *J. Clin. Hypertens.*, vol. 11, no. 11, pp. 611–614, 2009.

UNIVERSITY of the
WESTERN CAPE

[17] P. Martin, I. D. Wilson, and G. R. Jones, "Optimisation of procedures for the extraction of structural analogues of propranolol with molecular imprinted polymers for sample preparation," *J. Chromatogr. A*, vol. 889, no. 1, pp. 143–147, 2000.

[18] A. Kiriyama, A. Honbo, and K. Iga, "Analysis of hepatic metabolism affecting pharmacokinetics of propranolol in humans," *Int. J. Pharm.*, vol. 349, no. 1, pp. 53–60, 2008.

[19] B. Taylan, Y. Capan, O. Güven, S. Kes, and A. A. Hincal, "Design and evaluation of sustained-release and buccal adhesive propranolol hydrochloride tablets," *J. Controlled Release*, vol. 38, no. 1, pp. 11–20, 1996.

[20] G. Berglund and O. Andersson, "Beta-blockers or diuretics in hypertension? A six year follow-up of blood pressure and metabolic side effects," *The Lancet*, vol. 317, no. 8223, pp. 744–747, 1981.

http://etd.uwc.ac.za/

[21] L. Filipponi, D. Sutherland, and I. N. Center, “Introduction to nanoscience and nanotechnologies,” *NANOYOU Teach. Train. Kit Nanosci. Nanotechnologies*, pp. 1–29, 2010.

[22] S. K. Sahoo, S. Parveen, and J. J. Panda, “The present and future of nanotechnology in human health care,” *Nanomedicine Nanotechnol. Biol. Med.*, vol. 3, no. 1, pp. 20–31, 2007.

[23] N. Sanvicens and M. P. Marco, “Multifunctional nanoparticles–properties and prospects for their use in human medicine,” *Trends Biotechnol.*, vol. 26, no. 8, pp. 425–433, 2008.

[24] A. Dowling, “Nanoscience and nanotechnologies,” in *An international symposium on the nature, purposes, ethics and politics of evidence in a democracy*, 2006, pp. 61.

[25] F. Klaessig, M. Marrapese, and S. Abe, “Current perspectives in nanotechnology terminology and nomenclature,” in *Nanotechnology Standards*, Springer, 2011, pp. 21–52.

[26] S. R. Mudshinge, A. B. Deore, S. Patil, and C. M. Bhalgat, “Nanoparticles: emerging carriers for drug delivery,” *Saudi Pharm. J.*, vol. 19, no. 3, pp. 129–141, 2011.

[27] S. D. Paul and D. Dewangan, “Nanotechnology and Neutraceuticals,” *Int J Nanomater Nanotechnol Nanomed*, vol. 1, pp. 30–33, 2015.

[28] S. S. D. Kumar, M. Surianarayanan, R. Vijayaraghavan, A. B. Mandal, and D. R. MacFarlane, “Curcumin loaded poly (2-hydroxyethyl methacrylate) nanoparticles from gelled ionic liquid–In vitro cytotoxicity and anti-cancer activity in SKOV-3 cells,” *Eur. J. Pharm. Sci.*, vol. 51, pp. 34–44, 2014.

[29] A. Z. Wilczewska, K. Niemirowicz, K. H. Markiewicz, and H. Car, “Nanoparticles as drug delivery systems,” *Pharmacol. Rep.*, vol. 64, no. 5, pp. 1020–1037, 2012.

[30] B. Godin, J. H. Sakamoto, R. E. Serda, A. Grattoni, A. Bouamrani, and M. Ferrari, “Emerging applications of nanomedicine for the diagnosis and treatment of cardiovascular diseases,” *Trends Pharmacol. Sci.*, vol. 31, no. 5, pp. 199–205, 2010.

http://etd.uwc.ac.za/

[31] A. Dube, “Assessment of the impact of biopolymeric nanoparticles on the oral absorption of green tea catechins,” Ph.D. dissertation, Monash University. Faculty of Pharmacy and Pharmaceutical Sciences. Drug Delivery, Disposition and Dynamics, 2011.

[32] C. P. Reis, R. J. Neufeld, A. J. Ribeiro, and F. Veiga, “Nanoencapsulation II. Biomedical applications and current status of peptide and protein nanoparticulate delivery systems,” *Nanomedicine Nanotechnol. Biol. Med.*, vol. 2, no. 2, pp. 53–65, 2006.

[33] A. Dube and N. Ebrahim, “The nanomedicine landscape of South Africa.” *Nanotechnology Reviews*, 2017.

[34] M. A. Shetab Boushehri and A. Lamprecht, “Nanoparticles as drug carriers: current issues with *in-vitro* testing,” *Nanomed.*, vol. 10, no. 21, pp. 3213–3230, 2015.

[35] L. Zhang *et al.*, “Nanoparticles in medicine: therapeutic applications and developments,” *Clin. Pharmacol. Ther.*, vol. 83, no. 5, pp. 761–769, 2008.

[36] R. Duncan and R. Gaspar, “Nanomedicine (s) under the microscope,” *Mol. Pharm.*, vol. 8, no. 6, pp. 2101–2141, 2011.

[37] L. Y. Rizzo, B. Theek, G. Storm, F. Kiessling, and T. Lammers, “Recent progress in nanomedicine: Therapeutic, diagnostic and theranostic applications,” *Curr. Opin. Biotechnol.*, vol. 24, no. 6, pp. 1159–1166, 2013.

[38] S. M. Moghimi, A. C. Hunter, and J. C. Murray, “Nanomedicine: current status and future prospects,” *FASEB J.*, vol. 19, no. 3, pp. 311–330, 2005.

[39] R. Singh and J. W. Lillard, “Nanoparticle-based targeted drug delivery,” *Exp. Mol. Pathol.*, vol. 86, no. 3, pp. 215–223, 2009.

[40] V. J. Mohanraj, Y. Chen, and others, “Nanoparticles–a review,” *Trop J Pharm Res*, vol. 5, no. 1, pp. 561–573, 2006.

[41] D. Bobo, K. J. Robinson, J. Islam, K. J. Thurecht, and S. R. Corrie, “Nanoparticle-based medicines: A review of FDA-approved materials and clinical trials to date,” *Pharm. Res.*, vol. 33, no. 10, pp. 2373–2387, 2016.

http://etd.uwc.ac.za/

[42] J. C. Kraft, J. P. Freeling, Z. Wang, and R. J. Ho, “Emerging research and clinical development trends of liposome and lipid nanoparticle drug delivery systems,” *J. Pharm. Sci.*, vol. 103, no. 1, pp. 29–52, 2014.

[43] G. Dikmen, L. Genç, and G. Güney, “Advantage and disadvantage in drug delivery systems,” *J. Mater. Sci. Eng.*, vol. 5, no. 4, pp. 468, 2011.

[44] N. Naseri, H. Valizadeh, and P. Zakeri-Milani, “Solid lipid nanoparticles and nanostructured lipid carriers: structure, preparation and application,” *Adv. Pharm. Bull.*, vol. 5, no. 3, pp. 305, 2015.

[45] A. Z. Wilczewska, K. Niemirowicz, K. H. Markiewicz, and H. Car, “Nanoparticles as drug delivery systems,” *Pharmacol. Rep.*, vol. 64, no. 5, pp. 1020–1037, 2012.

[46] A. D’emanuele and D. Attwood, “Dendrimer–drug interactions,” *Adv. Drug Deliv. Rev.*, vol. 57, no. 15, pp. 2147–2162, 2005.

[47] S. Natali and J. Mijovic, “Dendrimers as drug carriers: dynamics of PEGylated and methotrexate-loaded dendrimers in aqueous solution,” *Macromolecules*, vol. 43, no. 6, pp. 3011–3017, 2010.

[48] L. Han, R. Huang, S. Liu, S. Huang, and C. Jiang, “Peptide-conjugated PAMAM for targeted doxorubicin delivery to transferrin receptor overexpressed tumors,” *Mol. Pharm.*, vol. 7, no. 6, pp. 2156–2165, 2010.

[49] A. Kumari, S. K. Yadav, and S. C. Yadav, “Biodegradable polymeric nanoparticles based drug delivery systems,” *Colloids Surf. B Biointerfaces*, vol. 75, no. 1, pp. 1–18, 2010.

[50] K. Landfester and V. Mailänder, “Nanocapsules with specific targeting and release properties using miniemulsion polymerization,” *Expert Opin. Drug Deliv.*, vol. 10, no. 5, pp. 593–609, 2013.

[51] V. Torchilin, *Multifunctional pharmaceutical nanocarriers*, vol. 4. New York USA: Springer Science & Business Media, 2008.

[52] A. Kumari, S. K. Yadav, and S. C. Yadav, “Biodegradable polymeric nanoparticles based drug delivery systems,” *Colloids Surf. B Biointerfaces*, vol. 75, no. 1, pp. 1–18, 2010.

http://etd.uwc.ac.za/

[53] B. K. Nanjwade, J. Singh, K. A. Parikh, and F. V. Manvi, “Preparation and evaluation of carboplatin biodegradable polymeric nanoparticles,” *Int. J. Pharm.*, vol. 385, no. 1, pp. 176–180, 2010.

[54] N. S. Rejinold, K. P. Chennazhi, S. V. Nair, H. Tamura, and R. Jayakumar, “Biodegradable and thermo-sensitive chitosan-g-poly (N-vinylcaprolactam) nanoparticles as a 5-fluorouracil carrier,” *Carbohydr. Polym.*, vol. 83, no. 2, pp. 776–786, 2011.

[55] J. Park *et al.*, “PEGylated PLGA nanoparticles for the improved delivery of doxorubicin,” *Nanomedicine Nanotechnol. Biol. Med.*, vol. 5, no. 4, pp. 410–418, 2009.

[56] G. K. Saraogi, P. Gupta, U. D. Gupta, N. K. Jain, and G. P. Agrawal, “Gelatin nanocarriers as potential vectors for effective management of tuberculosis,” *Int. J. Pharm.*, vol. 385, no. 1, pp. 143–149, 2010.

[57] A. Dev *et al.*, “Preparation of poly (lactic acid)/chitosan nanoparticles for anti-HIV drug delivery applications,” *Carbohydr. Polym.*, vol. 80, no. 3, pp. 833–838, 2010.

[58] R. Pandey, Z. Ahmad, S. Sharma, and G. K. Khuller, “Nano-encapsulation of azole antifungals: potential applications to improve oral drug delivery,” *Int. J. Pharm.*, vol. 301, no. 1, pp. 268–276, 2005.

UNIVERSITY of the
WESTERN CAPE

[59] D. Thassu, Y. Pathak, and M. Deleers, “Nanoparticulate Drug-Delivery Systems,” in *Nanoparticulate drug delivery systems*, CRC Press, 2007, pp. 1–31.

[60] C. Vauthier and K. Bouchemal, “Methods for the preparation and manufacture of polymeric nanoparticles,” *Pharm. Res.*, vol. 26, no. 5, pp. 1025–1058, 2009.

[61] V. R. Sinha, K. Bansal, R. Kaushik, R. Kumria, and A. Trehan, “Poly-ϵ-caprolactone microspheres and nanospheres: an overview,” *Int. J. Pharm.*, vol. 278, no. 1, pp. 1–23, 2004.

[62] L. S. Nair and C. T. Laurencin, “Biodegradable polymers as biomaterials,” *Prog. Polym. Sci.*, vol. 32, no. 8, pp. 762–798, 2007.

[63] H. Kweon *et al.*, “A novel degradable polycaprolactone networks for tissue engineering,” *Biomaterials*, vol. 24, no. 5, pp. 801–808, 2003.

http://etd.uwc.ac.za/

[64] D.-I. D. Cho and H. J. Yoo, "Microfabrication methods for biodegradable polymeric carriers for drug delivery system applications: a review," *J. Microelectromechanical Syst.*, vol. 24, no. 1, pp. 10–18, 2015.

[65] H. Devalpally, D. Shenoy, S. Little, R. Langer, and M. Amiji, "Poly (ethylene oxide)-modified poly (epsiloncaprolactone) nanoparticles for targeted delivery of tamoxifen in breast cancer," *Cancer Chemother Pharmacol*, vol. 59, no. 4, pp. 477, 2007.

[66] C. Choi, S. Y. Chae, and J.-W. Nah, "Thermosensitive poly (N-isopropylacrylamide)-b-poly (ε-caprolactone) nanoparticles for efficient drug delivery system," *Polymer*, vol. 47, no. 13, pp. 4571–4580, 2006.

[67] L. K. Shah and M. M. Amiji, "Intracellular delivery of saquinavir in biodegradable polymeric nanoparticles for HIV/AIDS," *Pharm. Res.*, vol. 23, no. 11, pp. 2638–2645, 2006.

[68] S. Y. Kim and Y. M. Lee, "Taxol-loaded block copolymer nanospheres composed of methoxy poly (ethylene glycol) and poly (ε-caprolactone) as novel anticancer drug carriers," *Biomaterials*, vol. 22, no. 13, pp. 1697–1704, 2001.

[69] C. Damgé, P. Maincent, and N. Ubrich, "Oral delivery of insulin associated to polymeric nanoparticles in diabetic rats," *J. Controlled Release*, vol. 117, no. 2, pp. 163–170, 2007.

UNIVERSITY of the
WESTERN CAPE

[70] D. Zheng, X. Li, H. Xu, X. Lu, Y. Hu, and W. Fan, "Study on docetaxel-loaded nanoparticles with high antitumor efficacy against malignant melanoma," *Acta Biochim. Biophys. Sin.*, vol. 41, no. 7, pp. 578–587, 2009.

[71] S. Y. Kim, J. C. Ha, and Y. M. Lee, "Poly (ethylene oxide)-poly (propylene oxide)-poly (ethylene oxide)/poly (ϵ-caprolactone)(PCL) amphiphilic block copolymeric nanospheres: II. Thermo-responsive drug release behaviors," *J. Controlled Release*, vol. 65, no. 3, pp. 345–358, 2000.

[72] P. Prabu, A. A. Chaudhari, N. Dharmaraj, M. S. Khil, S. Y. Park, and H. Y. Kim, "Preparation, characterization, in-vitro drug release and cellular uptake of poly (caprolactone) grafted dextran copolymeric nanoparticles loaded with anticancer drug," *J. Biomed. Mater. Res. A*, vol. 90, no. 4, pp. 1128–1136, 2009.

http://etd.uwc.ac.za/

[73] V. Labhasetwar, C. Song, W. Humphrey, R. Shebuski, and R. J. Levy, "Arterial uptake of biodegradable nanoparticles: effect of surface modifications," *J. Pharm. Sci.*, vol. 87, no. 10, pp. 1229–1234, 1998.

[74] M. Bharathi *et al.*, "Preparation and in vitro & in vivo characterization of valsartan loaded eudragit nanoparticles," *Pharm. Sin.*, vol. 3, no. 5, pp. 516–525, 2012.

[75] M. Leroueil-Le Verger, L. Fluckiger, Y.-I. Kim, M. Hoffman, and P. Maincent, "Preparation and characterization of nanoparticles containing an antihypertensive agent," *Eur. J. Pharm. Biopharm.*, vol. 46, no. 2, pp. 137–143, 1998.

[76] U. Jana, A. K. Mohanty, P. K. Manna, and G. P. Mohanta, "Preparation and characterization of nebivolol nanoparticles using Eudragit® RS100," *Colloids Surf. B Biointerfaces*, vol. 113, pp. 269–275, 2014.

[77] Y. I. Kim, L. Fluckiger, M. Hoffman, I. Lartaud-Idjouadiene, J. Atkinson, and T. Maincent, "The antihypertensive effect of orally administered nifedipine-loaded nanoparticles in spontaneously hypertensive rats," *Br. J. Pharmacol.*, vol. 120, no. 3, pp. 399–404, 1997.

[78] M. Sharma, R. Sharma, and D. K. Jain, "Nanotechnology Based Approaches for Enhancing Oral Bioavailability of Poorly Water Soluble Antihypertensive Drugs," *Scientifica*, vol. 2016, pp. 1–11, 2016.

UNIVERSITY of the
WESTERN CAPE

[79] K. Nakamura *et al.*, "Nanoparticle-Mediated Drug Delivery System for Pulmonary Arterial Hypertension," *J. Clinical medicine*, vol. 6, no. 5, pp. 48, 2017.

[80] L. Chen *et al.*, "Nanoparticle-mediated delivery of pitavastatin into lungs ameliorates the development and induces regression of monocrotaline-induced pulmonary artery hypertension," *Hypertension*, vol. 57, no. 2, pp. 343–350, 2011.

[81] S. Kimura *et al.*, "Nanoparticle-mediated delivery of nuclear factor κB decoy into lungs ameliorates monocrotaline-induced pulmonary arterial hypertension," *Hypertension*, vol. 53, no. 5, pp. 877–883, 2009.

[82] S. Akagi *et al.*, "Delivery of imatinib-incorporated nanoparticles into lungs suppresses the development of monocrotaline-induced pulmonary arterial hypertension," *Int. Heart. J.*, vol. 56, no. 3, pp. 354–359, 2015.

http://etd.uwc.ac.za/

[83] T. Ishihara *et al.*, "Encapsulation of beraprost sodium in nanoparticles: analysis of sustained release properties, targeting abilities and pharmacological activities in animal models of pulmonary arterial hypertension," *J. Controlled Release*, vol. 197, pp. 97–104, 2015.

[84] S. Akagi *et al.*, "Intratracheal Administration of Prostacyclin Analogue–incorporated Nanoparticles Ameliorates the Development of Monocrotaline and Sugen-Hypoxia-induced Pulmonary Arterial Hypertension," *J. Cardiovasc. Pharmacol.*, vol. 67, no. 4, pp. 290, 2016.

[85] J. M. McLendon *et al.*, "Lipid nanoparticle delivery of a microRNA-145 inhibitor improves experimental pulmonary hypertension," *J. Controlled Release*, vol. 210, pp. 67–75, 2015.

[86] M.-F. Ficheux, L. Bonakdar, F. Leal-Calderon, and J. Bibette, "Some stability criteria for double emulsions," *Langmuir*, vol. 14, no. 10, pp. 2702–2706, 1998.

[87] T. G. Mason, J. N. Wilking, K. Meleson, C. B. Chang, and S. M. Graves, "Nanoemulsions: formation, structure, and physical properties," *J. Phys. Condens. Matter*, vol. 18, no. 41, pp. R635, 2006.

[88] T. F. Tadros, *Emulsion formation and stability*. Berkshire, UK: John Wiley & Sons, 2013.

UNIVERSITY of the
WESTERN CAPE

[89] M. E. Aulton and K. M. Taylor, *Aulton's pharmaceutics: the design and manufacture of medicines*. Elsevier Health Sciences, 2013.

[90] D. Attwood, *Surfactant systems: their chemistry, pharmacy and biology*. Springer Science & Business Media, 2012.

[91] I. C. I. Americas, *The HLB System: A Time-saving Guide to Emulsifier Selection*. ICI Americas, Incorporated, 1984.

[92] A. Gadhave, "Determination of hydrophilic-lipophilic balance value," *Int J Sci Res*, vol. 3, no. 4, pp. 573–575, 2014.

[93] J.-L. Salager, "Surfactants types and uses," *FIRP Bookl.*, no. E300A, 2002.

http://etd.uwc.ac.za/

[94] M. Adamczak, “Surfactants, polyelectrolytes and nanoparticles as building blocks for nanocarriers,” Ph.D. dissertation, The Jerzy Haber Institute of Catalysis and Surface Chemistry Polish Academy of Sciences, Poland, 2013.

[95] P. I. Urrutia, “Predicting water-in-oil emulsion coalescence from surface pressure isotherms,” M. A. thesis, University of Calgary, Canada, 2006.

[96] L. L. Schramm, *Emulsions, foams, and suspensions: fundamentals and applications*. John Wiley & Sons, 2006.

[97] E. Sah and H. Sah, “Recent trends in preparation of poly (lactide-co-glycolide) nanoparticles by mixing polymeric organic solution with antisolvent,” *J. Nanomater.*, vol. 2015, pp. 61, 2015.

[98] S. K. Sahoo, J. Panyam, S. Prabha, and V. Labhasetwar, “Residual polyvinyl alcohol associated with poly (D, L-lactide-co-glycolide) nanoparticles affects their physical properties and cellular uptake,” *J. Controlled Release*, vol. 82, no. 1, pp. 105–114, 2002.

[99] T. S. Gaaz, A. B. Sulong, M. N. Akhtar, A. A. H. Kadhum, A. B. Mohamad, and A. A. Al-Amiery, “Properties and applications of polyvinyl alcohol, halloysite nanotubes and their nanocomposites,” *Molecules*, vol. 20, no. 12, pp. 22833–22847, 2015.

[100] Z. Zhang, S. Tan, and S.-S. Feng, “Vitamin E TPGS as a molecular biomaterial for drug delivery,” *Biomaterials*, vol. 33, no. 19, pp. 4889–4906, 2012.

[101] S.-W. Wu and W. K. Hopkins, “Characteristics of d-α-tocopheryl PEG 1000 succinate for applications as an absorption enhancer in drug delivery systems,” *Pharm. Technol.*, vol. 23, no. 10, pp. 52–68, 1999.

[102] L. Yu *et al.*, “Vitamin E-TPGS increases absorption flux of an HIV protease inhibitor by enhancing its solubility and permeability1,” *Pharm. Res.*, vol. 16, no. 12, pp. 1812–1817, 1999.

[103] J. M. Dintaman and J. A. Silverman, “Inhibition of P-glycoprotein by D-α-tocopheryl polyethylene glycol 1000 succinate (TPGS),” *Pharm. Res.*, vol. 16, no. 10, pp. 1550–1556, 1999.

UNIVERSITY of the WESTERN CAPE
http://etd.uwc.ac.za/

[104] Z. Zhang, S. H. Lee, C. W. Gan, and S.-S. Feng, “In vitro and in vivo investigation on PLA–TPGS nanoparticles for controlled and sustained small molecule chemotherapy,” *Pharm. Res.*, vol. 25, no. 8, pp. 1925–1935, 2008.

[105] P. Parhi, C. Mohanty, and S. K. Sahoo, “RETRACTED: Enhanced cellular uptake and in vivo pharmacokinetics of rapamycin loaded cubic phase nanoparticles for cancer therapy,” *Acta Biomater.*, vol. 7, no. 10, pp. 3656–3669, 2011.

[106] D. Kumar, K. Singh, S. Kumar, H. S. Bhatti, and others, “Photoluminescent properties of SPAN-80 coated intrinsic and extrinsic ZnO nanostructures,” *Phys. E Low-Dimens. Syst. Nanostructures*, vol. 79, pp. 188–197, 2016.

[107] I. S. Ahmed, R. El Hosary, S. Shalaby, and S. Nour, “Preparation and in-vitro Evaluation of Poly Caprolactone Nanoparticles Containing Atorvastation Calcium,” *J. Pharm. Res. Opin.*, vol. 4, no. 1, pp. 8–18, 2014.

[108] C. P. Reis, R. J. Neufeld, A. J. Ribeiro, and F. Veiga, “Nanoencapsulation I. Methods for preparation of drug-loaded polymeric nanoparticles,” *Nanomedicine Nanotechnol. Biol. Med.*, vol. 2, no. 1, pp. 8–21, 2006.

[109] D. Bennet and S. Kim, “Polymer nanoparticles for smart drug delivery”, in *Application of Nanotechnology in Drug Delivery*, InTech, 2014, pp. 257–312.

UNIVERSITY of the
WESTERN CAPE

[110] S. L. Pal, U. Jana, P. K. Manna, G. P. Mohanta, and R. Manavalan, “Nanoparticle: An overview of preparation and characterization,” *J. Applied Pharmaceutical Science*, vol. 1, no. 6, pp. 228–234, 2011.

[111] S. Desgouilles *et al.*, “The design of nanoparticles obtained by solvent evaporation: a comprehensive study,” *Langmuir*, vol. 19, no. 22, pp. 9504–9510, 2003.

[112] C. Vauthier and G. Ponchel, *Polymer Nanoparticles for Nanomedicines*. Springer International Publishing Switzerland, 2016.

[113] J. P. Rao and K. E. Geckeler, “Polymer nanoparticles: preparation techniques and size-control parameters,” *Prog. Polym. Sci.*, vol. 36, no. 7, pp. 887–913, 2011.

http://etd.uwc.ac.za/

[114] C. X. Song *et al.*, "Formulation and characterization of biodegradable nanoparticles for intravascular local drug delivery," *J. Controlled Release*, vol. 43, no. 2, pp. 197–212, 1997.

[115] M. L. Hans and A. M. Lowman, "Biodegradable nanoparticles for drug delivery and targeting," *Curr. Opin. Solid State Mater. Sci.*, vol. 6, no. 4, pp. 319–327, 2002.

[116] J. Xu, "Synthesis of polymeric nanoparticles for the controlled release of hydrophobic and hydrophilic therapeutic compounds," Ph.D. dissertation, University Of Waterloo, Canada, 2016.

[117] D. Quintanar-Guerrero, E. Allémann, E. Doelker, and H. Fessi, "A mechanistic study of the formation of polymer nanoparticles by the emulsification-diffusion technique," *Colloid Polym. Sci.*, vol. 275, no. 7, pp. 640–647, 1997.

[118] B. Mandal, "Preparation and physicochemical characterization of Eudragit® RL100 nanosuspension with potential for ocular delivery of sulfacetamide," M.A. thesis, University of Toledo, United States, 2010.

[119] M. J. Hey, D. P. Jackson, and H. Yan, "The salting-out effect and phase separation in aqueous solutions of electrolytes and poly (ethylene glycol)," *Polymer*, vol. 46, no. 8, pp. 2567–2572, 2005.

UNIVERSITY of the
WESTERN CAPE

[120] B. V. N. Nagavarma, H. K. Yadav, A. Ayaz, L. S. Vasudha, and H. G. Shivakumar, "Different techniques for preparation of polymeric nanoparticles—a review," *Asian J Pharm Clin Res*, vol. 5, no. 3, pp. 16–23, 2012.

[121] X. Liu *et al.*, "A one-step homogeneous immunoassay for cancer biomarker detection using gold nanoparticle probes coupled with dynamic light scattering," *J. Am. Chem. Soc.*, vol. 130, no. 9, pp. 2780–2782, 2008.

[122] K. Ranjit and A. A. Baquee, "Nanoparticle: an overview of preparation, characterization and application," *Int Res J Pharm*, vol. 4, no. 4, pp. 47–57, 2013.

[123] S. Charurvedi and P. N. Dave, "Microscopy in nanotechnology. Microscopy contributions to advances in science and technology,"*Microscopy: advances in scientific research and education*, 2012.

http://etd.uwc.ac.za/

[124] S. L. Pal, U. Jana, P. K. Manna, G. P. Mohanta, and R. Manavalan, "Nanoparticle: An overview of preparation and characterization (2000-2010).," *Journal of Appli ed Pharmaceutical Science*, vol. 1, no. 6, pp. 228–234, 2011.

[125] M. Kaszuba, J. Corbett, F. M. Watson, and A. Jones, "High-concentration zeta potential measurements using light-scattering techniques," *Philos. Trans. R. Soc. Lond. Math. Phys. Eng. Sci.*, vol. 368, no. 1927, pp. 4439–4451, 2010.

[126] M. M. Domingues, P. S. Santiago, M. A. Castanho, and N. C. Santos, "What can light scattering spectroscopy do for membrane-active peptide studies?," *J. Pept. Sci.*, vol. 14, no. 4, pp. 394–400, 2008.

[127] O. Popovska, "An overview: methods for preparation and characterization of liposomes as drug delivery systems," *Int. J. Pharm. Phytopharm. Res.*, vol. 3, no. 3 pp. 182–189, 2014.

[128] J. H. Lee and Y. Yeo, "Controlled drug release from pharmaceutical nanocarriers," *Chem. Eng. Sci.*, vol. 125, pp. 75–84, 2015.

[129] G. Singhvi and M. Singh, "Review: in-vitro drug release characterization models," *Int J Pharm Stud Res*, vol. 2, no. 1, pp. 77–84, 2011.

[130] J. Siepmann and F. Siepmann, "Mathematical modeling of drug dissolution," *Int. J. Pharm.*, vol. 453, no. 1, pp. 12–24, 2013.

[131] J. Siepmann and A. Göpferich, "Mathematical modeling of bioerodible, polymeric drug delivery systems," *Adv. Drug Deliv. Rev.*, vol. 48, no. 2, pp. 229–247, 2001.

[132] J. Siepmann and F. Siepmann, "Mathematical modeling of drug delivery," *Int. J. Pharm.*, vol. 364, no. 2, pp. 328–343, 2008.

[133] Y. Agata, Y. Iwao, A. Miyagishima, and S. Itai, "Novel mathematical model for predicting the dissolution profile of spherical particles under non-sink conditions," *Chem. Pharm. Bull. Tokyo*, vol. 58, no. 4, pp. 511, 2010.

http://etd.uwc.ac.za/

[134] P. Costa and J. M. S. Lobo, "Modeling and comparison of dissolution profiles," *Eur. J. Pharm. Sci.*, vol. 13, no. 2, pp. 123–133, 2001.

[135] M. A. Kalam *et al.*, "Release kinetics of modified pharmaceutical dosage forms: a review," *Cont J Pharm Sci*, vol. 1, no. 3, pp. 30–35, 2007.

[136] R. Grillo, N. Z. P. dos Santos, C. R. Maruyama, A. H. Rosa, R. de Lima, and L. F. Fraceto, "Poly (ε-caprolactone) nanocapsules as carrier systems for herbicides: Physico-chemical characterization and genotoxicity evaluation," *J. Hazard. Mater.*, vol. 231, pp. 1–9, 2012.

[137] R. W. Korsmeyer, R. Gurny, E. Doelker, P. Buri, and N. A. Peppas, "Mechanisms of solute release from porous hydrophilic polymers," *Int. J. Pharm.*, vol. 15, no. 1, pp. 25–35, 1983.

[138] M. Gierszewska-Drużyńska and J. Ostrowska-Czubenko, "Mechanism of water diffusion into noncrosslinked and ionically crosslinked chitosan membranes," *Prog. Chem. Appl. Chitin Its Deriv.*, vol. 17, pp. 59–66, 2012.

[139] F. Langenbucher, "Letters to the Editor: Linearization of dissolution rate curves by the Weibull distribution," *J. Pharm. Pharmacol.*, vol. 24, no. 12, pp. 979–981, 1972.

UNIVERSITY of the WESTERN CAPE

[140] Y. Zhang *et al.*, "DDSolver: an add-in program for modeling and comparison of drug dissolution profiles," *AAPS J.*, vol. 12, no. 3, pp. 263–271, 2010.

[141] N. Anton and T. F. Vandamme, "The universality of low-energy nano-emulsification," *Int. J. Pharm.*, vol. 377, no. 1, pp. 142–147, 2009.

[142] T. Niwa, H. Takeuchi, T. Hino, M. Nohara, and Y. Kawashima, "Biodegradable submicron carriers for peptide drugs: preparation of DL-lactide/glycolide copolymer (PLGA) nanospheres with nafarelin acetate by a novel emulsion-phase separation method in an oil system," *Int. J. Pharm.*, vol. 121, no. 1, pp. 45–54, 1995.

[143] S. Cristina, Z. Gheorghe, and P. Sandu, "Factors influencing the obtaining and the stability of double emulsions made of corn oil," *Ann. Univ. Dunarea Jos Galati Fascicle VI Food Technol.*, vol. 33, pp. 57, 2009.

http://etd.uwc.ac.za/

[144] Z. Zhang and S.-S. Feng, “Nanoparticles of poly (lactide)/vitamin E TPGS copolymer for cancer chemotherapy: synthesis, formulation, characterization and in vitro drug release,” *Biomaterials*, vol. 27, no. 2, pp. 262–270, 2006.

[145] L. Mu and S. S. Feng, “A novel controlled release formulation for the anticancer drug paclitaxel (Taxol®): PLGA nanoparticles containing vitamin E TPGS,” *J. Controlled Release*, vol. 86, no. 1, pp. 33–48, 2003.

[146] M. H. Perez *et al.*, “The preparation and evaluation of poly (ϵ-caprolactone) microparticles containing both a lipophilic and a hydrophilic drug,” *J. Controlled Release*, vol. 65, no. 3, pp. 429–438, 2000.

[147] C. T. Sengel Türk, Z. Sezgin Bayindir, and U. Badilli, “Preparation of polymeric nanoparticles using different stabilizing agents,” *J Fac Pharm Ank.*, vol. 38, no. 4, pp. 257–268, 2009.

[148] J. Liu, Z. Qiu, S. Wang, L. Zhou, and S. Zhang, “A modified double-emulsion method for the preparation of daunorubicin-loaded polymeric nanoparticle with enhanced in vitro anti-tumor activity,” *Biomed. Mater.*, vol. 5, no. 6, pp. 065002, 2010.

[149] A. Saez, M. Guzman, J. Molpeceres, and M. R. Aberturas, “Freeze-drying of polycaprolactone and poly (D, L-lactic-glycolic) nanoparticles induce minor particle size changes affecting the oral pharmacokinetics of loaded drugs,” *Eur. J. Pharm. Biopharm.*, vol. 50, no. 3, pp. 379–387, 2000.

[150] W. Abdelwahed, G. Degobert, S. Stainmesse, and H. Fessi, “Freeze-drying of nanoparticles: formulation, process and storage considerations,” *Adv. Drug Deliv. Rev.*, vol. 58, no. 15, pp. 1688–1713, 2006.

[151] W. Zhou, R. Apkarian, Z. L. Wang, and D. Joy, “Fundamentals of scanning electron microscopy (SEM),” in *Scanning Microscopy for Nanotechnology*, Springer, 2006, pp. 1–40.

[152] M. D. Coffin and J. W. McGinity, “Biodegradable pseudolatexes: the chemical stability of poly (D, L-lactide) and poly (ε-caprolactone) nanoparticles in aqueous media,” *Pharm. Res.*, vol. 9, no. 2, pp. 200–205, 1992.

[153] V. Mirshafiee, R. Kim, M. Mahmoudi, and M. L. Kraft, “The importance of selecting a proper biological milieu for protein corona analysis in vitro: Human plasma versus human serum,” *Int. J. Biochem. Cell Biol.*, vol. 75, no. 2016, pp. 188–195, 2015.

UNIVERSITY of the WESTERN CAPE

http://etd.uwc.ac.za/

[154] M. S. Cartiera, K. M. Johnson, V. Rajendran, M. J. Caplan, and W. M. Saltzman, "The uptake and intracellular fate of PLGA nanoparticles in epithelial cells," *Biomaterials*, vol. 30, no. 14, pp. 2790–2798, 2009.

[155] R. L. McCall and R. W. Sirianni, "PLGA nanoparticles formed by single-or double-emulsion with vitamin E-TPGS," *JoVE J. Vis. Exp.*, no. 82, pp. e51015–e51015, 2013.

[156] J. Vandervoort and A. Ludwig, "Biocompatible stabilizers in the preparation of PLGA nanoparticles: a factorial design study," *Int. J. Pharm.*, vol. 238, no. 1, pp. 77–92, 2002.

[157] J. W. Fong, *Process for preparation of microspheres*. Google Patents, 1990.

[158] M. M. Elsayed and G. Cevc, "Turbidity spectroscopy for characterization of submicroscopic drug carriers, such as nanoparticles and lipid vesicles: size determination," *Pharm. Res.*, vol. 28, no. 9, pp. 2204–2222, 2011.

[159] J. S. Chawla and M. M. Amiji, "Biodegradable poly (ε-caprolactone) nanoparticles for tumor-targeted delivery of tamoxifen," *Int. J. Pharm.*, vol. 249, no. 1, pp. 127–138, 2002.

[160] L. Tshweu, L. Katata, L. Kalombo, and H. Swai, "Nanoencapsulation of water-soluble drug, lamivudine, using a double emulsion spray-drying technique for improving HIV treatment," *J. Nanoparticle Res.*, vol. 15, no. 11, p. 2040, 2013.

UNIVERSITY of the
WESTERN CAPE

[161] C. E. Mora-Huertas, H. Fessi, and A. Elaissari, "Polymer-based nanocapsules for drug delivery," *Int. J. Pharm.*, vol. 385, no. 1, pp. 113–142, 2010.

[162] C. R. Müller *et al.*, "Degradation and stabilization of diclofenac in polymeric nanocapsules," *Quím. Nova*, vol. 27, no. 4, pp. 555–560, 2004.

[163] S. R. Schaffazick, S. S. Guterres, L. de L. Freitas, and A. R. Pohlmann, "Physicochemical characterization and stability of the polymeric nanoparticle systems for drug administration," *Quím. Nova*, vol. 26, no. 5, pp. 726–737, 2003.

[164] S. R. Saptarshi, A. Duschl, and A. L. Lopata, "Interaction of nanoparticles with proteins: relation to bio-reactivity of the nanoparticle," *J. Nanobiotechnology*, vol. 11, no. 1, pp. 1, 2013.

http://etd.uwc.ac.za/

[165] Q. Xu *et al.*, "Impact of surface polyethylene glycol (PEG) density on biodegradable nanoparticle transport in mucus ex vivo and distribution in vivo," *ACS Nano*, vol. 9, no. 9, pp. 9217, 2015.

[166] S. Winzen, J. C. Schwabacher, J. Müller, K. Landfester, and K. Mohr, "Small Surfactant Concentration Differences Influence Adsorption of Human Serum Albumin on Polystyrene Nanoparticles," *Biomacromolecules*, vol. 17, no. 11, pp. 3845–3851, 2016.

[167] S. P. Boulos *et al.*, "Nanoparticle–protein interactions: a thermodynamic and kinetic study of the adsorption of bovine serum albumin to gold nanoparticle surfaces," *Langmuir*, vol. 29, no. 48, pp. 14984–14996, 2013.

[168] S. H. Jeong, K. K. Kim, S. J. Jeong, K. H. An, S. H. Lee, and Y. H. Lee, "Optical absorption spectroscopy for determining carbon nanotube concentration in solution," *Synth. Met.*, vol. 157, no. 13, pp. 570–574, 2007.

[169] ICH, "Validation of analytical procedures: text and methodology," vol. 1, 2005.

[170] D. Wang, J. He, N. Rosenzweig, and Z. Rosenzweig, "Superparamagnetic Fe2O3 beads-CdSe/ZnS quantum dots core-shell nanocomposite particles for cell separation," *Nano Lett.*, vol. 4, no. 3, pp. 409–413, 2004.

UNIVERSITY of the
WESTERN CAPE

[171] Y. Baimark and Y. Srisuwan, "Biodegradable nanoparticles of methoxy poly (ethylene glycol)-b-poly (d, l-lactide)/methoxy poly (ethylene glycol)-b-poly (ϵ-caprolactone) blends for drug delivery," *Nanoscale Res. Lett.*, vol. 7, no. 1, pp. 1, 2012.

[172] G. A. Shabir, "A practical approach to validation of HPLC methods under current good manufacturing practices," *J. Valid. Technol.*, vol. 10, pp. 210–218, 2004.

[173] A. Dube, J. L. Reynolds, W.-C. Law, C. C. Maponga, P. N. Prasad, and G. D. Morse, "Multimodal nanoparticles that provide immunomodulation and intracellular drug delivery for infectious diseases," *Nanomedicine Nanotechnol. Biol. Med.*, vol. 10, no. 4, pp. 831–838, 2014.

[174] M. Tukulula *et al.*, "Curdlan-conjugated PLGA nanoparticles possess macrophage stimulant activity and drug delivery capabilities," *Pharm. Res.*, vol. 32, no. 8, pp. 2713–2726, 2015.

http://etd.uwc.ac.za/

[175] H. K. Shaikh, R. V. Kshirsagar, and S. G. Patil, "Mathematical models for drug release characterization: a review," *WJPPS*, vol. 4, no. 4, pp. 324–338, 2015.

[176] T. Verrecchia, G. Spenlehauer, D. V. Bazile, A. Murry-Brelier, Y. Archimbaud, and M. Veillard, "Non-stealth (poly (lactic acid/albumin)) and stealth (poly (lactic acid-polyethylene glycol)) nanoparticles as injectable drug carriers," *J. Controlled Release*, vol. 36, no. 1, pp. 49–61, 1995.

[177] T. Govender, S. Stolnik, M. C. Garnett, L. Illum, and S. S. Davis, "PLGA nanoparticles prepared by nanoprecipitation: drug loading and release studies of a water soluble drug," *J. Controlled Release*, vol. 57, no. 2, pp. 171–185, 1999.

[178] D. S. Jones and K. J. Pearce, "An investigation of the effects of some process variables on the microencapsulation of propranolol hydrochloride by the solvent evaporation method," *Int. J. Pharm.*, vol. 118, no. 2, pp. 199–205, 1995.

[179] H. Danafar, "MPEG–PCL copolymeric nanoparticles in drug delivery systems," *Cogent Med.*, vol. 3, no. 1, pp. 1142411, 2016.

[180] M. V. Srikanth, N. S. Rao, S. A. Sunil, B. J. Ram, and V. R. M. Kolapalli, "Statistical design and evaluation of a propranolol HCl gastric floating tablet," *Acta Pharm. Sin. B*, vol. 2, no. 1, pp. 60–69, 2012.

UNIVERSITY of the
WESTERN CAPE

[181] F. Kedzierewicz, P. Thouvenot, I. Monot, M. Hoffman, and P. Maincent, "Influence of different physicochemical conditions on the release of indium oxine from nanocapsules," *J. Biomed. Mater. Res.*, vol. 39, no. 4, pp. 588–593, 1998.

[182] W. Lu and T. G. Park, "Protein release from poly (lactic-co-glycolic acid) microspheres: protein stability problems," *PDA J. Pharm. Sci. Technol.*, vol. 49, no. 1, pp. 13–19, 1995.

[183] M. T. Peracchia, R. Gref, Y. Minamitake, A. Domb, N. Lotan, and R. Langer, "PEG-coated nanospheres from amphiphilic diblock and multiblock copolymers: investigation of their drug encapsulation and release characteristics," *J. Controlled Release*, vol. 46, no. 3, pp. 223–231, 1997.

[184] S. K. Das and N. G. Das, "Preparation and in vitro dissolution profile of dual polymer (Eudragit RS100 and RL100) microparticles of diltiazem hydrochloride," *J. Microencapsul.*, vol. 15, no. 4, pp. 445–452, 1998.

http://etd.uwc.ac.za/

[185] J.-H. Ha, S.-H. Kim, and C.-S. Cho, “Albumin Release from Bioerodible Hydrogels Based on Semi-Interpenetrating Polymer Networks Composed of Poly(ε-Caprolactone) and Poly (Ethylene Glycol) Macromer,” in *Advanced Biomaterials in Biomedical Engineering and Drug Delivery Systems*, N. Ogata, S. W. Kim, J. Feijen, and T. Okano, Eds. Tokyo: Springer Japan, 1996, pp. 343–344.

[186] P. Fonte *et al.*, “Effect of cryoprotectants on the porosity and stability of insulin-loaded PLGA nanoparticles after freeze-drying,” *Biomatter*, vol. 2, no. 4, pp. 329–339, 2012.

[187] C. E. Mora-Huertas, H. Fessi, and A. Elaissari, “Polymer-based nanocapsules for drug delivery,” *Int. J. Pharm.*, vol. 385, no. 1–2, pp. 113–142, Jan. 2010.

[188] S. Pandav and J. Naik, “Preparation and in vitro evaluation of ethylcellulose and polymethacrylate resins loaded microparticles containing hydrophilic drug,” *J. Pharm.*, vol. 2014, pp. 5, 2014.

[189] A. Lokhande, S. Mishra, R. Kulkarni, and J. Naik, “Formulation and Evaluation of Glipizide loaded nanoparticles,” *J Pharm Pharm Sci*, vol. 5, no. 975-1491, pp. 147–151, 2013.

UNIVERSITY of the
WESTERN CAPE

http://etd.uwc.ac.za/